CAVITY LIMITATIONS

Gianluigi Ciovati

Thomas Jefferson National Accelerator Facility

Outline

- Residual resistance
- Multipacting
- Field emission
- Quench
- High-field Q-slope

The Real World

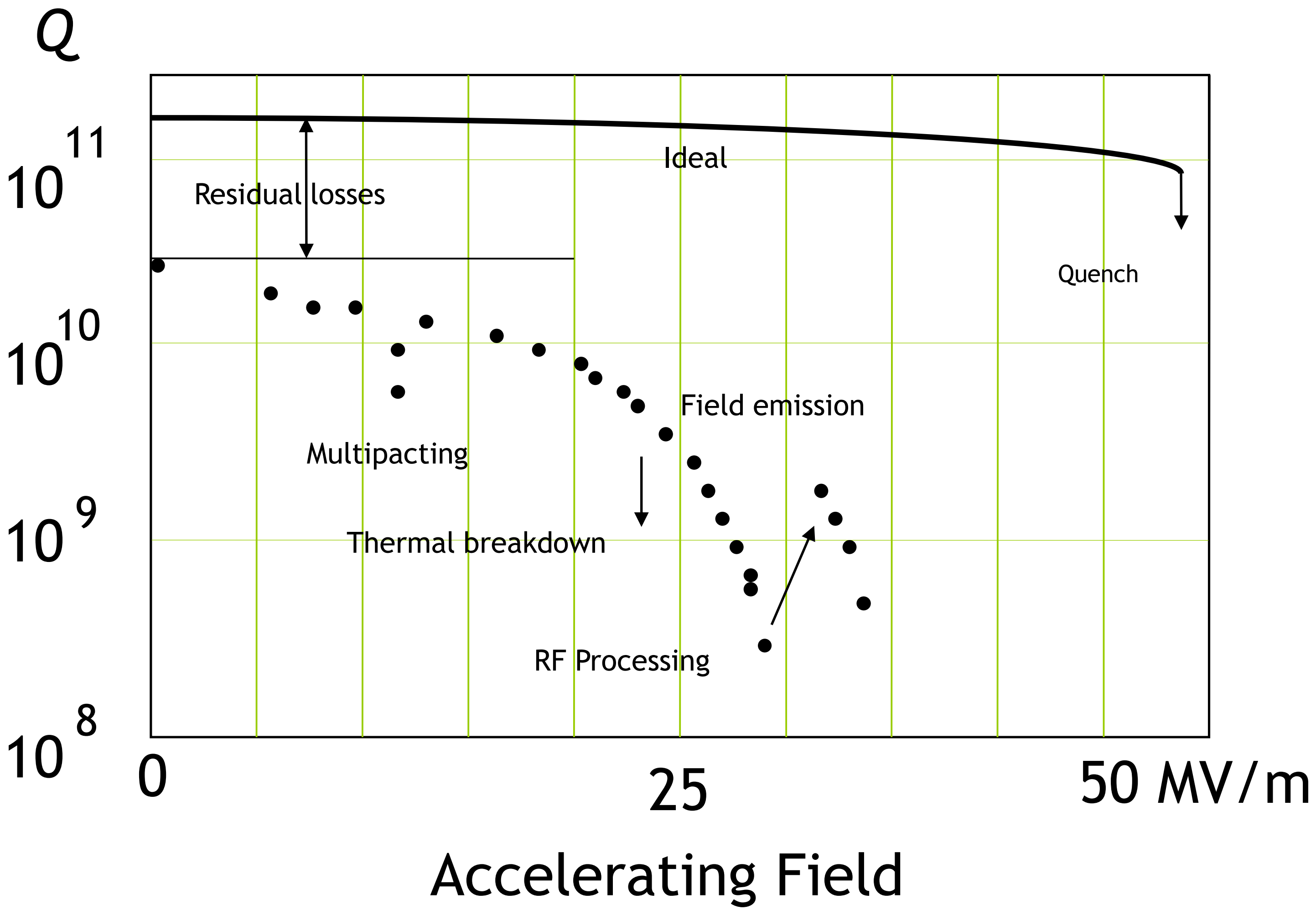

Losses in SRF Cavities

- Different loss mechanism are associated with different regions of the cavity surface

Electric field high at iris

$E_p/E_{acc} \sim 2$

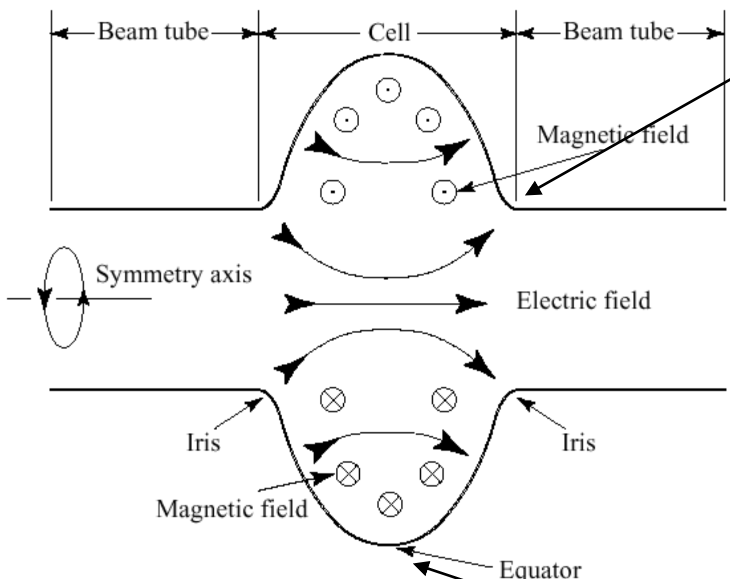

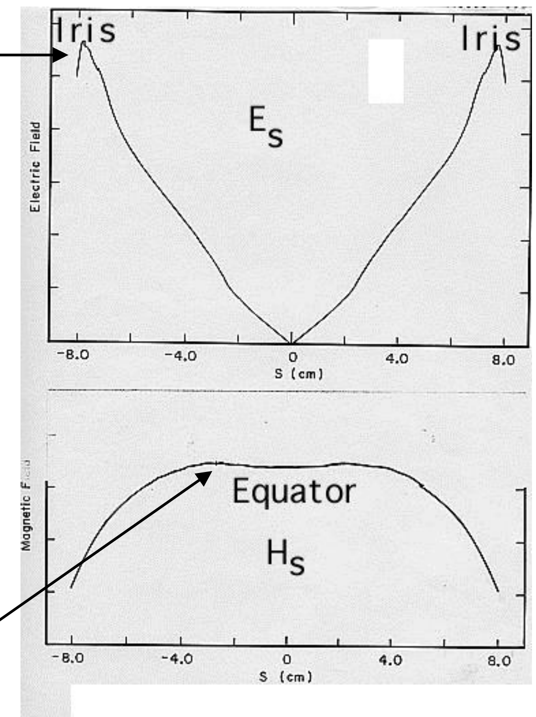

Magnetic field high at equator

$B_p/E_{acc} \sim 4.2$ mT/(MV/m)

Origin of Residual Surface Resistance

- Dielectric surface contaminants (gases, chemical residues, dust, adsorbates)
- Normal conducting defects, inclusions
- Surface imperfections (cracks, scratches, delaminations)
- **Trapped magnetic flux**
- **Hydride precipitation**
- Localized electron states in the oxide (photon absorption)

R_{res} is typically 5-10 nΩ at 1-1.5 GHz

Trapped Magnetic Field

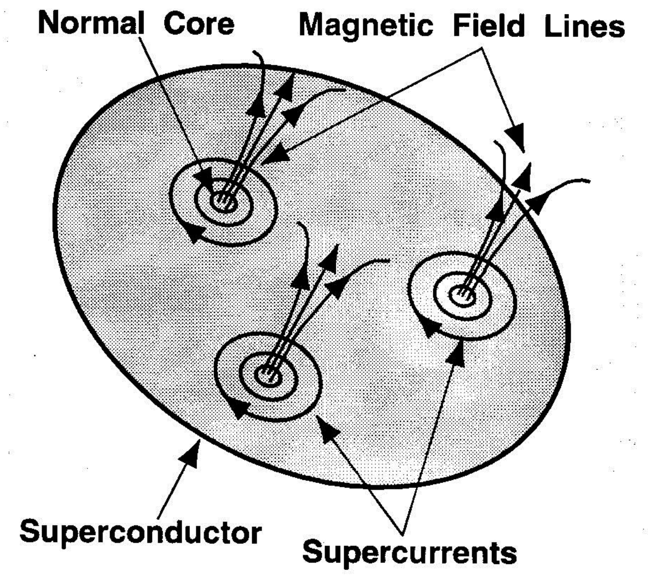

- Vortices are normal to the surface
- 100% flux trapping
- RF dissipation is due to the normal conducting core, of resistance R_n

$$R_{res} \cong R_n \frac{H_i}{H_{c2}}$$

H_i = residual DC magnetic field

• For Nb: $R_{res} \approx$ 0.3 to 1 nΩ/mG around 1 GHz

Depends on material treatment

• While a cavity goes through the superconducting transition, the ambient magnetic filed cannot be more than a few mG.
• The earth's magnetic shield must be effectively shielded.
• Thermoelectric currents can cause trapped magnetic field, especially in cavities made of composite materials.

Trapped Magnetic Field

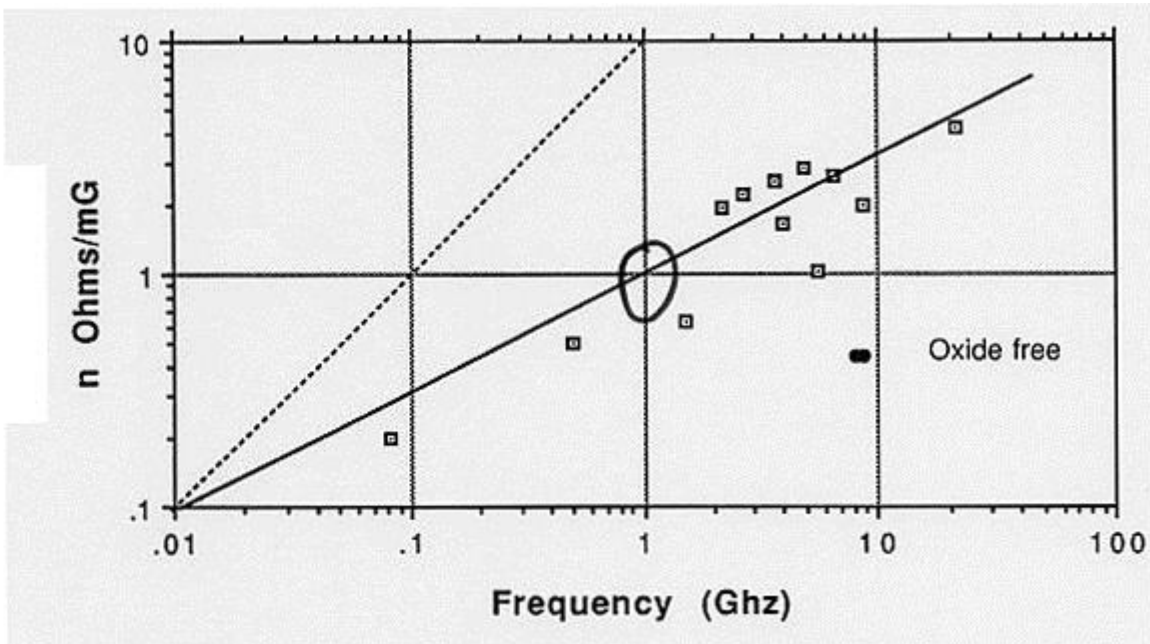

R_{res} Due to Hydrides (Q-Disease)

- Cavities that remain at 70-150 K for several hours (or slow cool-down, < 1 K/min) experience a sharp increase of residual resistance
- More severe in cavities which have been heavily chemically etched

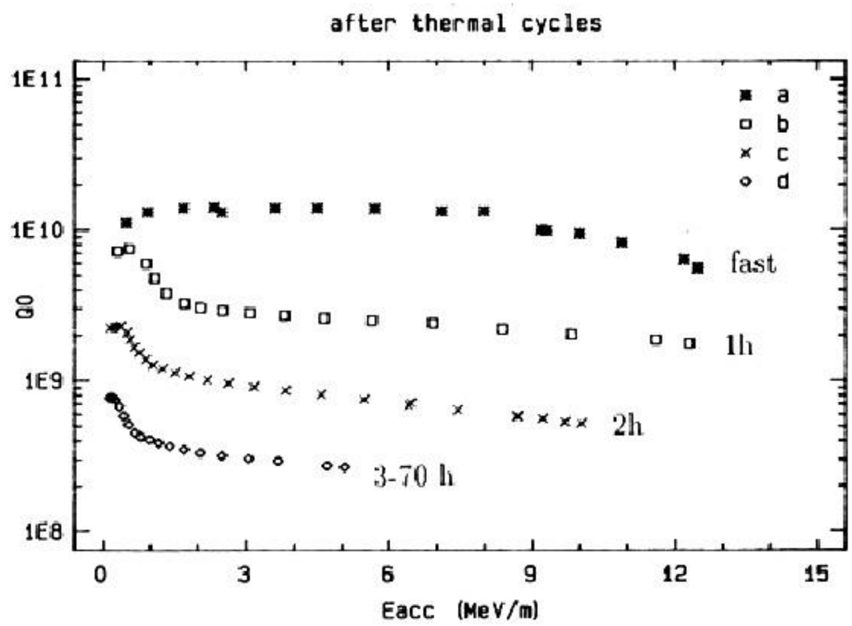

Hydrogen: “Q-disease”

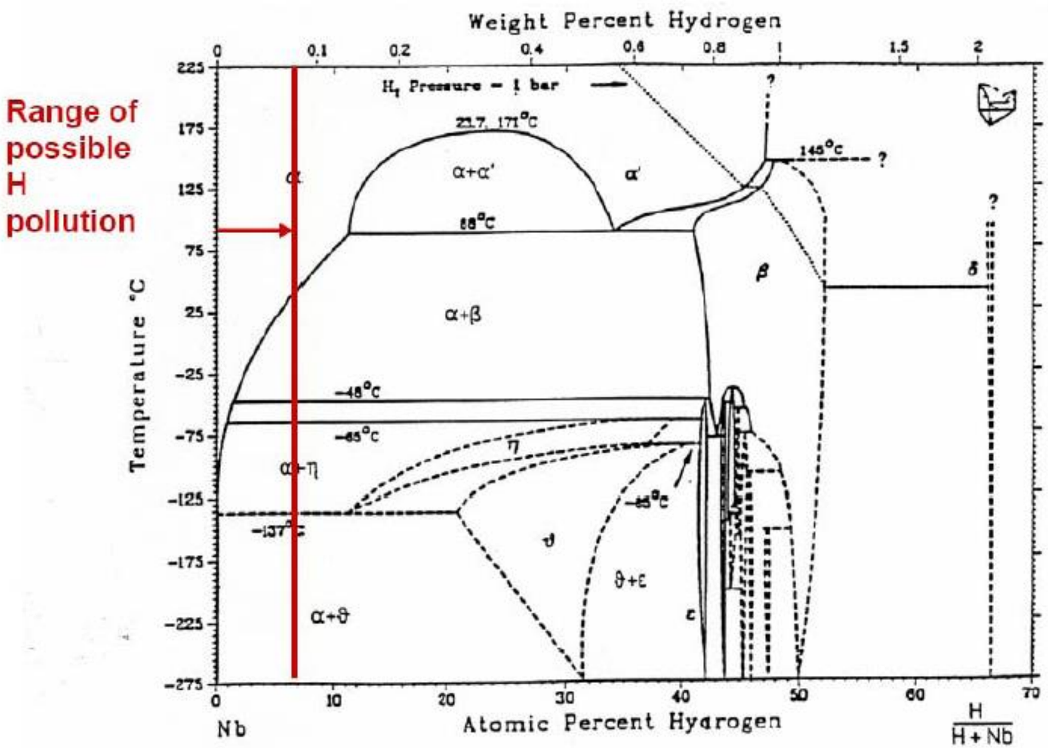

- H is readily absorbed into Nb where the oxide layer is removed (during chemical etching or mechanical grinding)
- H has high diffusion rate in Nb, even at low temperatures.
- H precipitates to form a hydride phase with poor superconducting properties: T_c=2.8 K, H_c=60 G

- At room temperature the required concentration to form a hydride is 10^3-10^4 wppm
- At 150K it is < **10 wppm**

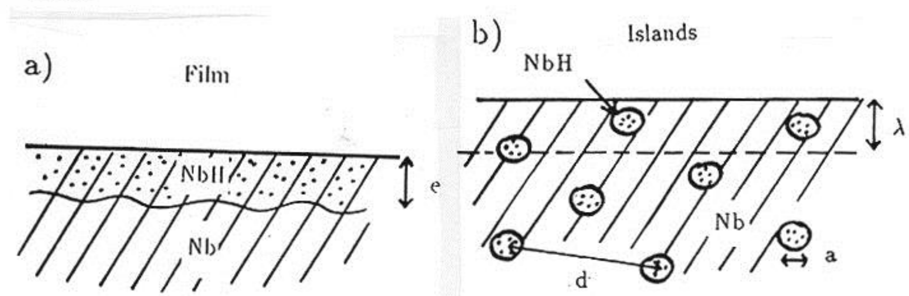

Cures for Q-disease

- Fast cool-down
- Maintain acid temperature below ~ 20 °C during BCP
- “Purge” H_2 with N_2 “blanket” and cover cathode with Teflon cloth during EP
- “Degas” Nb in vacuum furnace at T > 600 °C

Q_0 Record

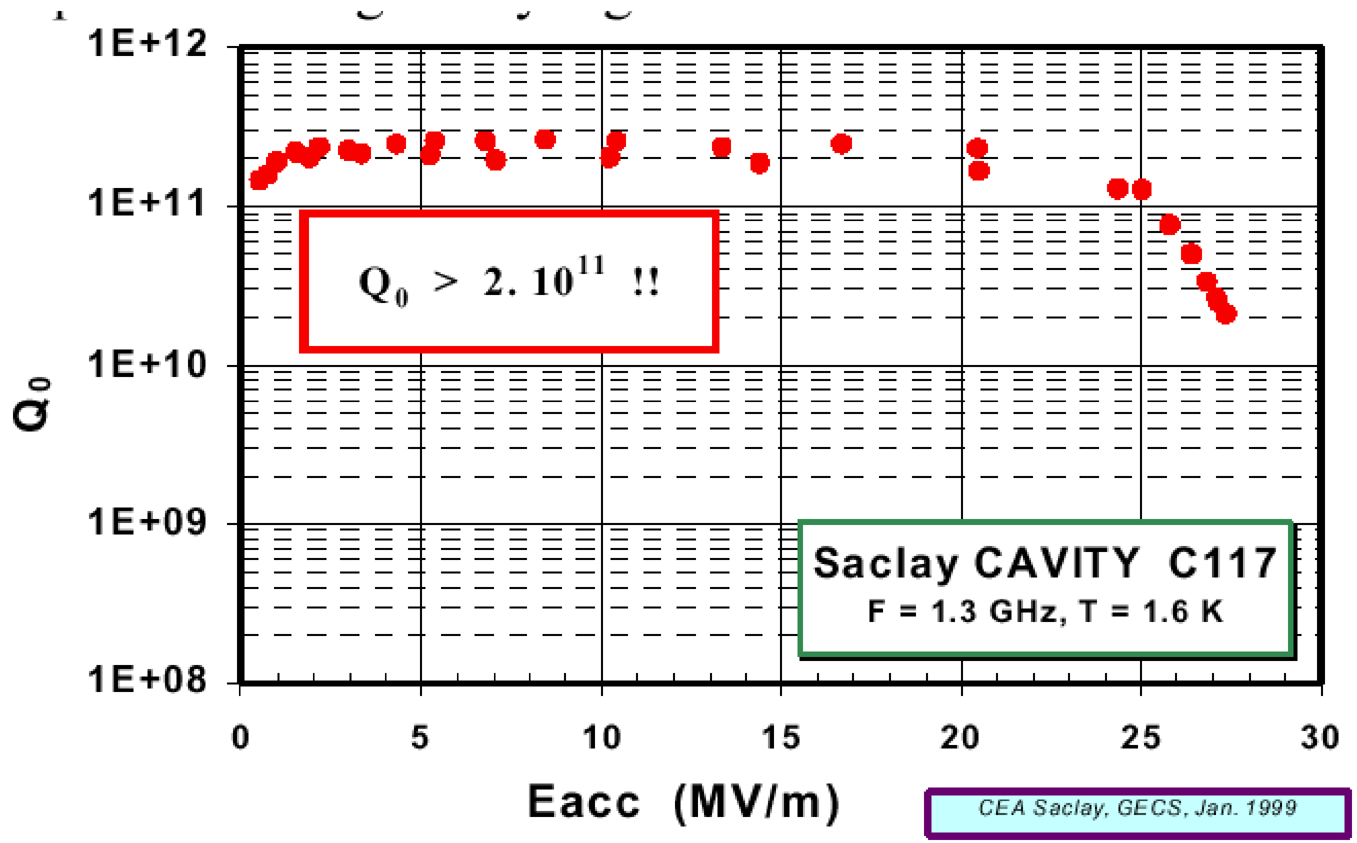

Figure 2 – Residual resistance as low as 0.5 nΩ is actually measured on large area cavities, giving an intrinsic quality factor Q_0 exceeding 2.10^{11}.

Multipacting

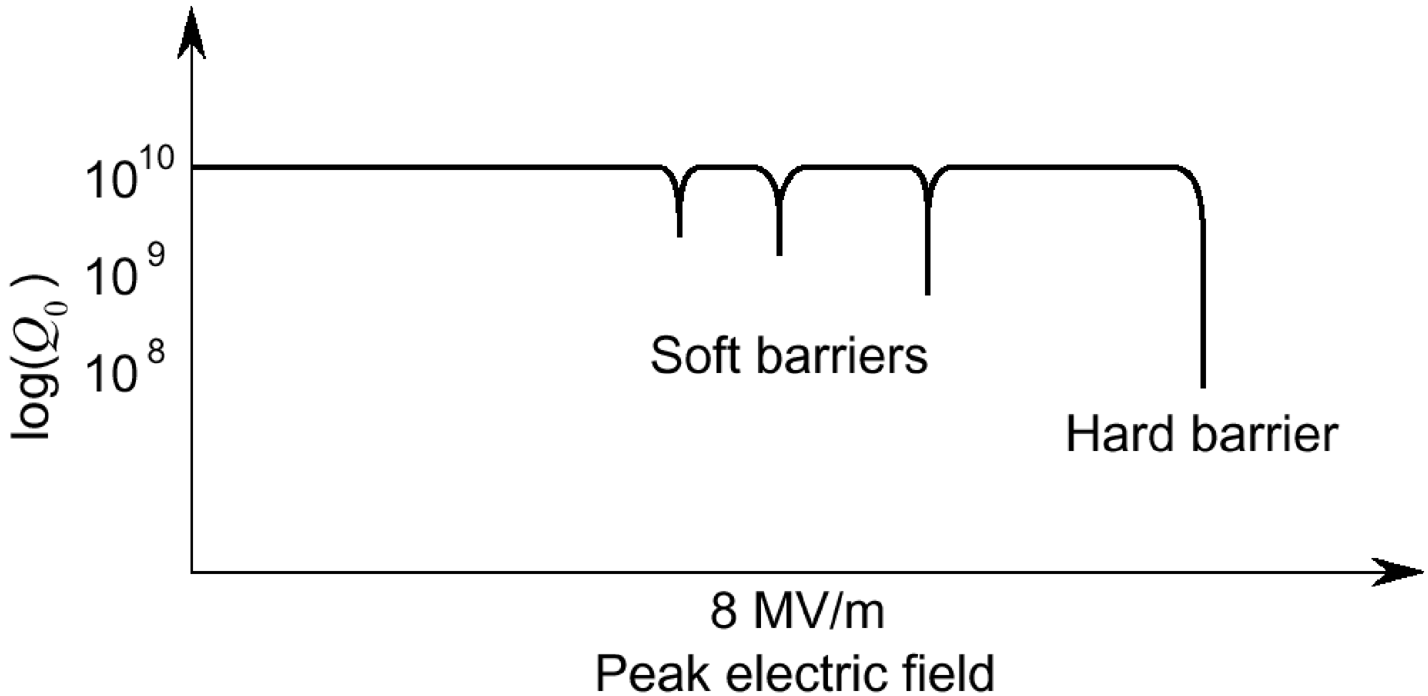

- No increase of P_t for increased P_i during MP
- Can induce quenches and trigger field emission

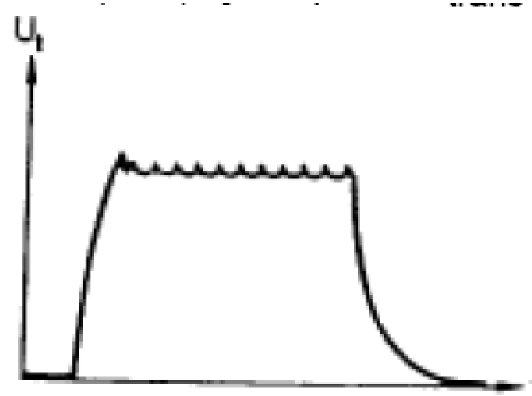

Multipacting

Multipacting is characterized by an exponential growth in the number of electrons in a cavity

Common problems of RF structures (Power couplers, NC cavities…)

Multipacting requires 2 conditions:

- Electron motion is periodic (resonance condition)
- Impact energy is such that secondary emission coefficient is >1

One-Point Multipacting

One-point MP

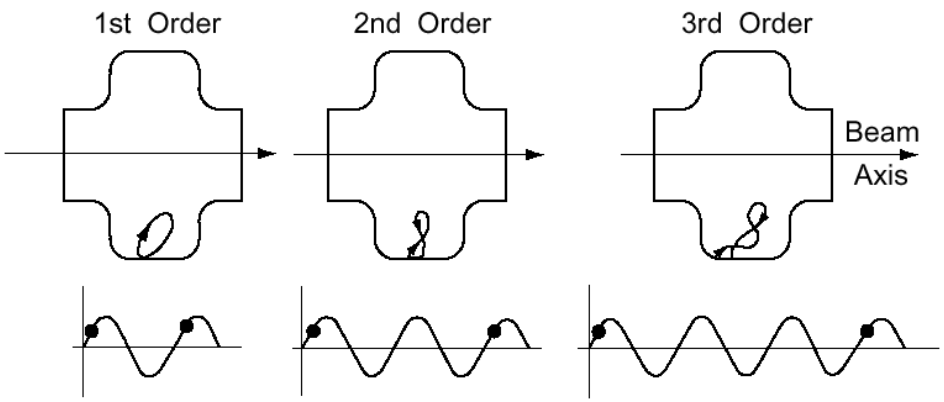

Cyclotron frequency: $\omega_c \propto \frac{\mu_0 H e}{m}$

Resonance condition:

Cavity frequency (ω_g) = n x cyclotron frequency $\omega_g = n\omega_c$ n: MP order

→ Possible MP barriers given by $H_n \propto \frac{m\omega_g}{n\mu_0 e}$ + SEY, δ(K), > 1 = MP

The impact energy scales as $K \propto \frac{e^2 E_\perp^2}{m\omega_g^2}$

Empirical formula: $H_n[\mathrm{Oe}] = \frac{0.3}{n} f_0[\mathrm{MHz}]$

Two-Point Multipacting

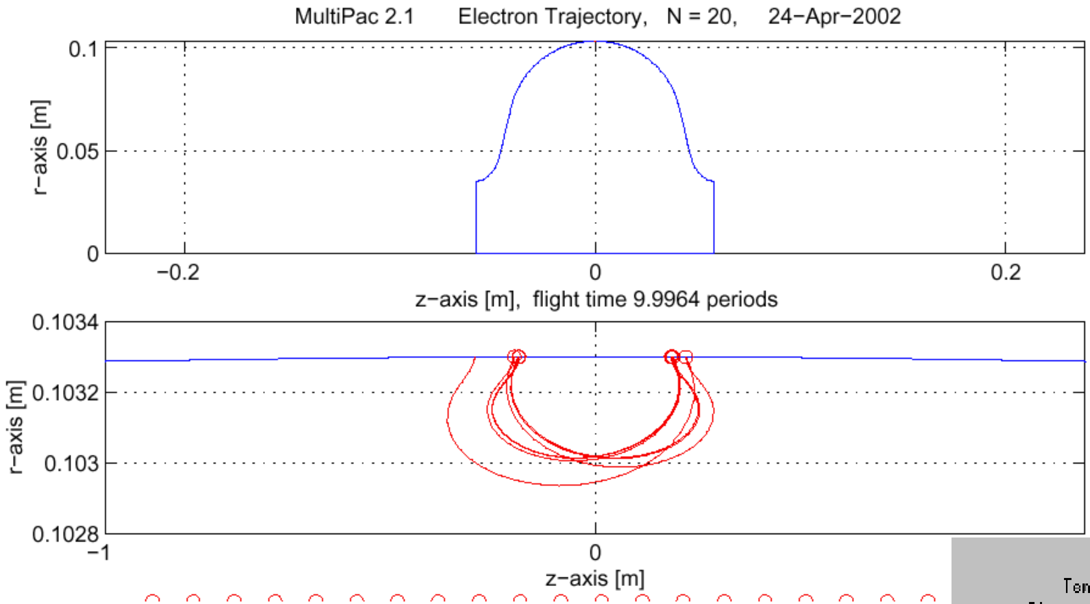

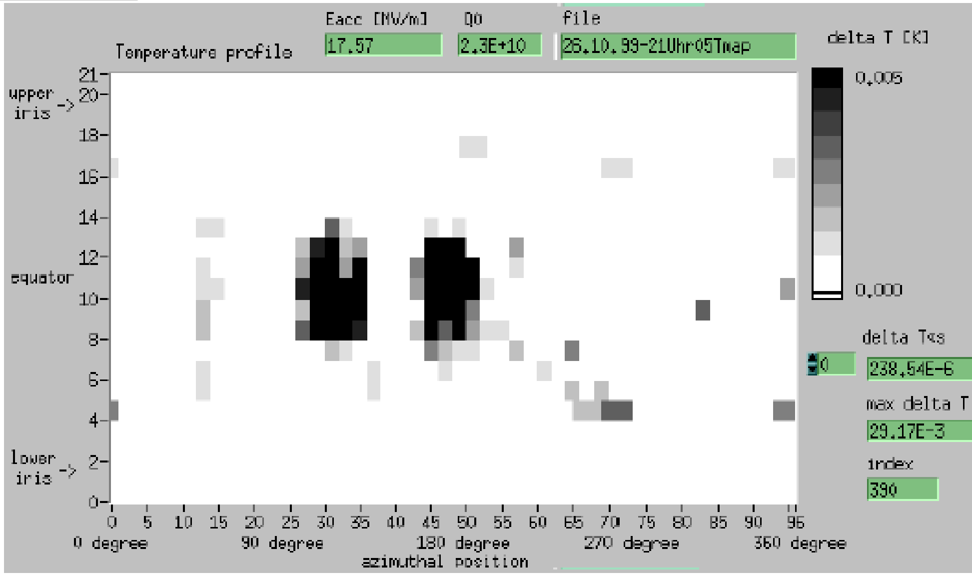

Empirical formula:

$$H_n\,[\mathrm{Oe}] = \frac{0.6}{2n-1}\, f_0\,[\mathrm{MHz}]$$

Two-Side Multipacting

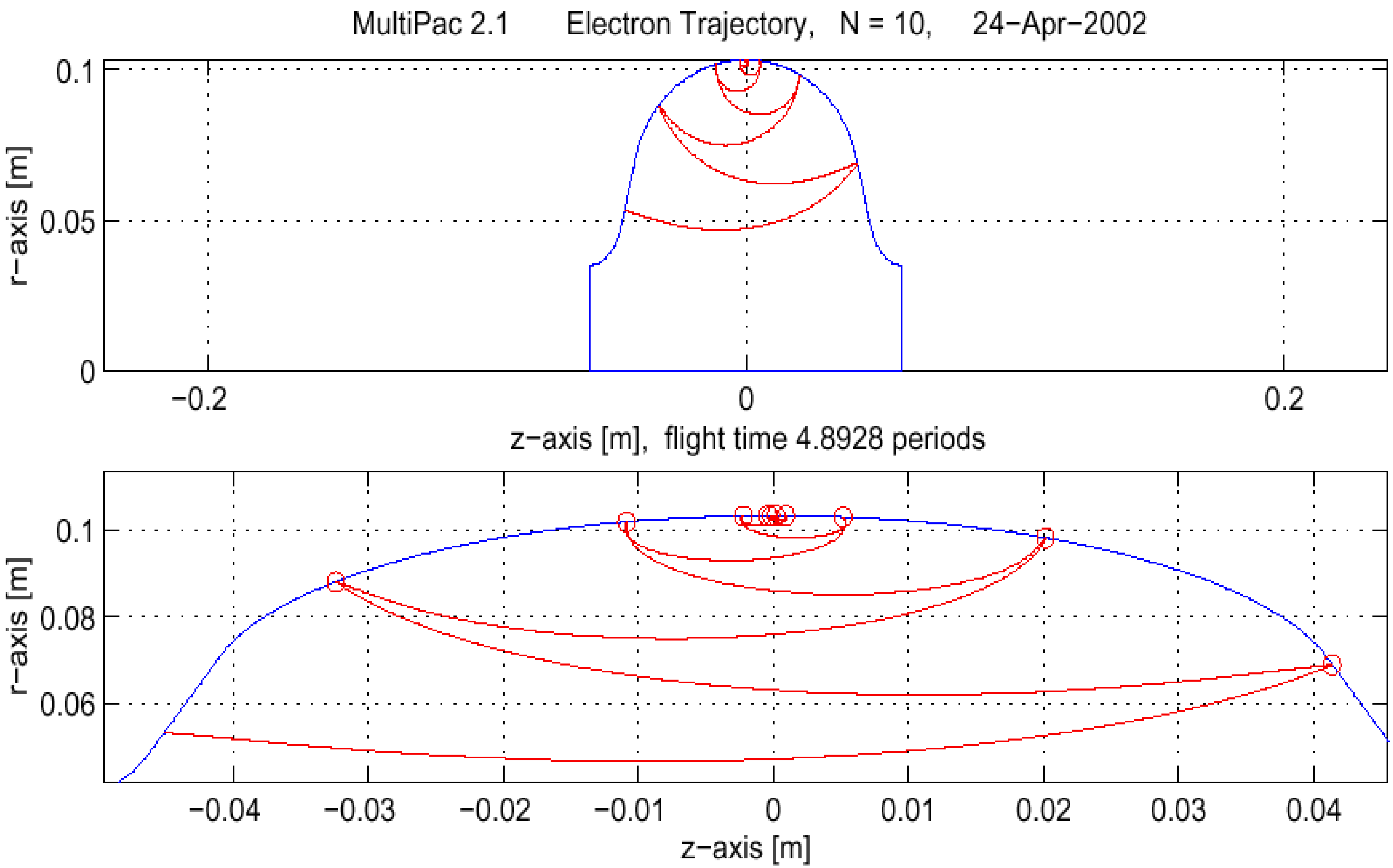

Secondary Emission in Niobium

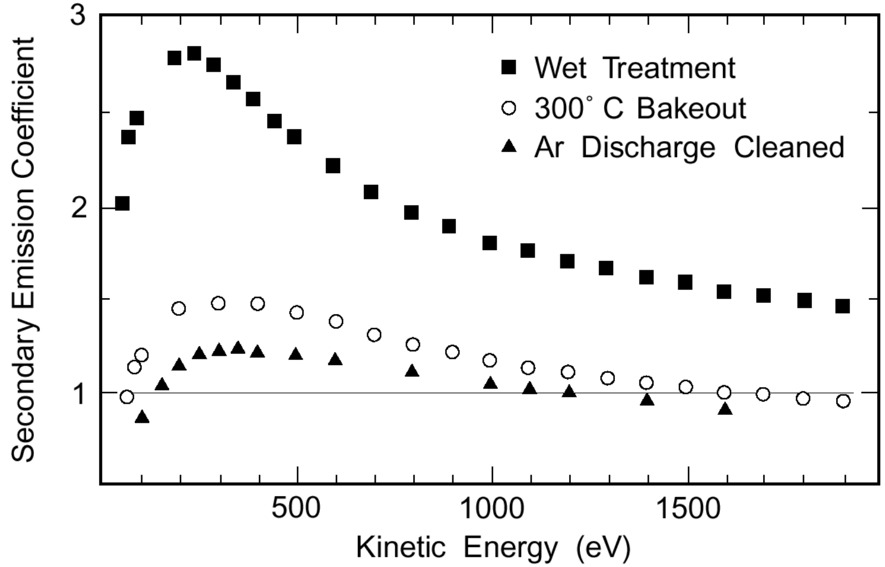

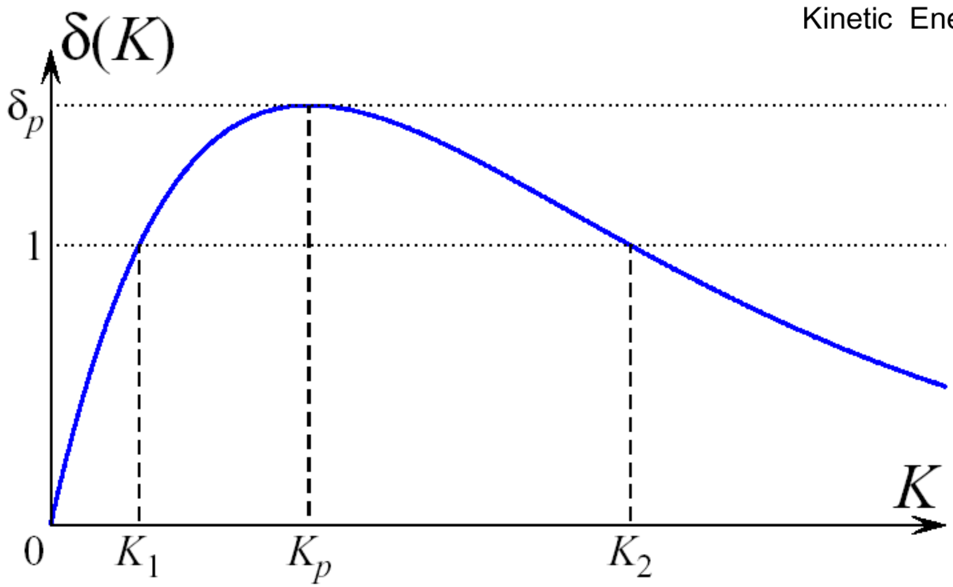

Condition	K_1	K_2
high SEY	$\sim$ 27 eV	$\gtrsim$ 2000 eV
typical SEY	$\sim$ 40 eV	$\sim$ 1000 eV
low SEY	$\sim$ 150 eV	$\sim$ 750 eV

MP in SRF Cavities

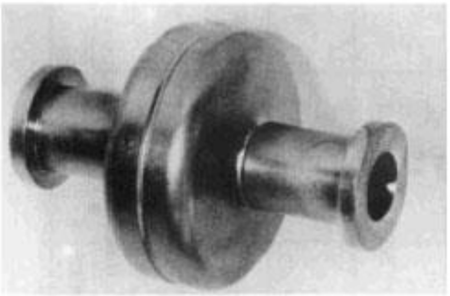
(a)

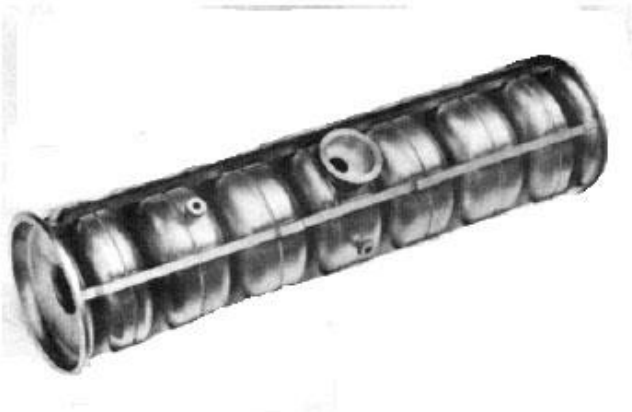
(b)

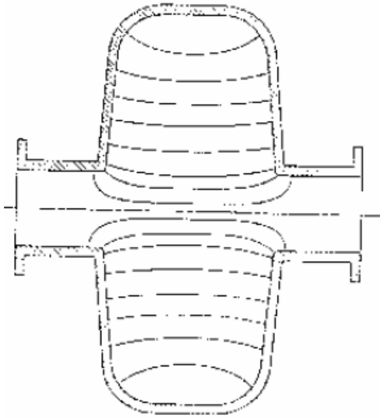
"Near pill-box" shape

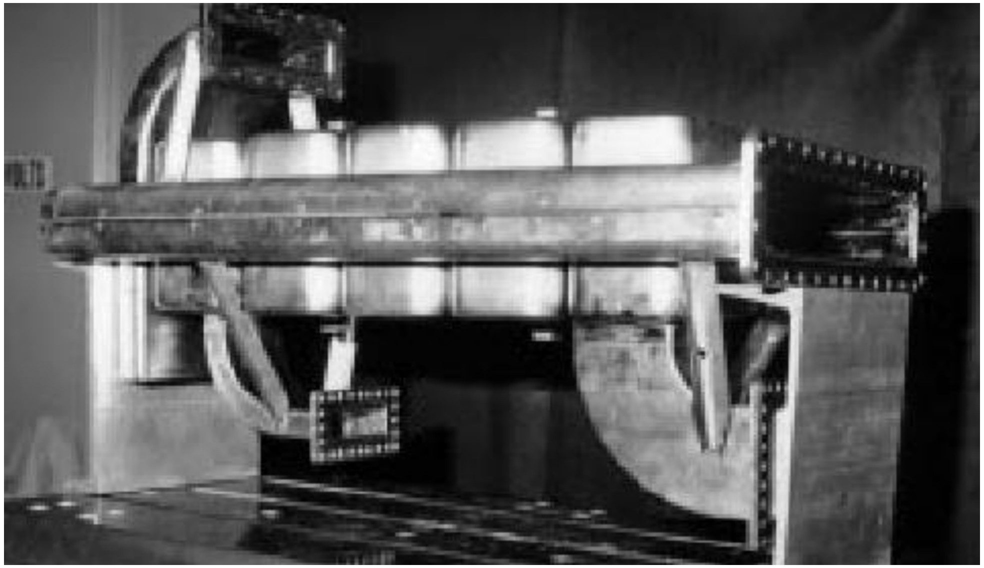

Early SRF cavity geometries (1960s-'70s) frequently limited by multipacting, usually at < 10 MV/m

MP in SRF Cavities

"Elliptical" cavity shape (1980s)

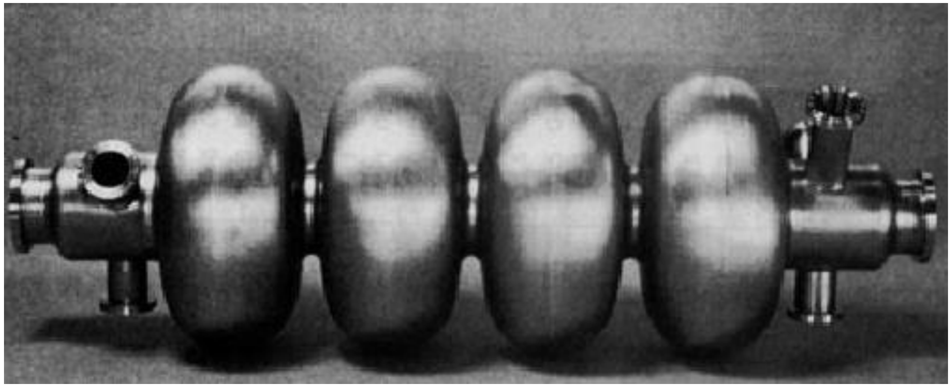

350-MHz LEP-II cavity (CERN)

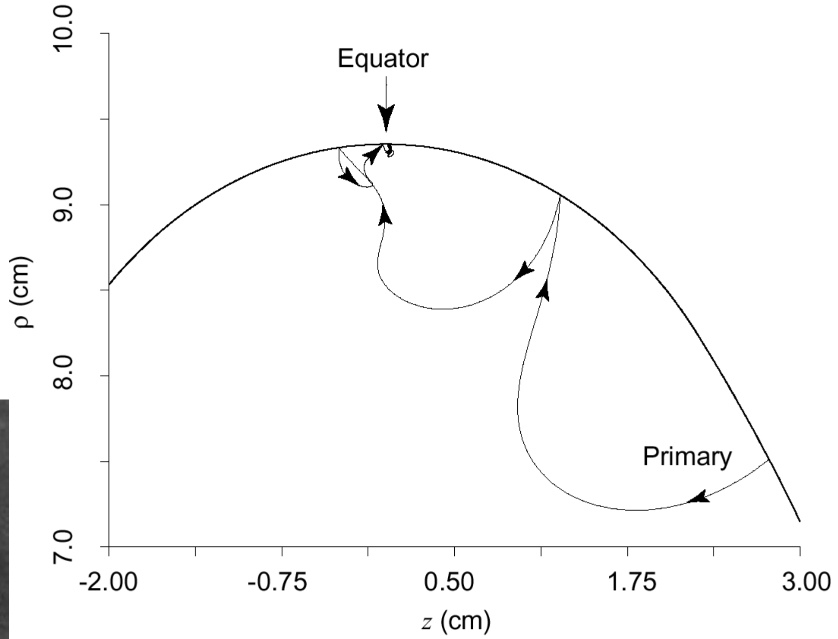

Electrons drift to equator
Electric field at equator is ≈ 0
→MP electrons don't gain energy
→MP stops

Cures for Multipacting

- Cavity design

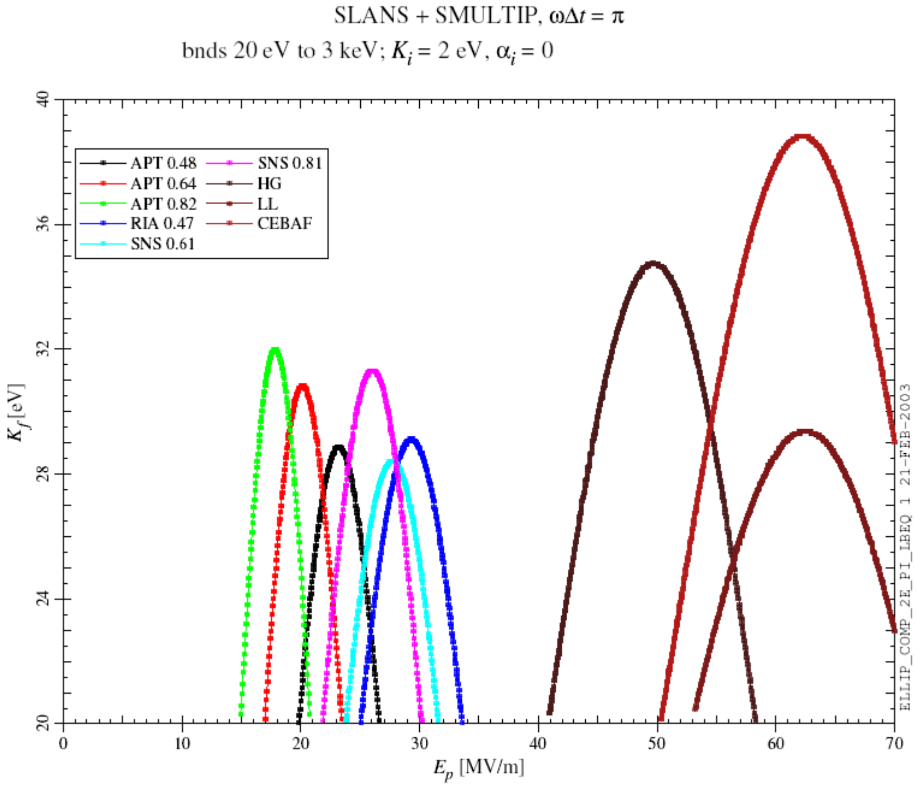

- Lower SEY: clean vacuum systems (low partial pressure of hydrocarbons, hydrogen and water), Ar discharge
- RF Processing: lower SEY by e^- bombardment (minutes to several hours)

Recent Examples of Multipacting

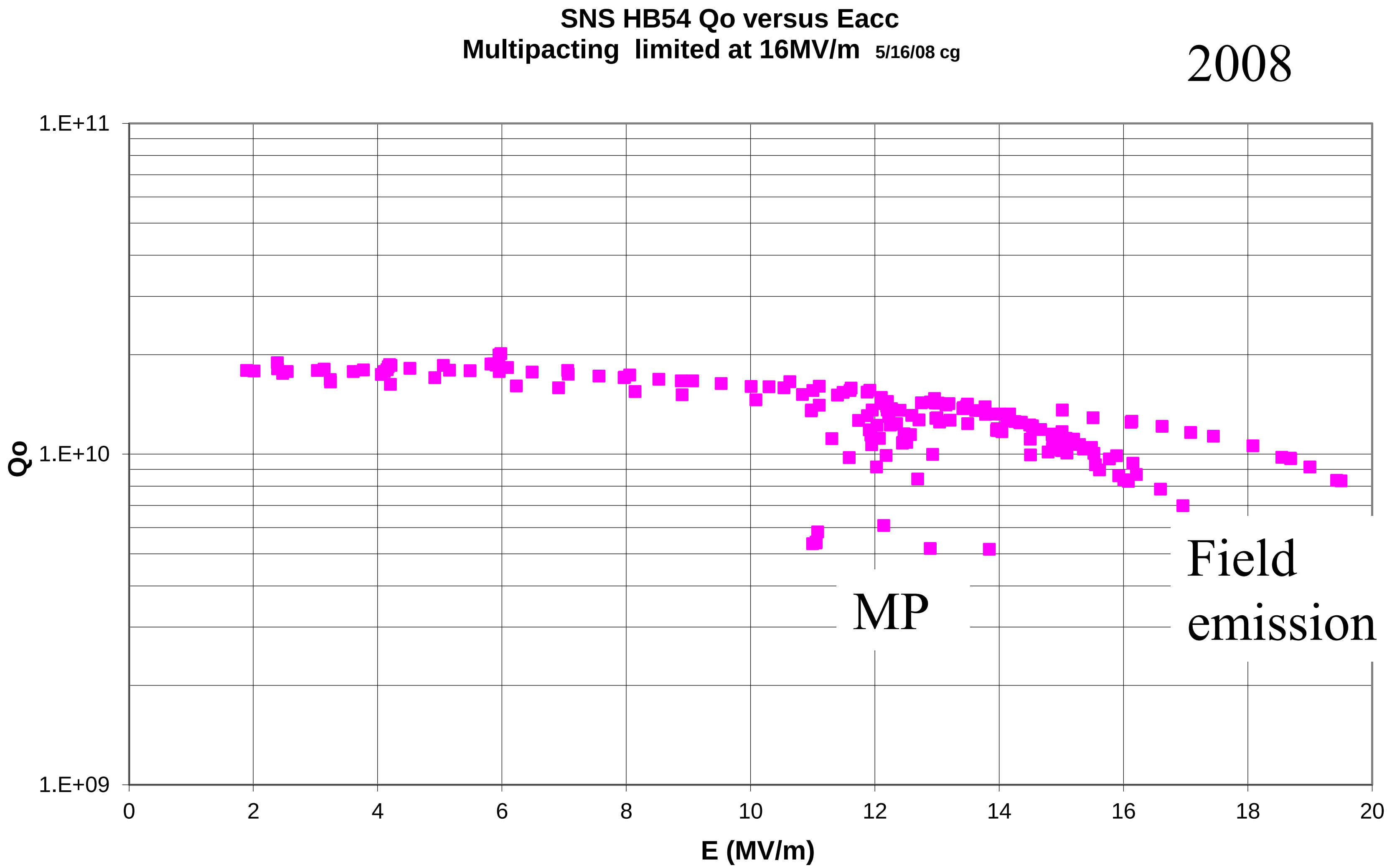

Field Emission

- Characterized by an exponential drop of the Q_0
- Associated with production of x-rays and emission of dark current

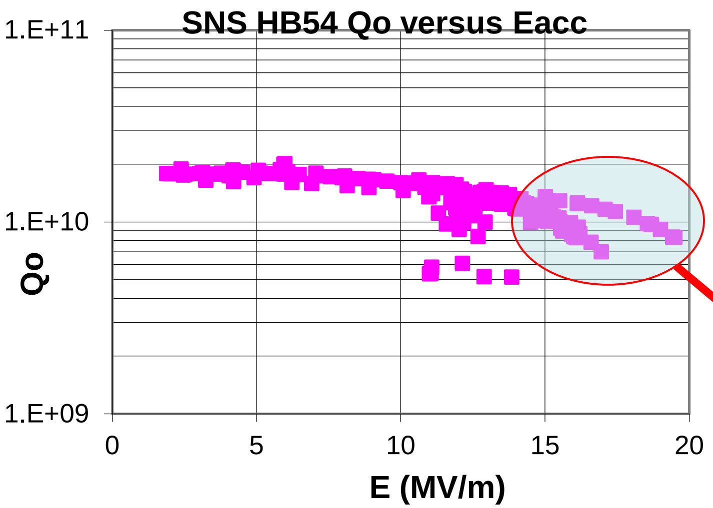

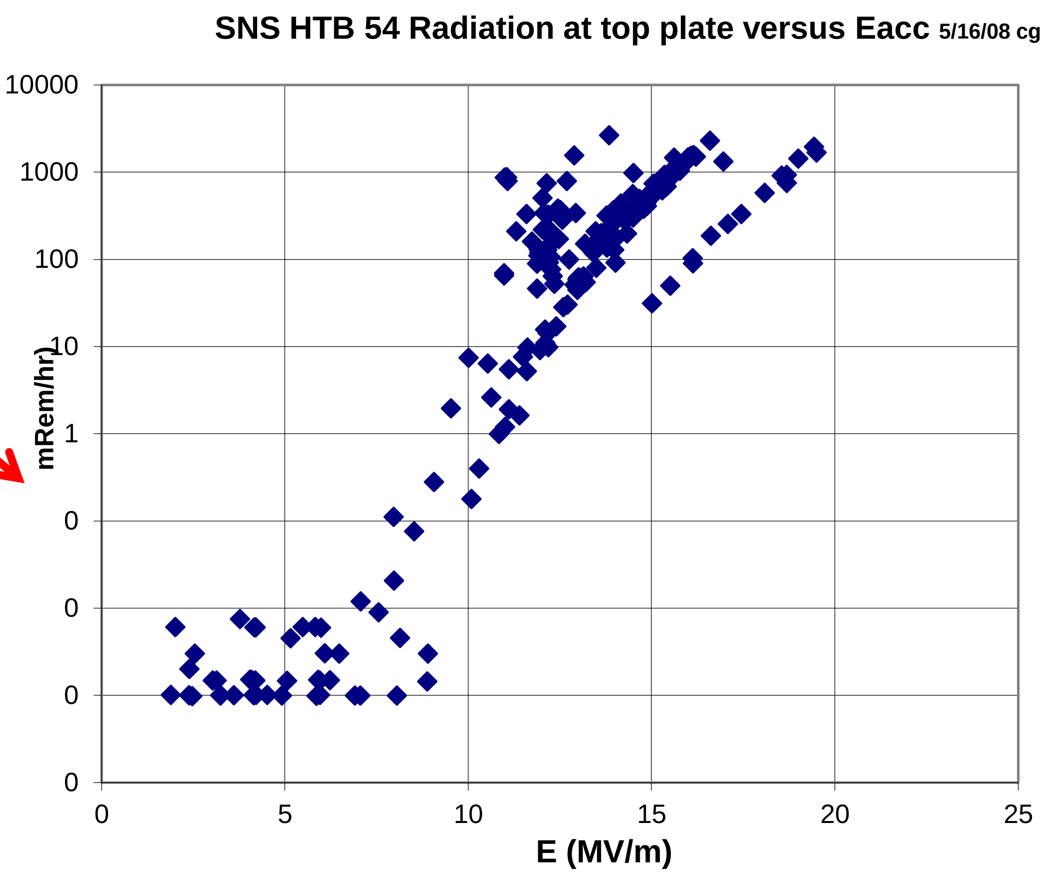

DC Field Emission from Ideal Surface

Fowler-Nordheim model

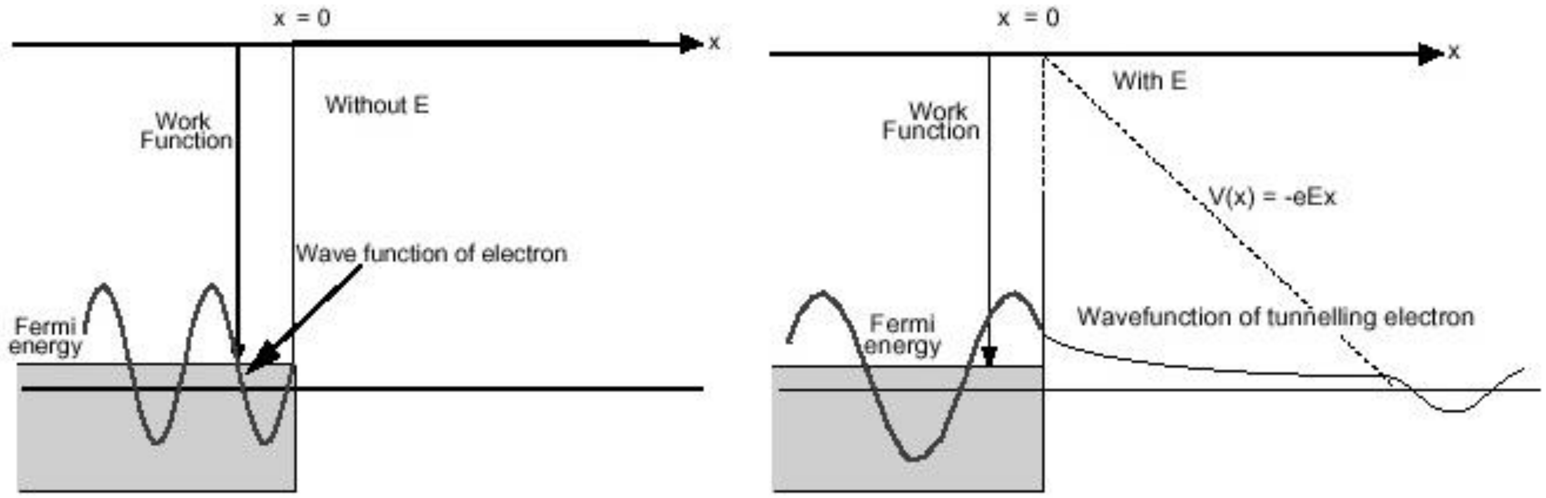

$$J = \frac{1.54 \times 10^6 E^2}{\Phi} e^{-6.83 \times 10^3 \Phi^{3/2}/E}$$

J: current density (A/m^2)
E: electric field (MV/m)
Φ: work function (eV)

Field Emission in RF Cavities

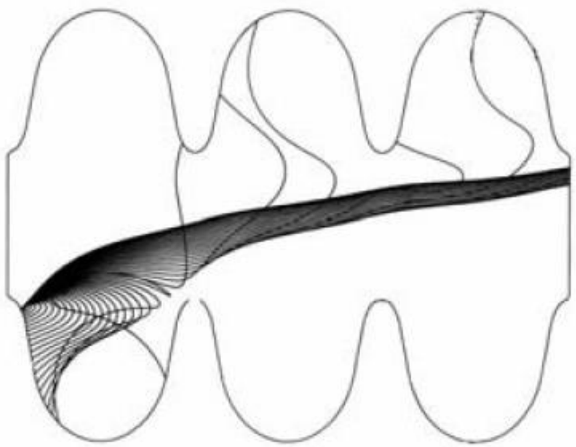

Acceleration of electrons drains cavity energy

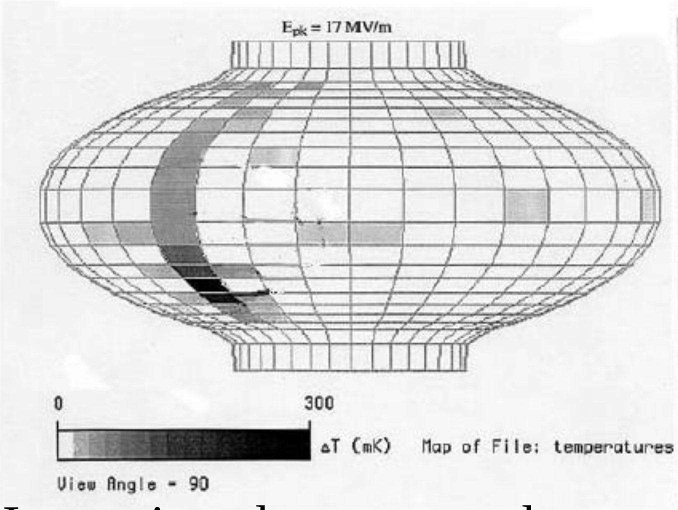

Impacting electrons produce:

- line heating detected by thermometry
- bremsstrahlung X rays

Foreign particulate found at emission site

Intensity of x-rays and field emission current is many orders of magnitude higher than predicted by FN theory…

$$J = \boldsymbol{k}\,\frac{1.54\times 10^{6}(\boldsymbol{\beta} E)^{5/2}}{\Phi}\,e^{-6.83\times 10^{3}\Phi^{3/2}/\boldsymbol{\beta} E}$$

β: enhancement factor (10s to 100s)
k: effective emitting surface

How to Investigate Field Emission

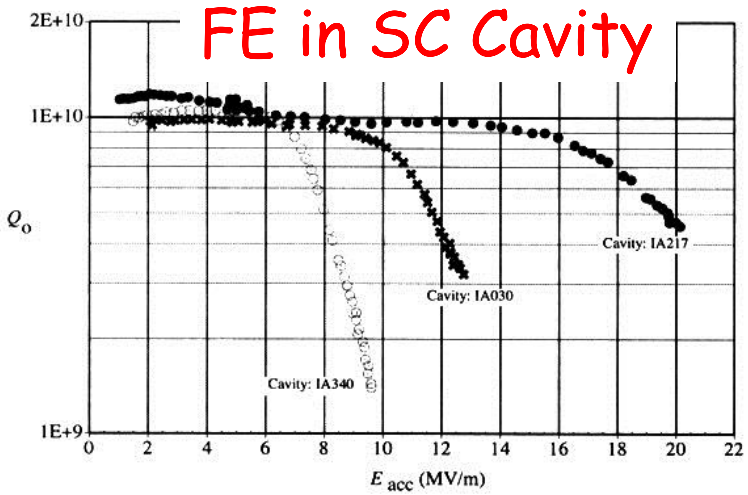

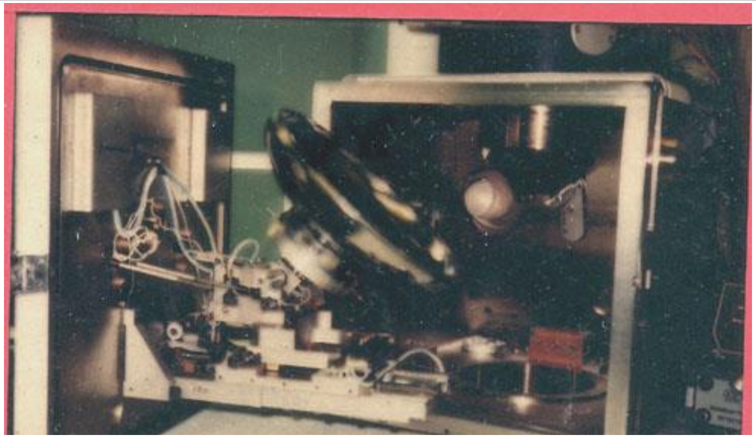

Dissection and analysis

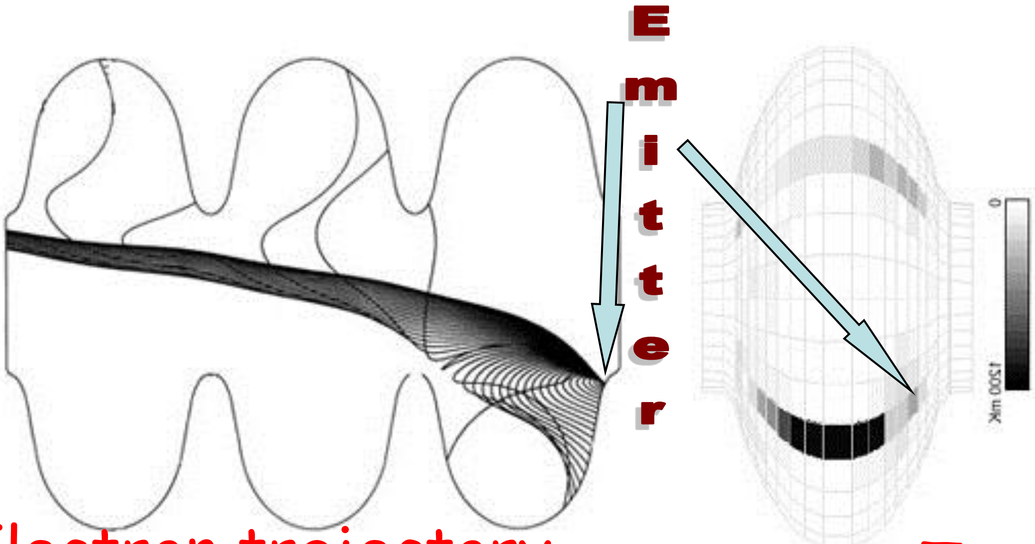

Electron trajectory

T-map

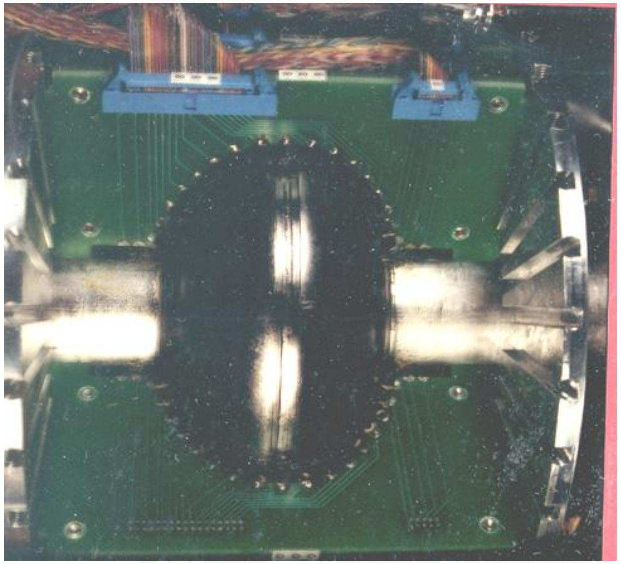

Dissection and SEM

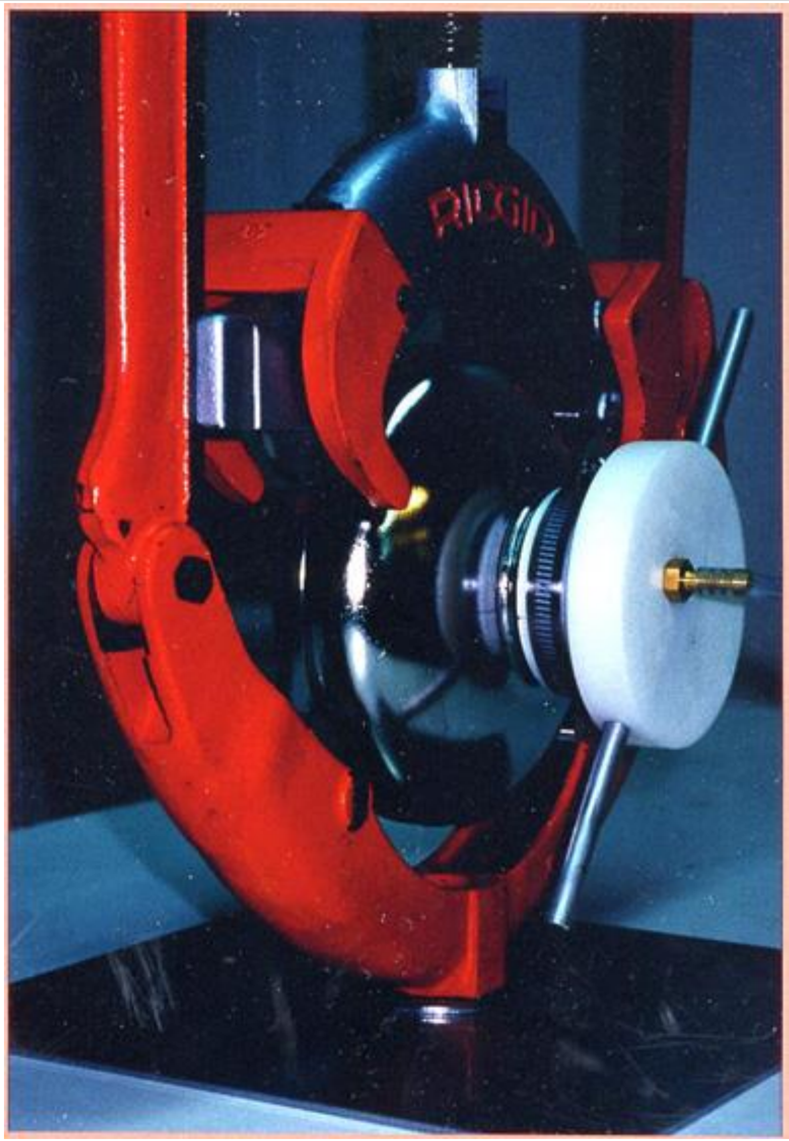

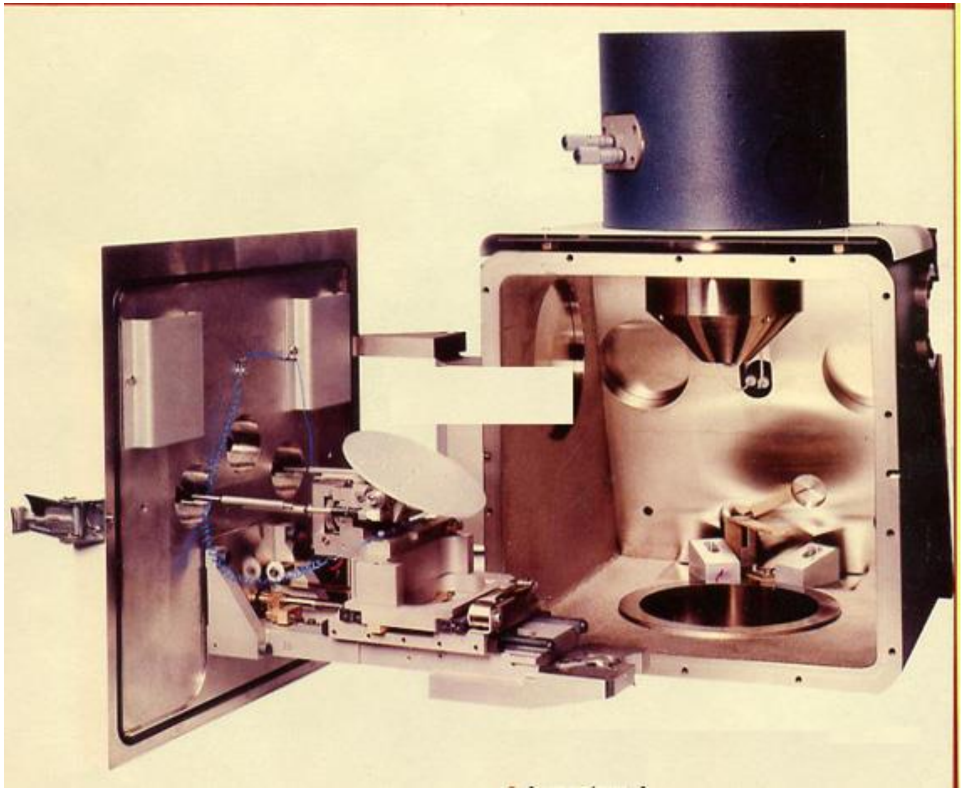

Example of Field Emitters

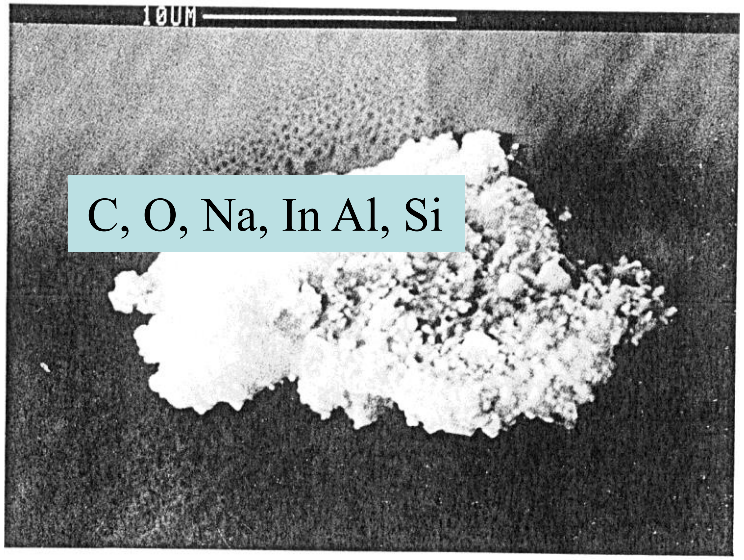

Stainless steel

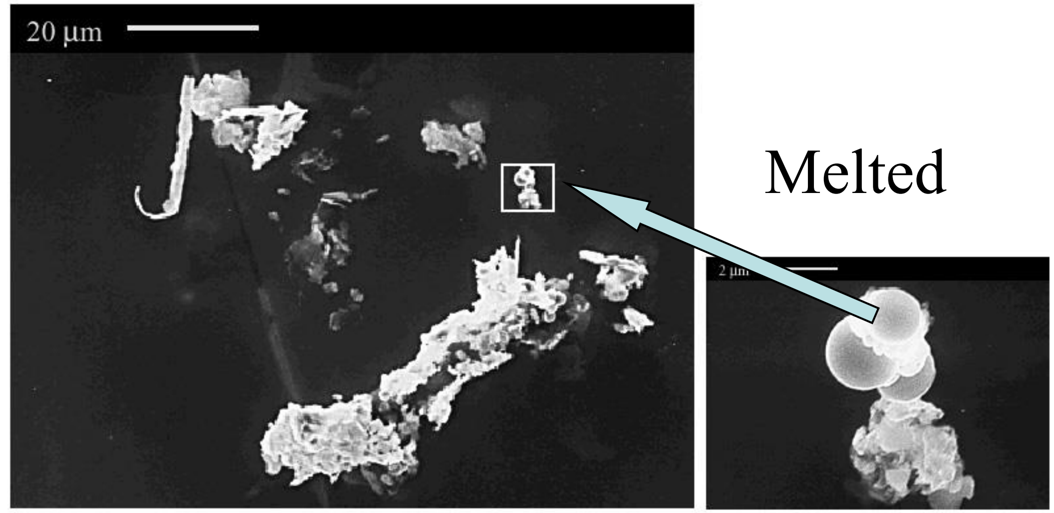

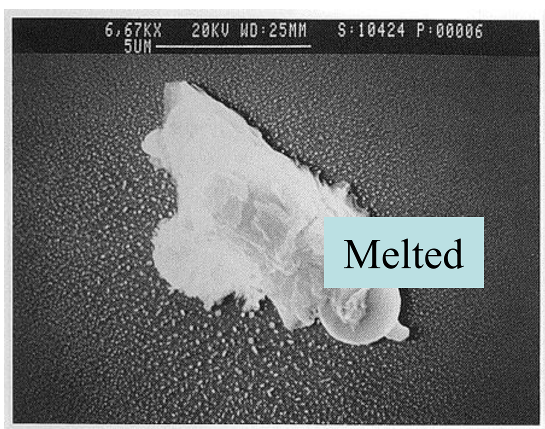

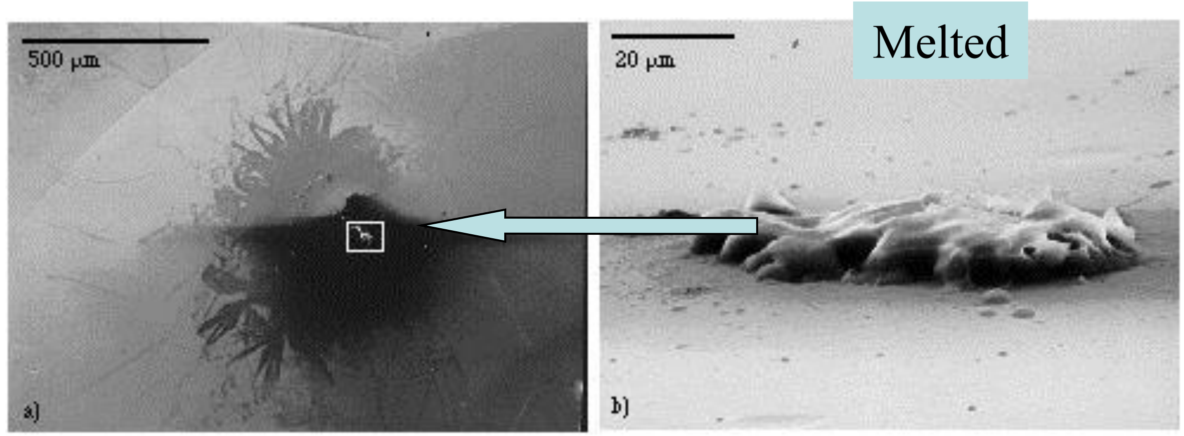

DC Field Emission Microscope

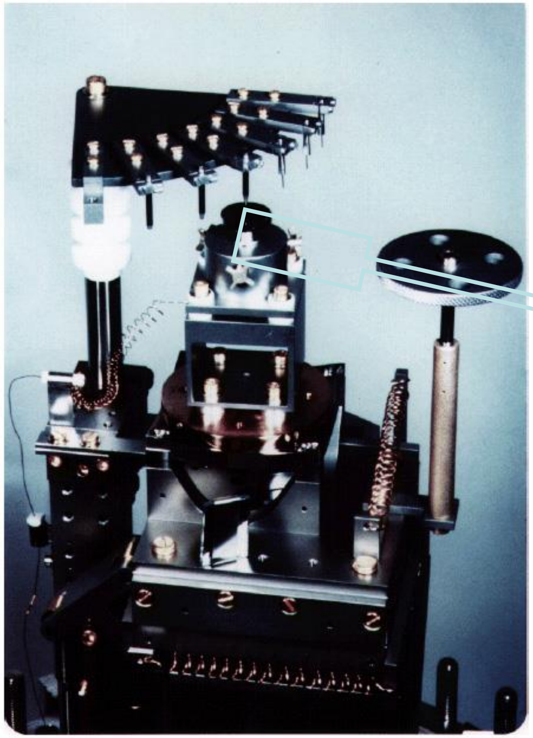

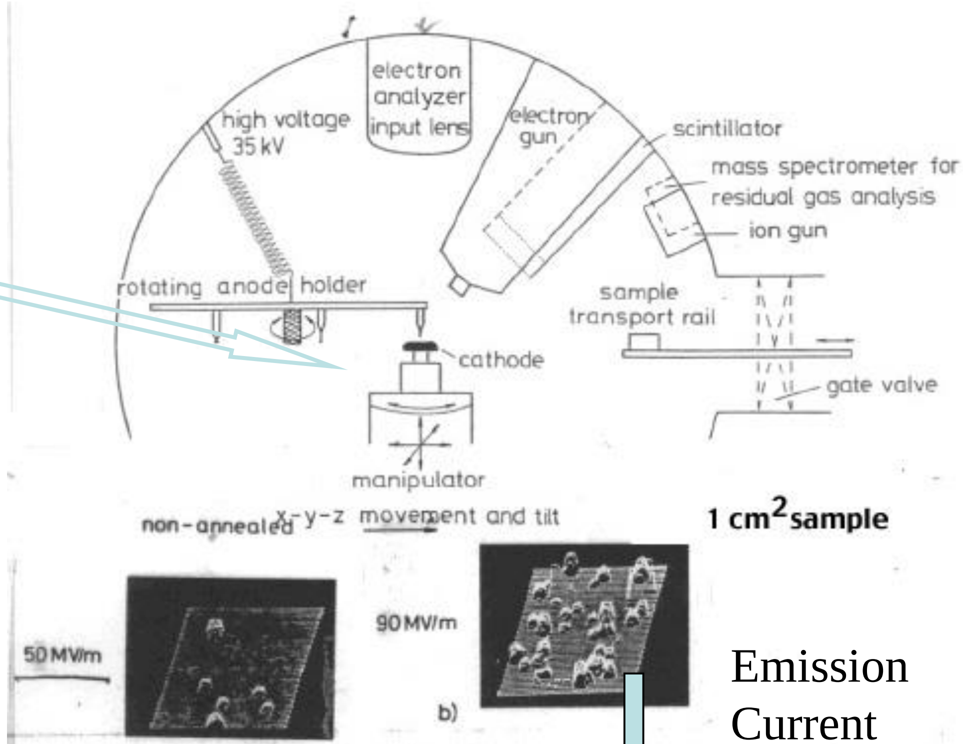

Emission Current

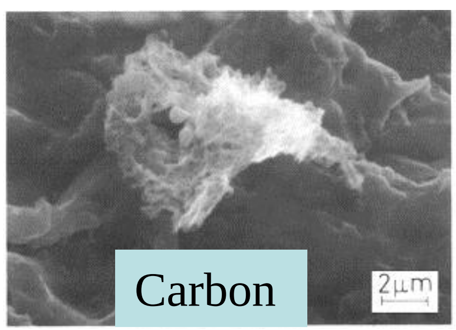

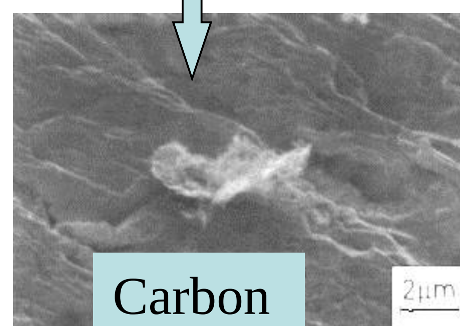

Type of Emitters

V

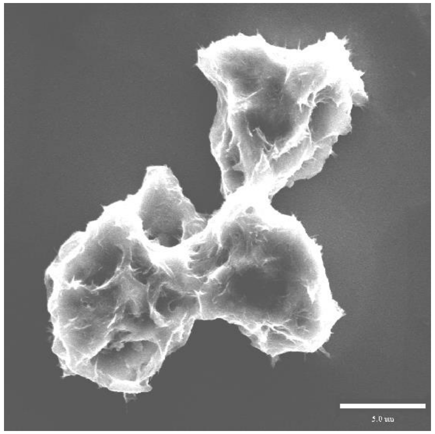

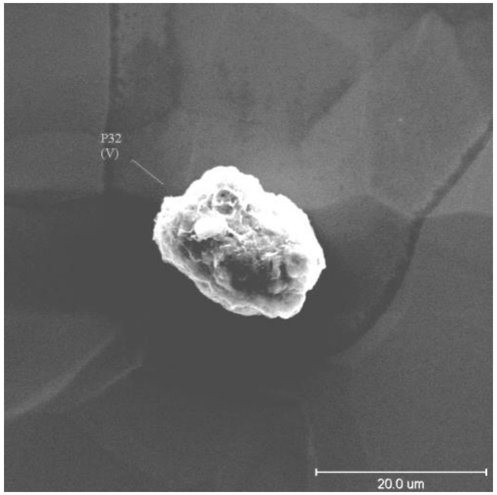

•*Tip-on-tip* model can explain why only 10% of particles are emitters for Epk < 200 MV/m.

Ni

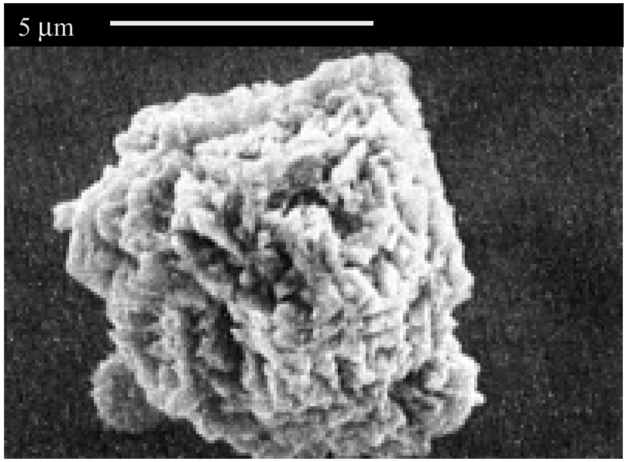

Smooth nickel particles emit less or emit at higher fields.

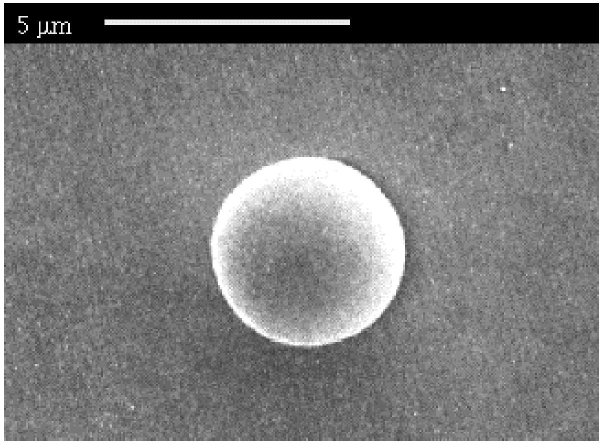

Tip-on-tip Model

- Smooth particles show little field emission
- Simple protrusions are not sufficient to explain the measured enhancement factors
- Possible explanation: tip-on-tip (compounded enhancement)

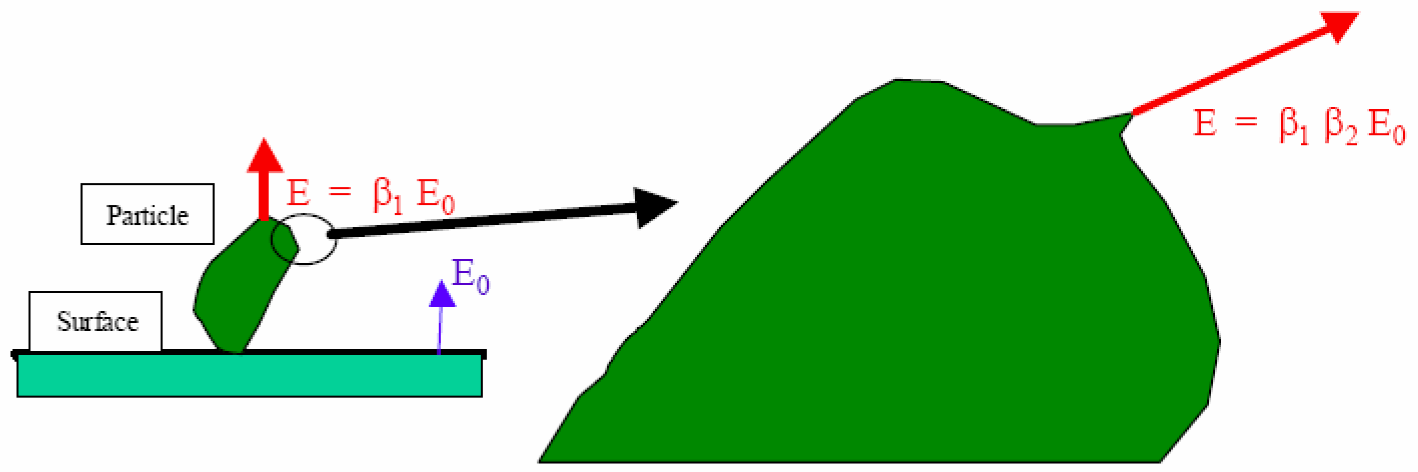

FE onset vs. Particulate Size

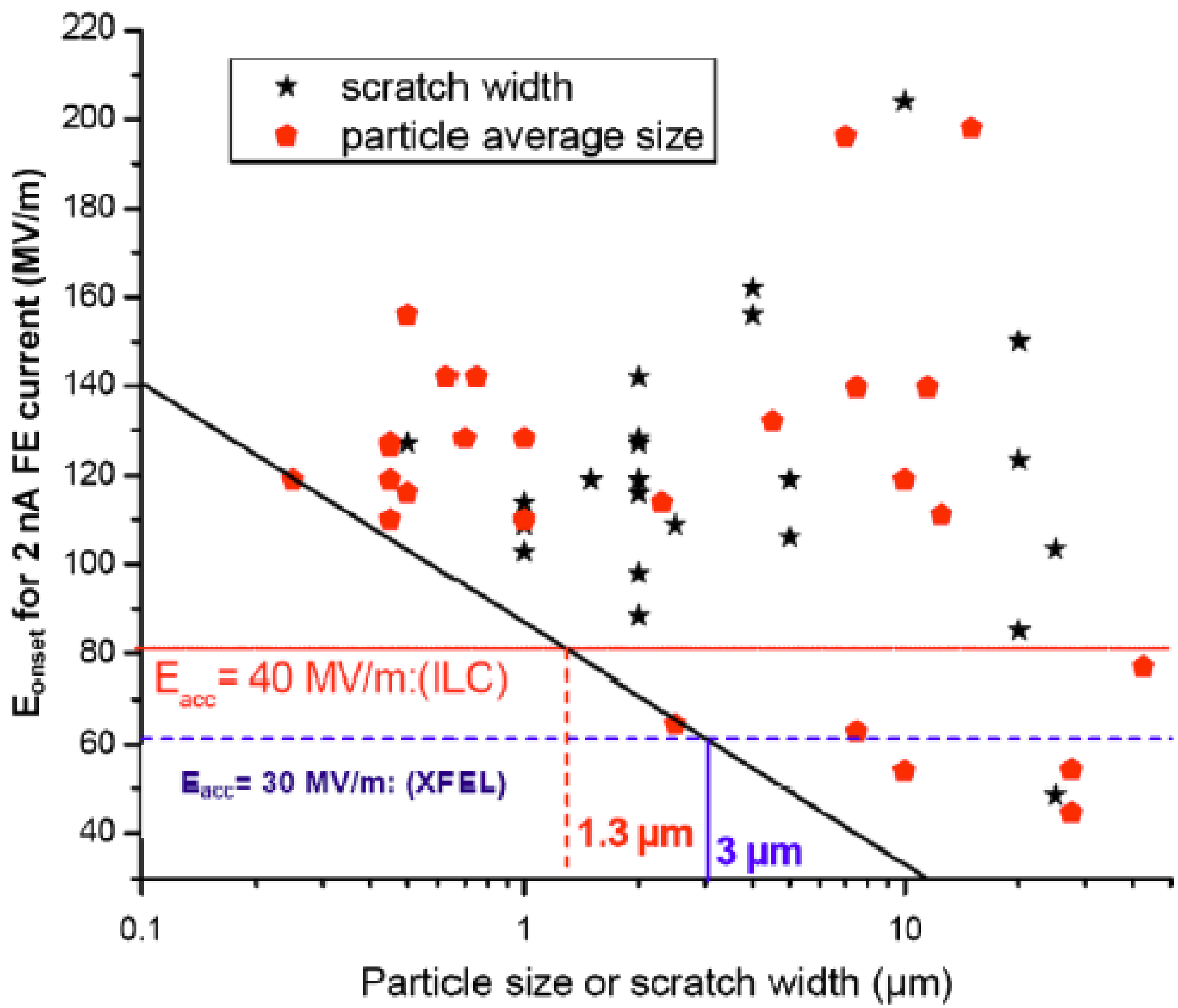

Enhancement by Absorbates

Adsorbed atoms on the surface can enhance the tunneling of electrons from the metal and increase field emission

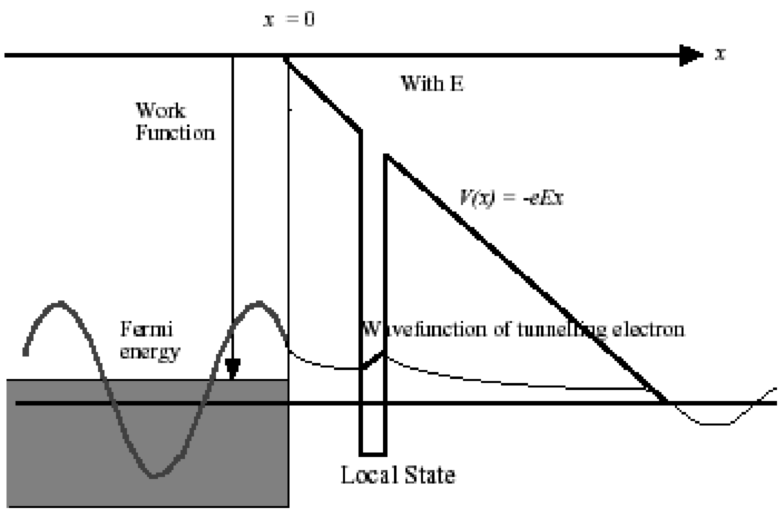

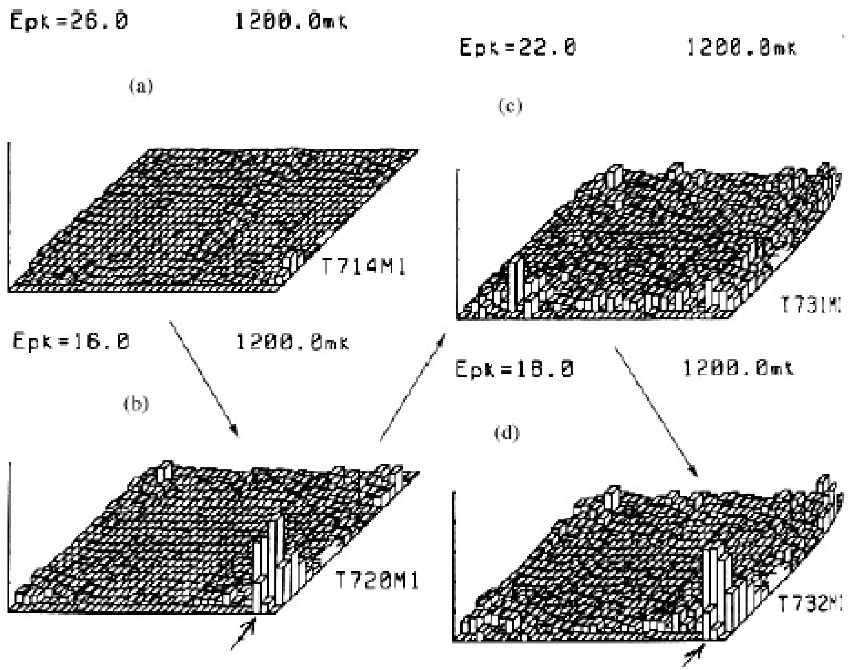

Intrinsic FE of Nb

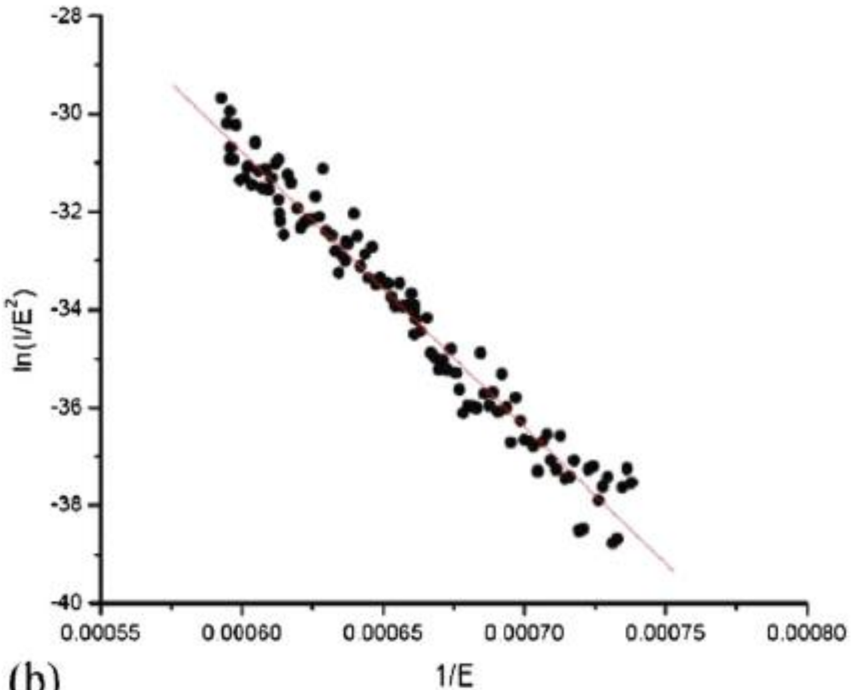

(b)

Single-crystal Nb samples showed FE onset higher than 1 GV/m.

The work function was obtained from the I-V curves:

Φ = 4.05 ± 17% eV for Nb (111)
Φ = 3.76 ± 27% eV for Nb (100)

Cures for Field Emission

- **Prevention:**
  - Semiconductor grade acids and solvents
  - High-Pressure Rinsing with ultra-pure water
  - Clean-room assembly
  - Simplified procedures and components for assembly
  - Clean vacuum systems (evacuation and venting without re-contamination)

- **Post-processing:**
  - Helium processing
  - High Peak Power (HPP) processing

Helium Processing

- Helium gas is introduced in the cavity at a pressure just below breakdown (~10^{-5} torr)
- Cavity is operating at the highest field possible (in heavy field emission regime)
- Duty cycle is adjusted to remain thermally stable
- Field emitted electrons ionized helium gas
- Helium ions stream back to emitting site
    - Cleans surface contamination
    - Sputters sharp protrusions

Helium Processing

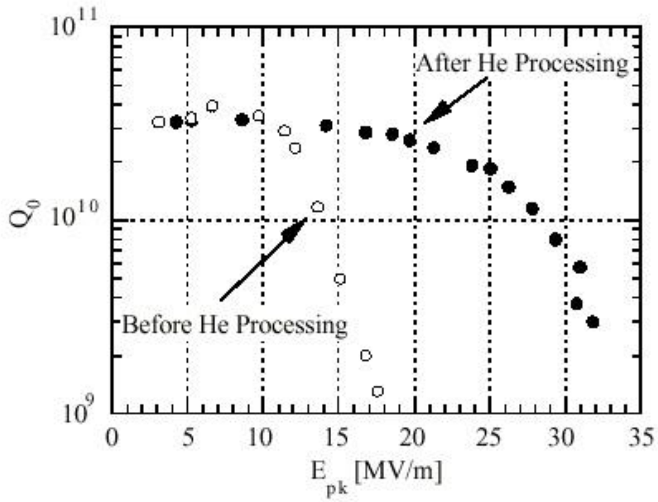

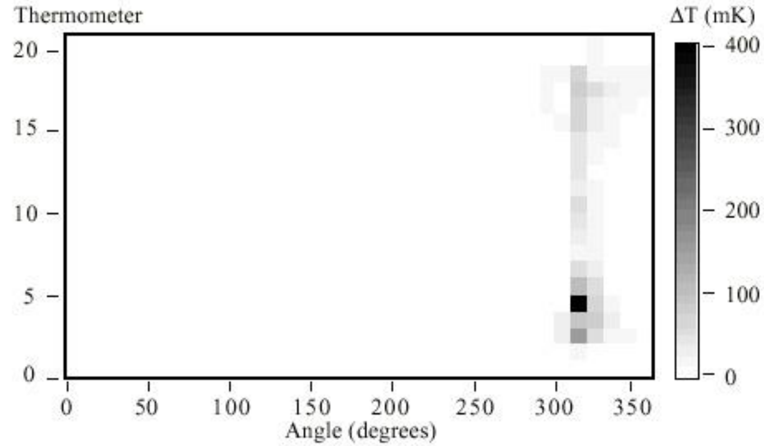

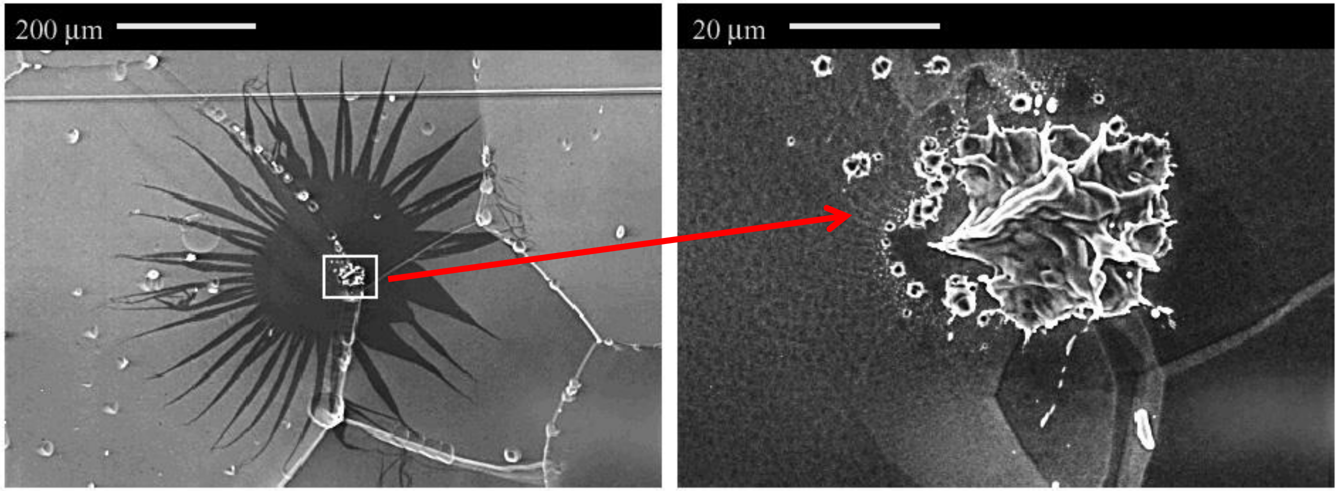

Helium Processing

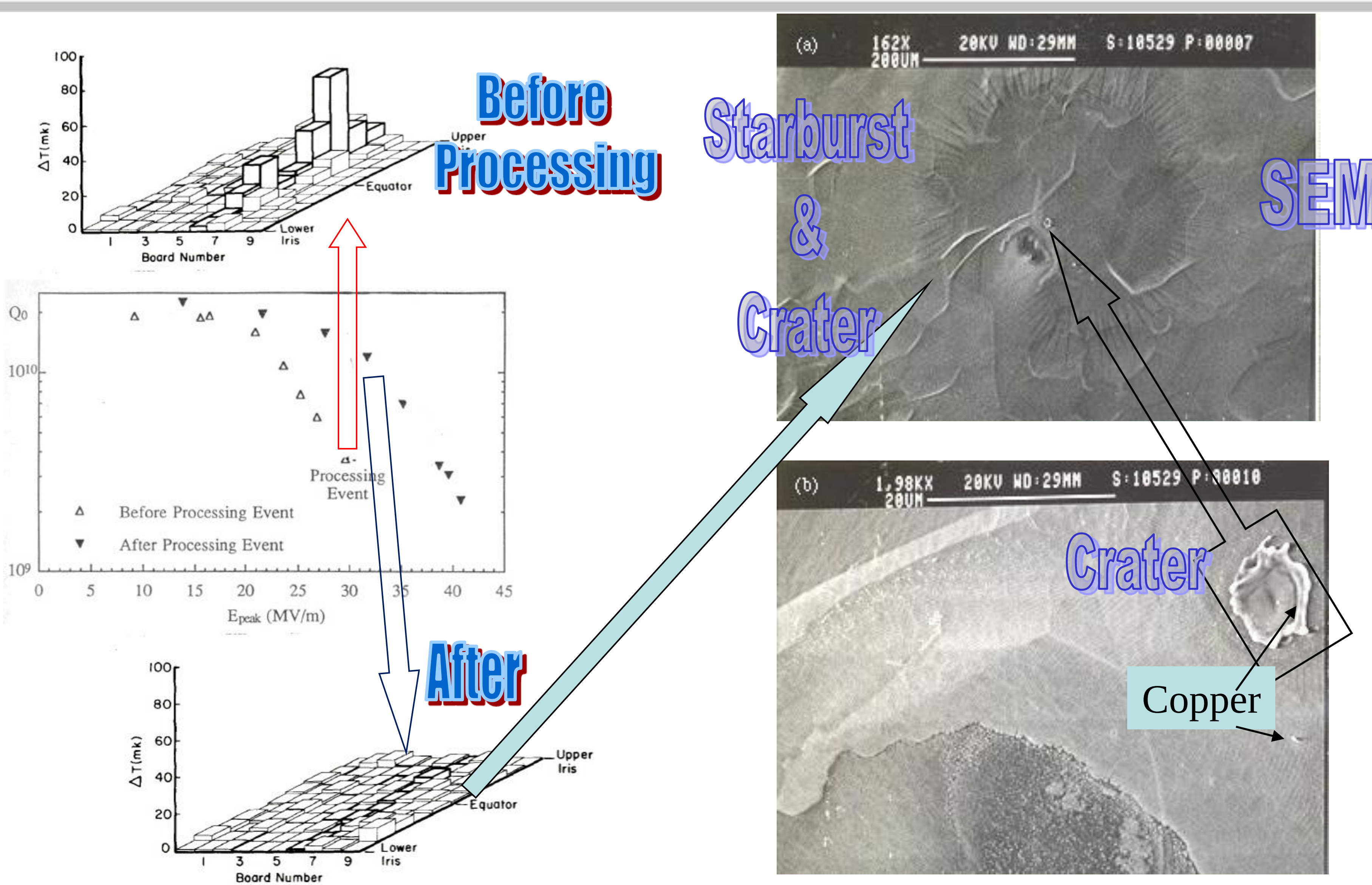

Helium Processing in CEBAF

Improvement of Cavity Performance with Helium Processing

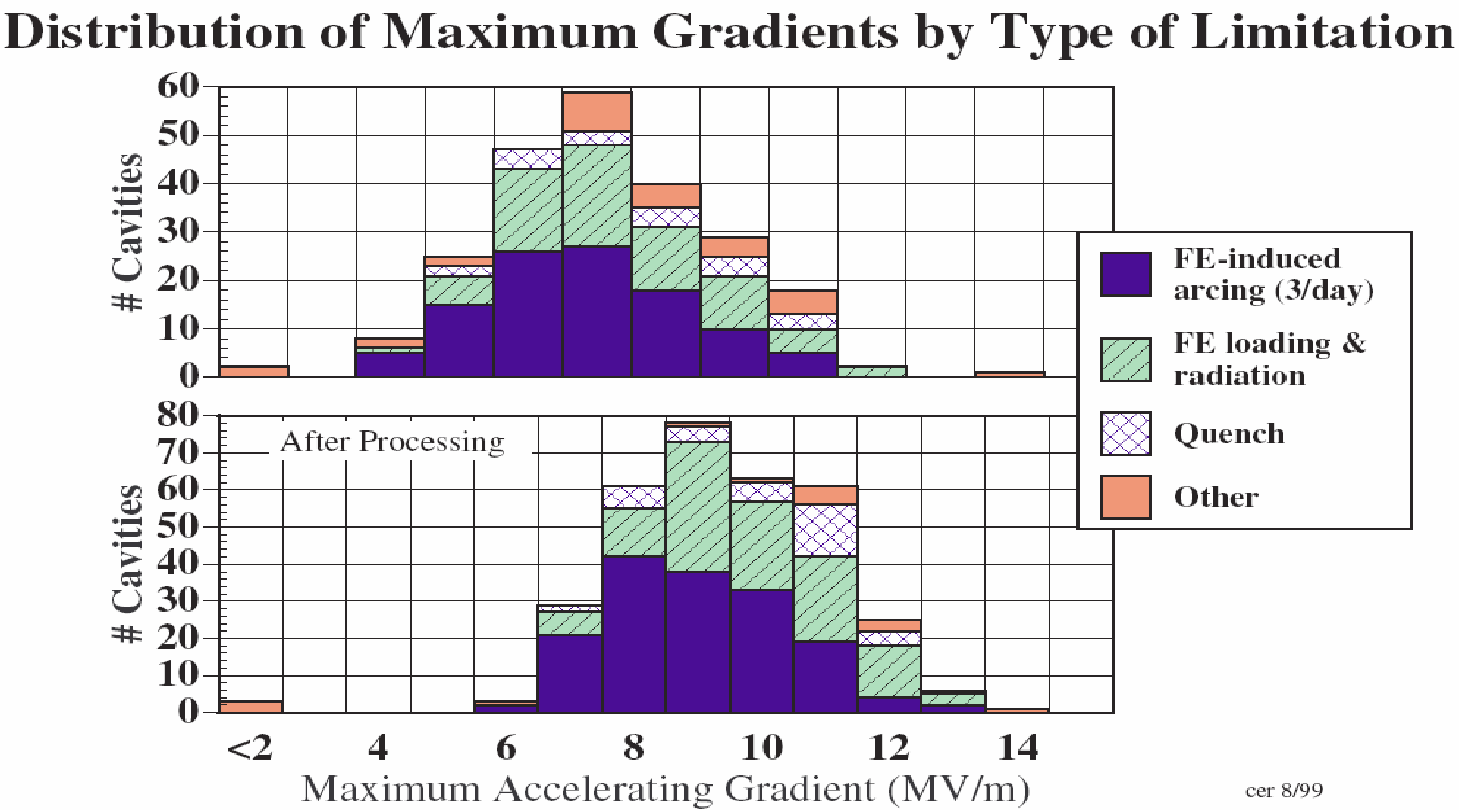

Helium Processing in CEBAF

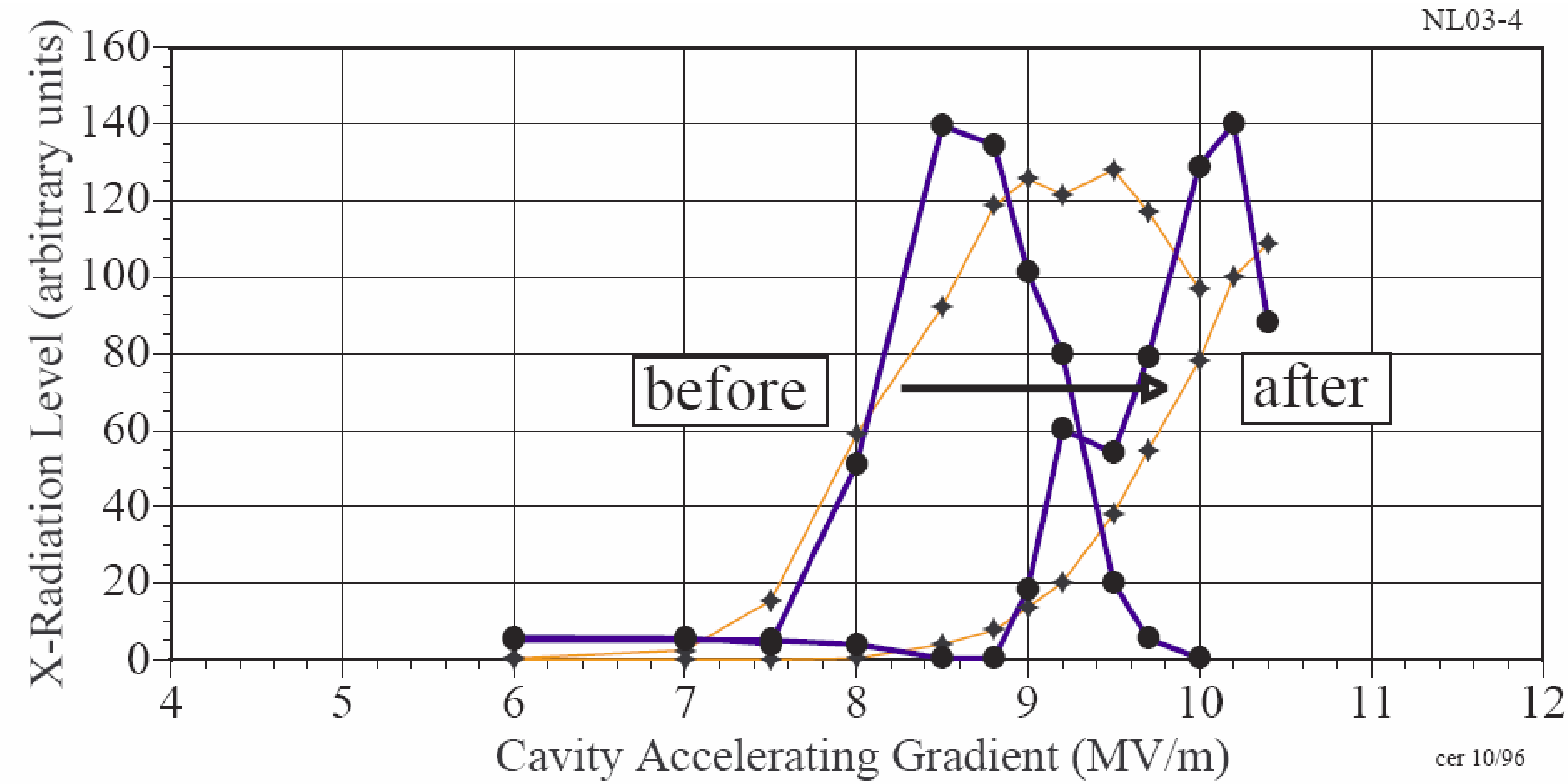

Figure 1. Radiation reduction with He processing.

Practical Limitations (CEBAF)

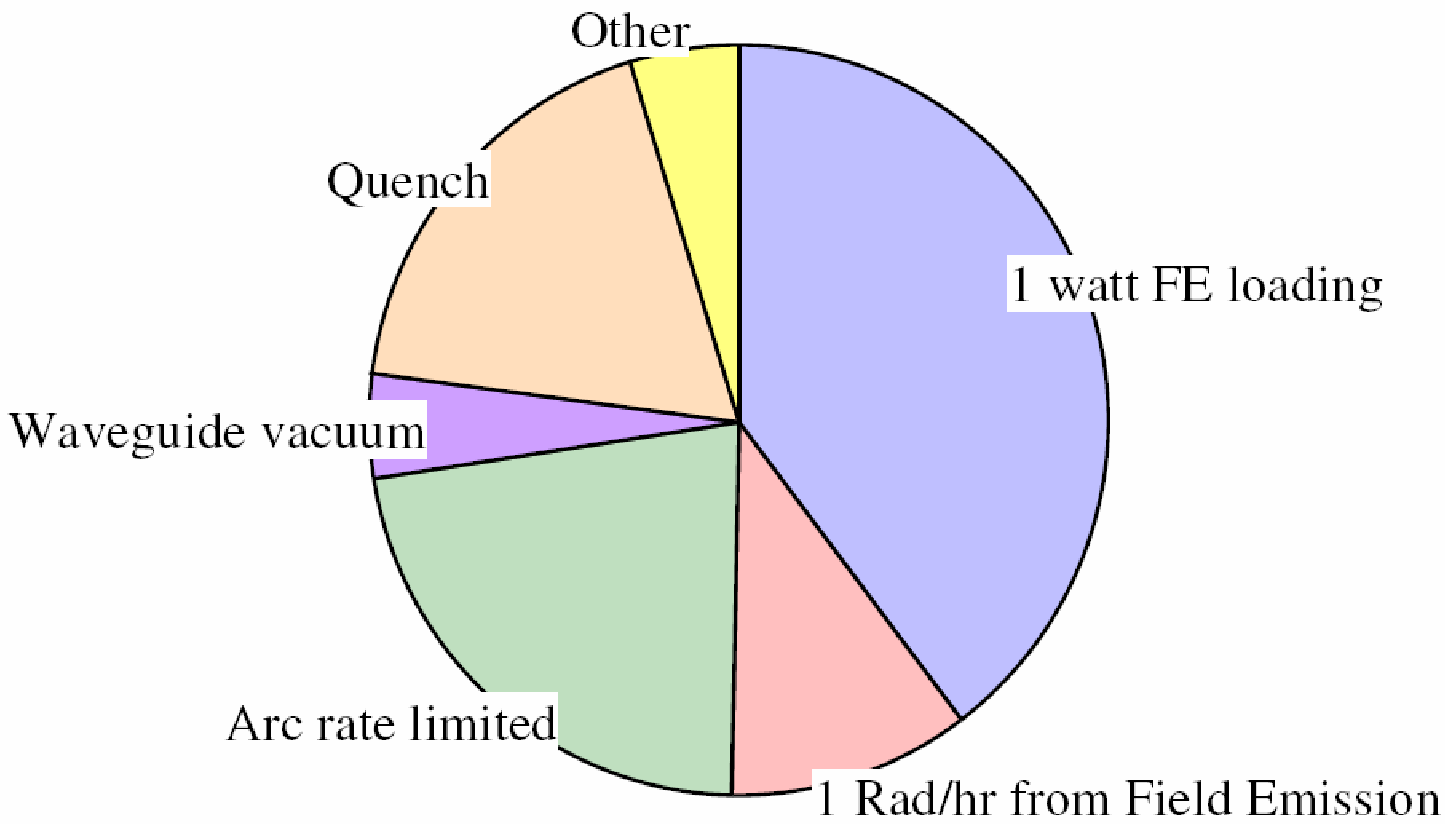

High Peak Power Processing

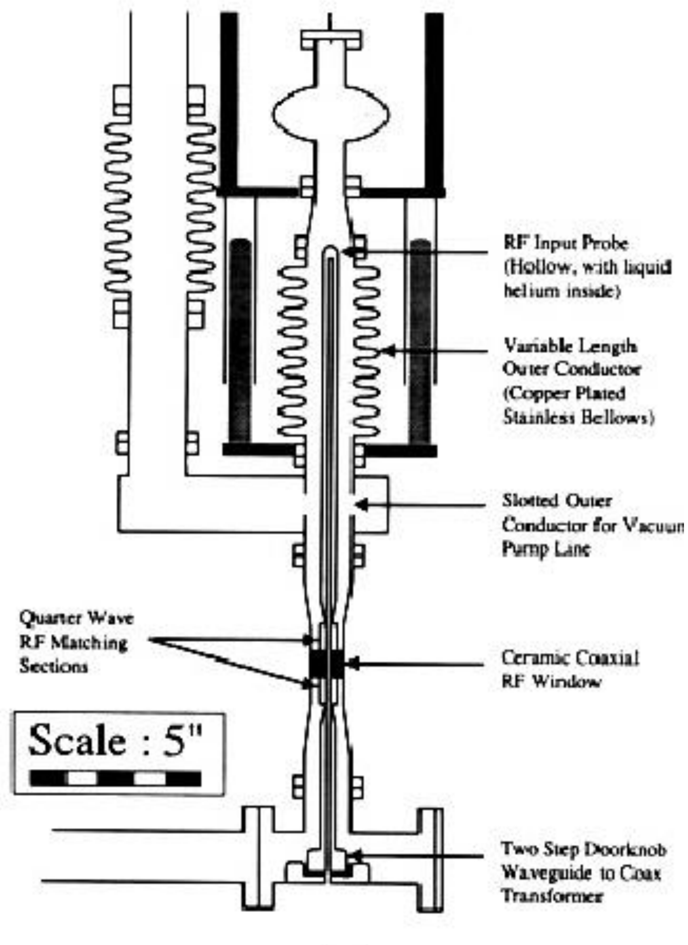

Power = 1.5 MW
Pulse Length = 250 us

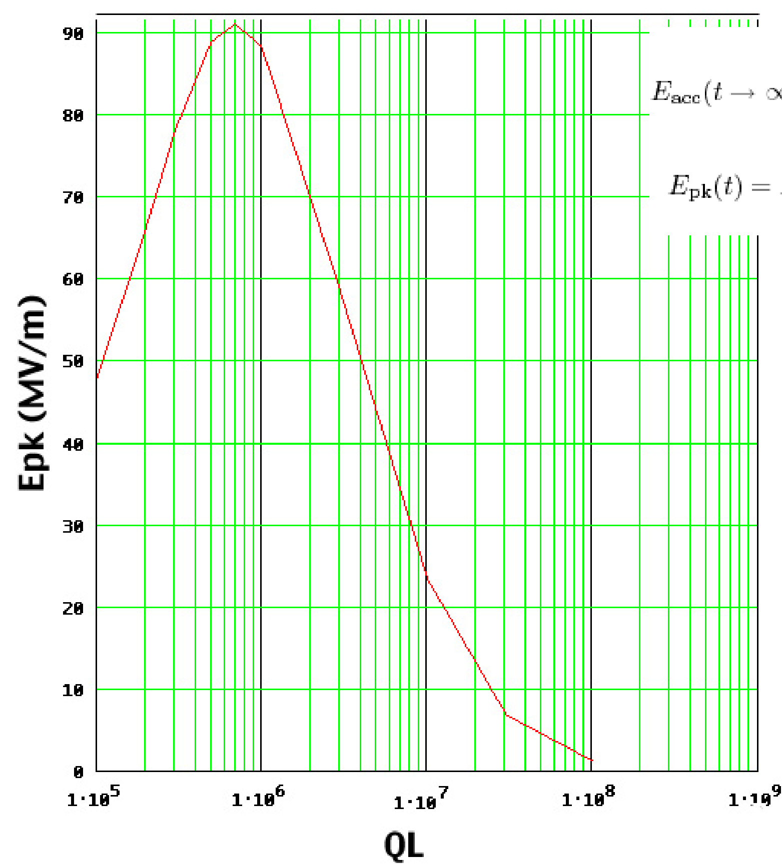

$$E_{\mathrm{acc}}(t \to \infty) = \sqrt{\frac{4\beta P_{\mathrm{g}}(r_{\mathrm{a}}/Q_0)Q_0}{(1+\beta)^2 L}},$$

$$E_{\mathrm{pk}}(t) = E_{\mathrm{pk}}\left[1 - \exp\left(\frac{-t}{2\tau_{\mathrm{L}}}\right)\right],$$

$$Q_L = \omega\ \tau_L$$

$$\beta = \frac{Q_0}{Q_L}$$

High Peak Power Processing

5-cell 1.3 GHz cavities
High Pulse Power Processing
with one MW

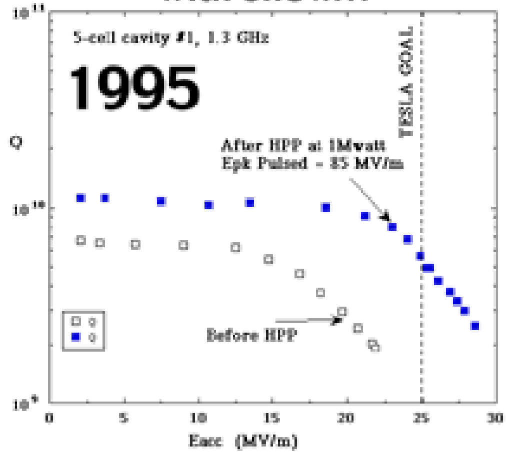

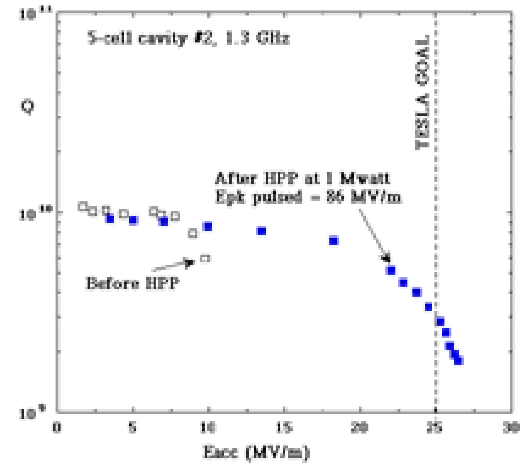

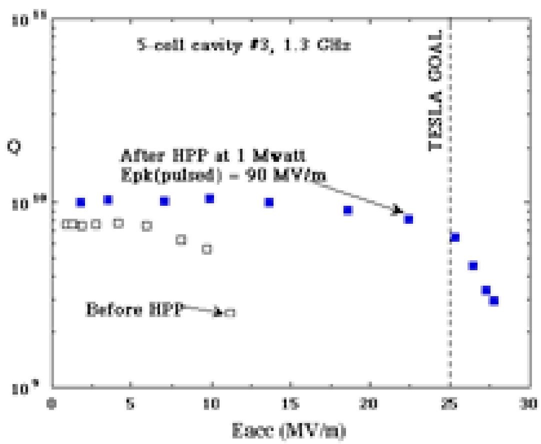

local melting leads to formation of a plasma and finally to the explosion of the emitter
→ "star bursts" caused by the plasma

High Peak Power Processing

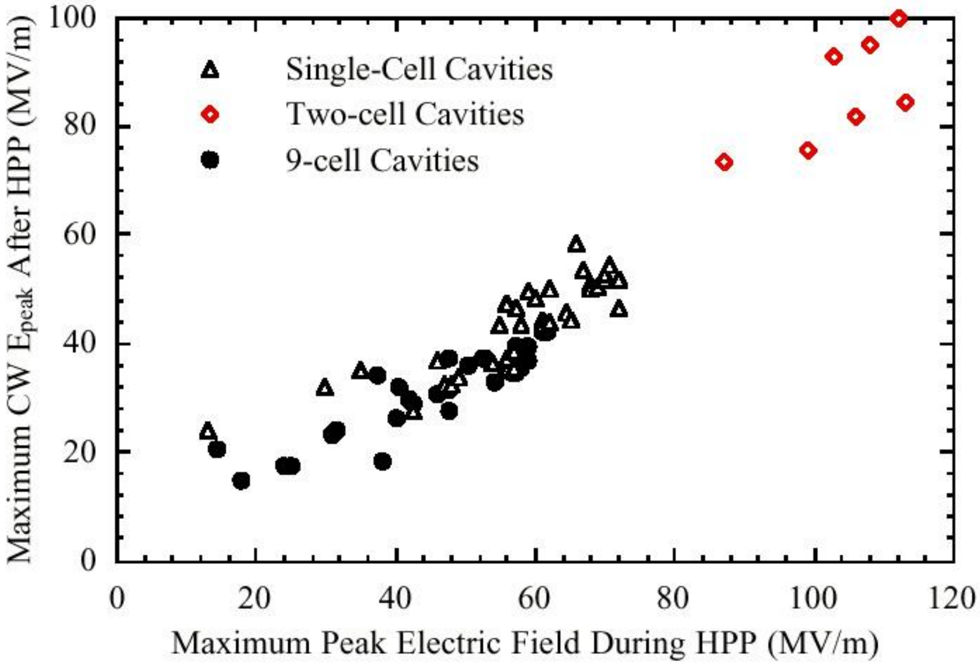

For field emission free

E_p (pulsed) = 2×E_p (cw)

High Peak Power Processing

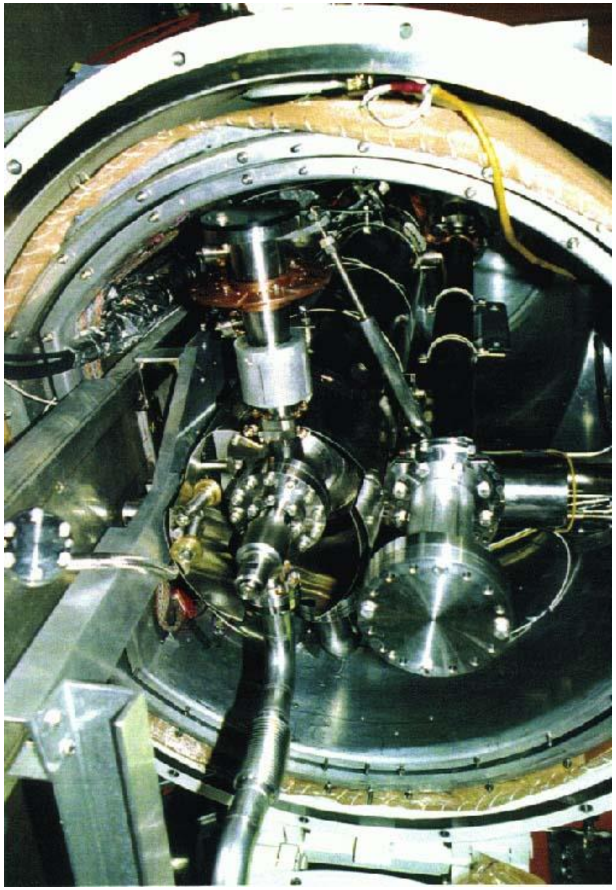

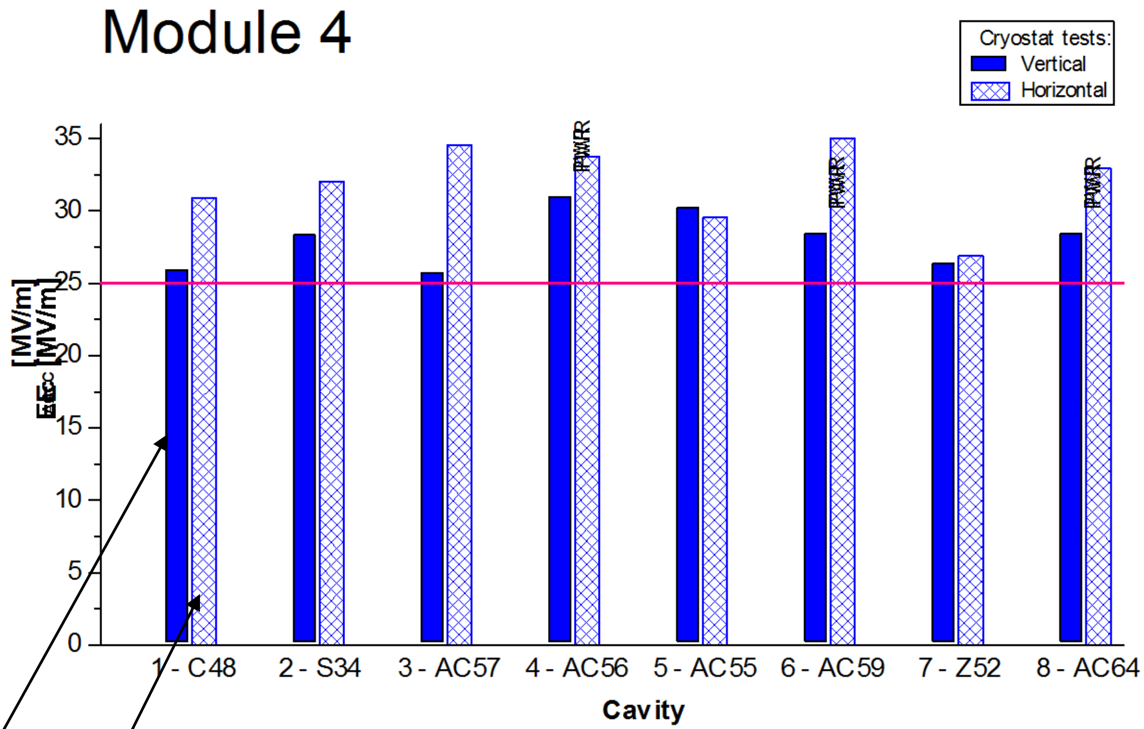

Bare Vert. Cavity vs. Equipped Hor. Cavity Test

Issues with HPP

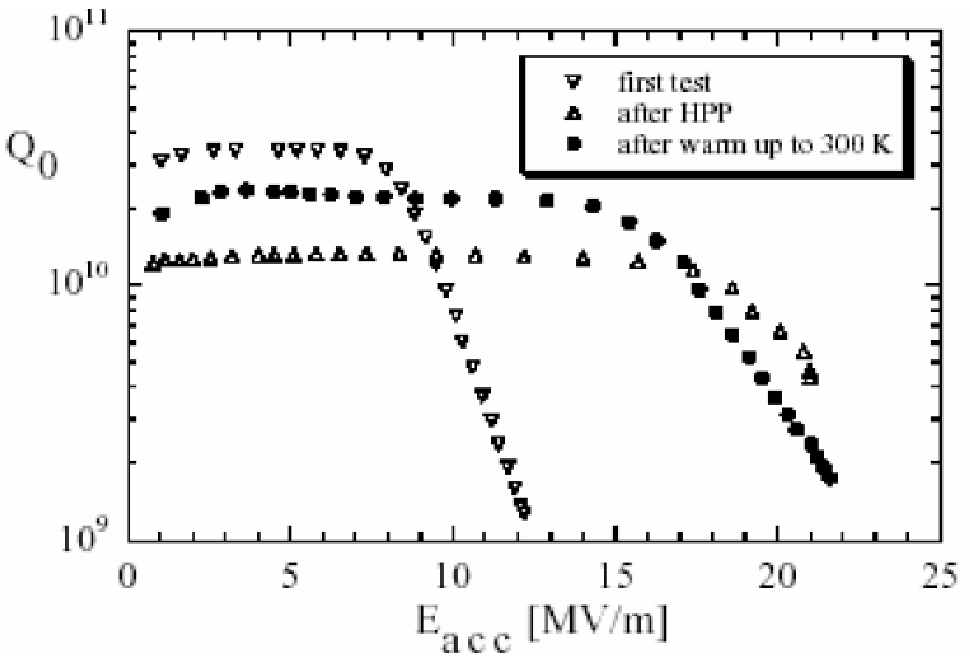

Fig. 2: Cavity C19 before and after HPP. The Q_0 recovered partially after warm up to room temperature.

- Reduced Q_0 after processing
- No experience with HPP above E_{acc} = 30 MV/m in 9-cell cavities
- Very high power required

Thermal Breakdown (Quench)

Localized heating

Hot area increases with field

At a certain field there is a thermal runaway, the field collapses

- sometimes displays a oscillator behavior
- sometimes settles at a lower value
- sometimes displays a hysteretic behavior

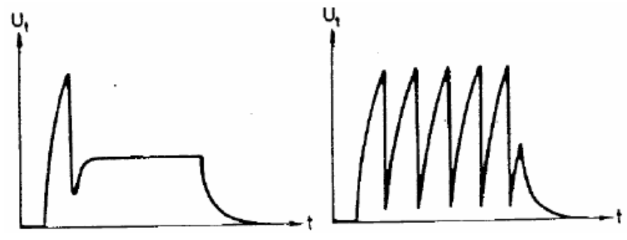

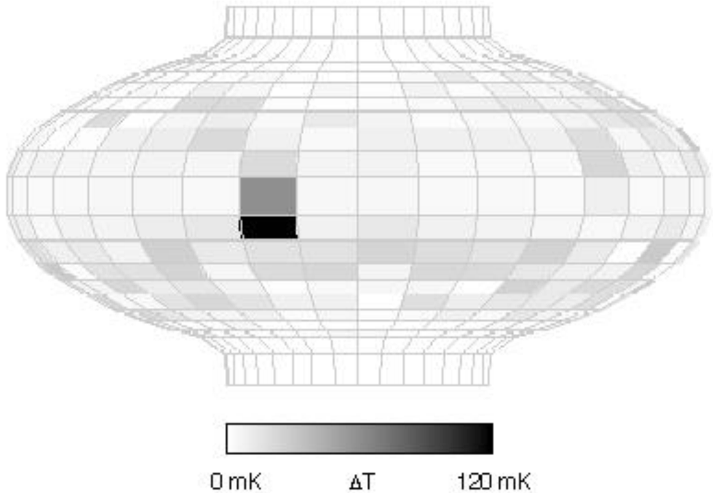

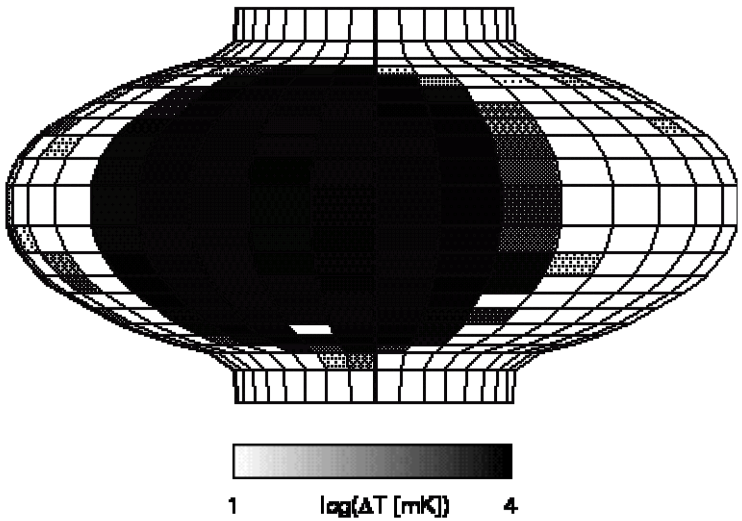

Thermal Breakdown

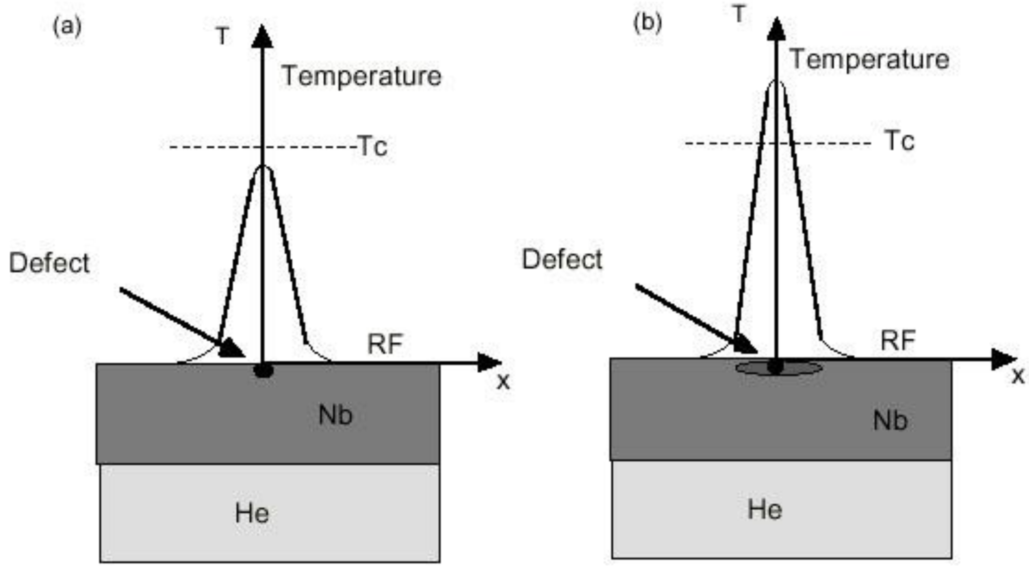

Thermal breakdown occurs when the heat generated at the hot spot is larger than that can be transferred to the helium bath causing $T > T_c$: "quench" of the superconducting state

Quench Mechanism

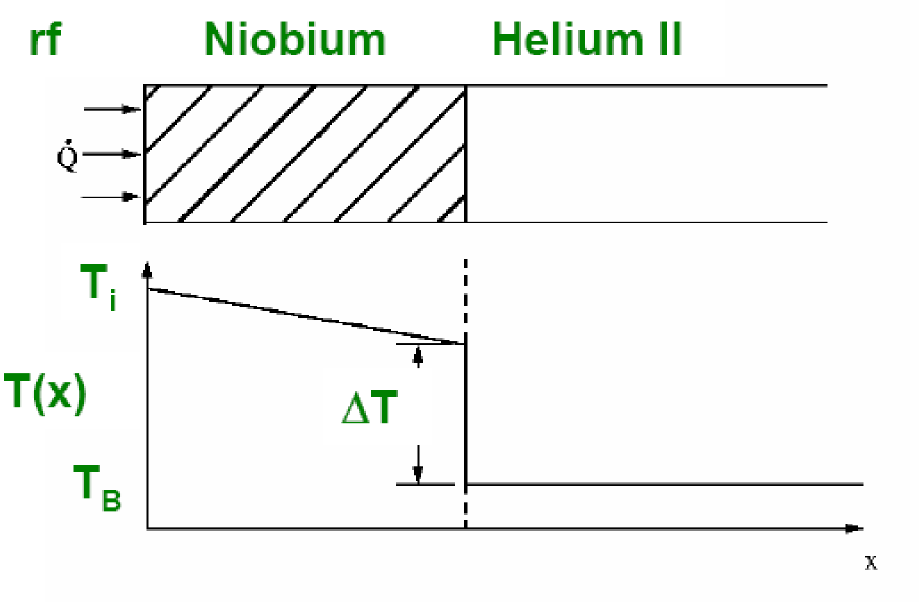

Temperature difference between inner surface and helium bath temperature (two dimensional case)**:**

- The RF current produces heat
- Superconductors are bad thermal conductors:
  - Thermal conductivity
  - Kapitza Nb/He interface resistance
- A small normalconducting defect can produce a very large heating (Factor 10^6 surface resistance!)

$$T_\mathrm{i} - T_\mathrm{B} = \frac{\dot{Q}}{A}\left(\frac{d}{\lambda} + \frac{1}{h_\mathrm{k}}\right)$$

High thermal and Kapitza conductivity required !!

Thermal Breakdown: Simple Model

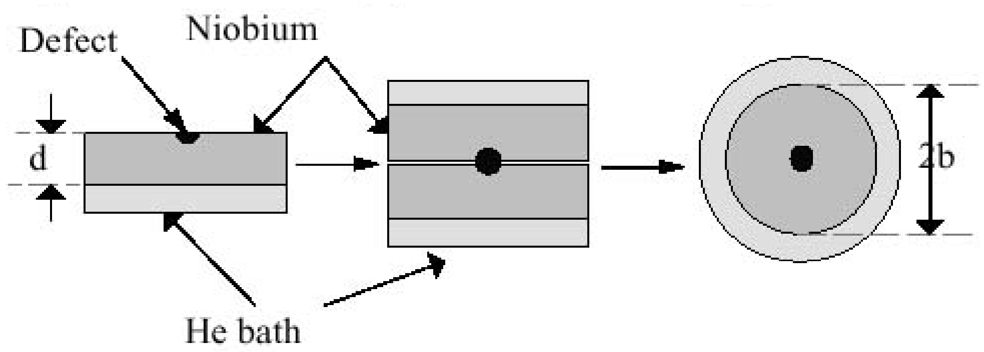

The power dissipation (in watts) at the defect is

$$\dot{Q}_{\mathrm{T}} = \frac{1}{2} R_n H^2 \pi a^2.$$

Heat flow out through a spherical surface:

$$-4\pi r^2 \kappa \frac{\partial T}{\partial r} = 2\dot{Q}_T$$

When the defect reaches T_c, the field reaches its maximum value

$$H_{\max} = \sqrt{\frac{4\kappa(T_c - T_b)}{a R_n}}.$$

Breakdown field given by (very approximately):

$$H_{tb} = \sqrt{\frac{4k_T (T_c - T_b)}{r_d R_d}}$$

κ_T: Thermal conductivity of Nb
R_d: Defect surface resistance
T_c: Critical temperature of Nb
T_b: Bath temperature

Thermal Conductivity of Nb

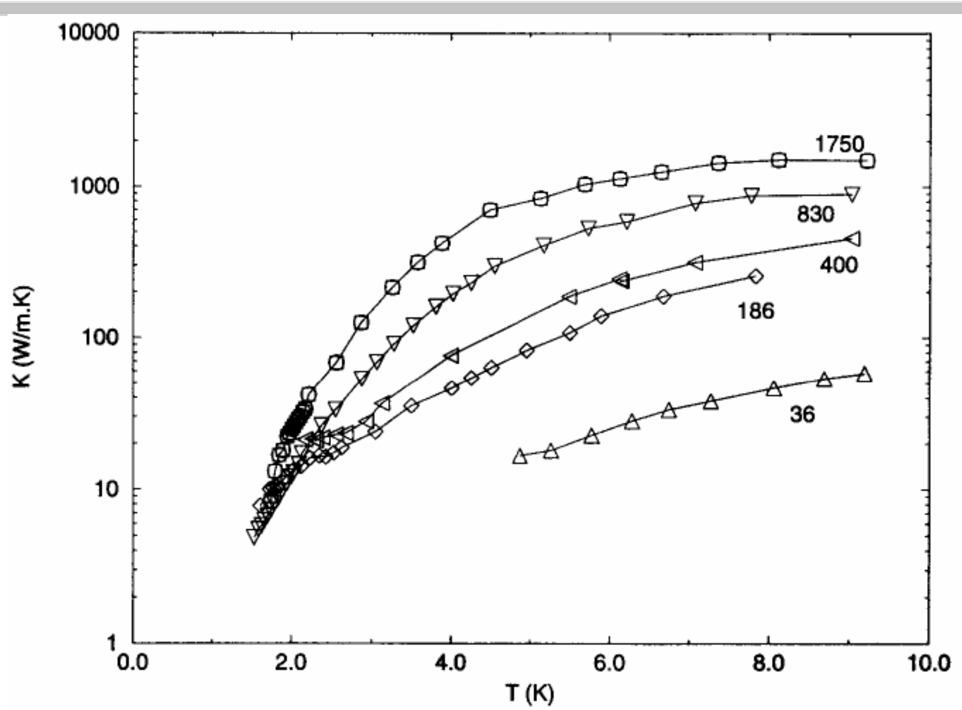

Fig. 3 The thermal conductivity of niobium as a function of temperature, for various RRR values.

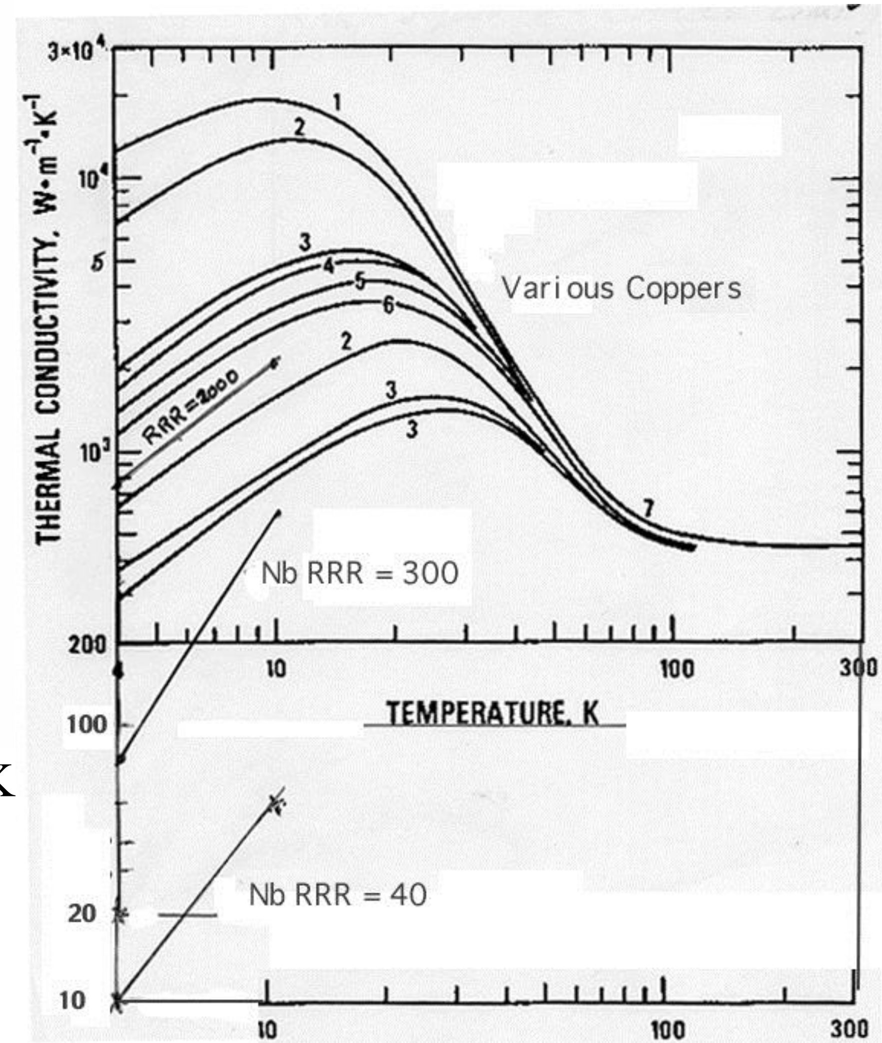

RRR is the ratio of the resistivity at 300K and 4.2K

$$RRR = \frac{r\,(300K)}{r\,(4.2K)}$$

RRR is related to the thermal conductivity

For Nb: $l\,(T = 4.2K) \gg RRR\,/\,4\,(\mathrm{W.\,m^{-1}.\,K^{-1}})$

Numerical Thermal Model Calculations

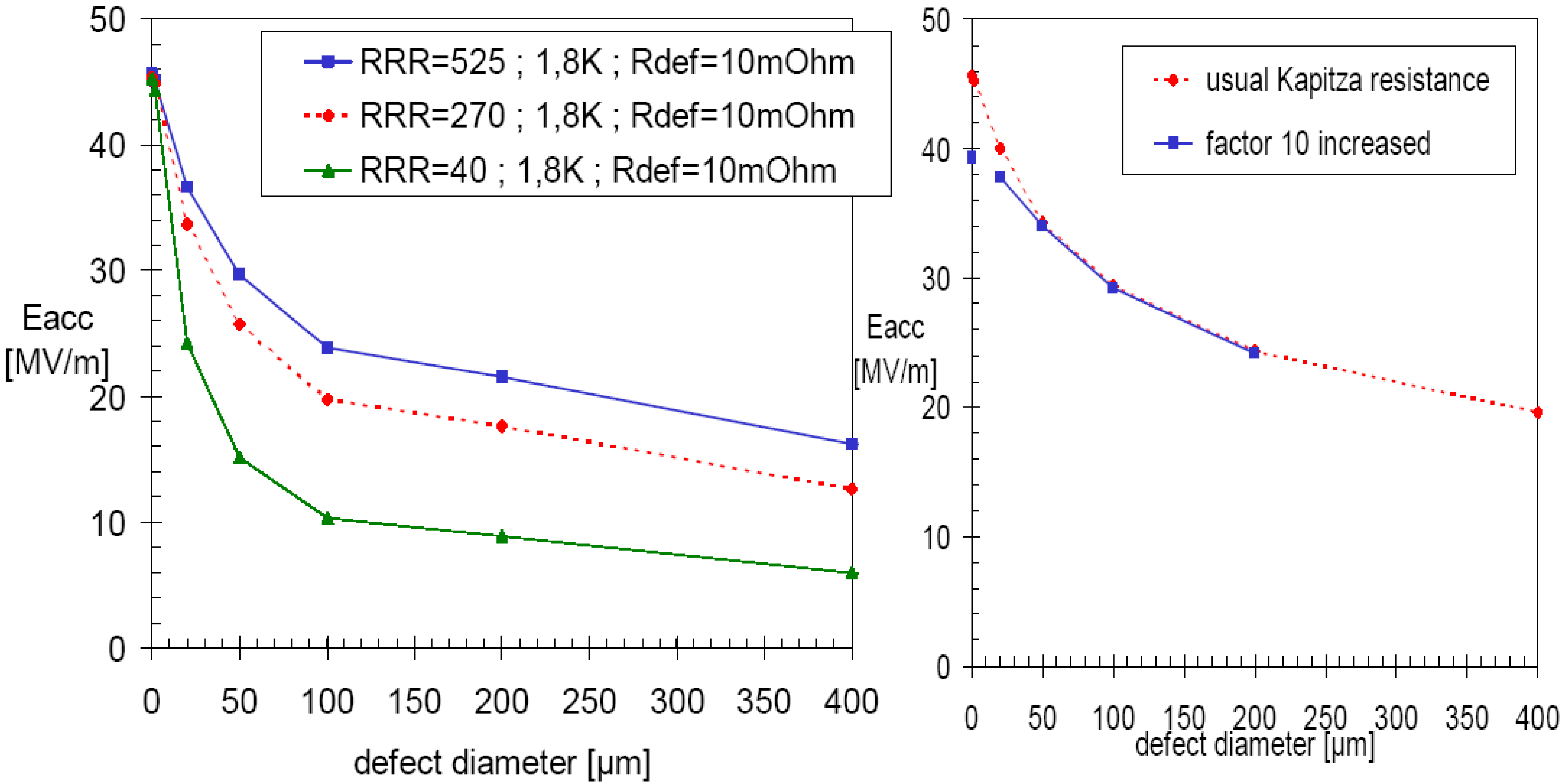

Note: H_{tb} has nearly no dependence on $T_B < 2.1$ K

Magneto-thermal Breakdown

- Quench location identified by T-mapping
- Morphology of quench site reproduced by replica technique

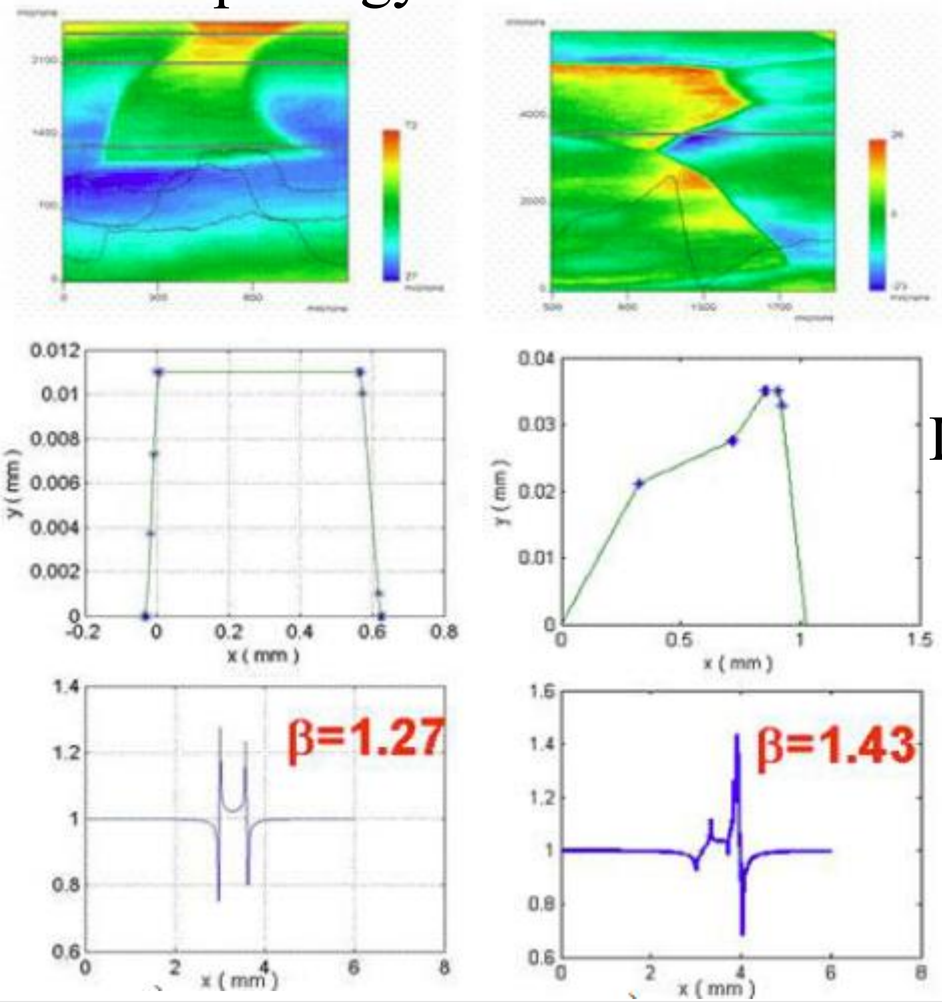

Local Magnetic Field Enhancement:
Quench when $\beta\, H > H_c$

Magneto-thermal Breakdown: Maximum E_{acc}

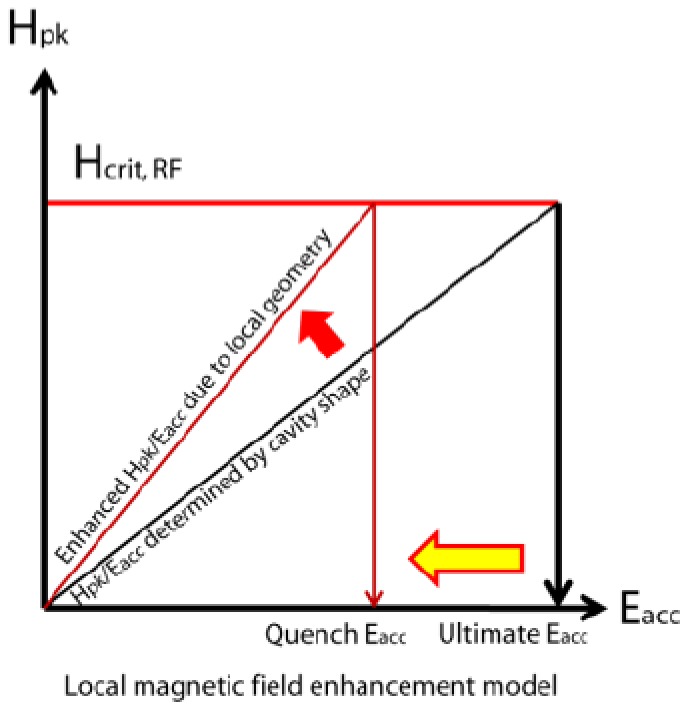

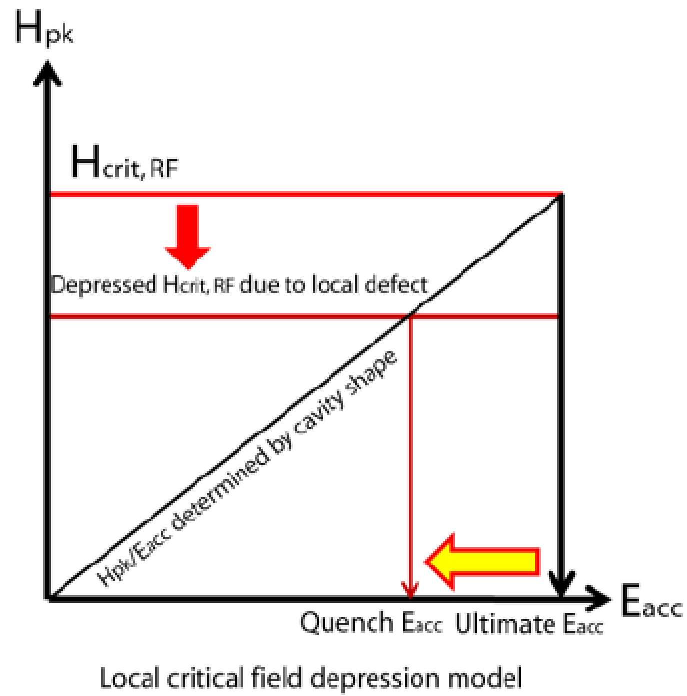

$$E_{acc}^{max} = d \frac{r\, H_{c,RF}}{\beta_m \left(H_p / E_{acc} \right)}$$

$r \leq 1$, reduction of the local critical field within the penetration depth, due to impurities or lattice imperfection

d, thermal stabilization parameter $\propto \sqrt{\kappa}$

$\beta_m > 1$, geometric field enhancement factor

Type of Defects

SEM

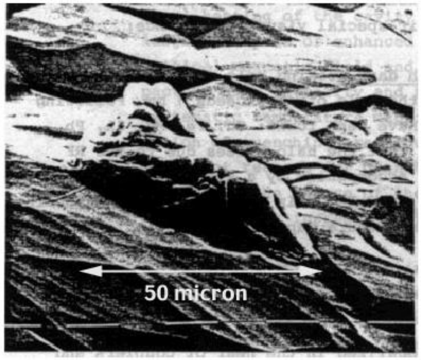

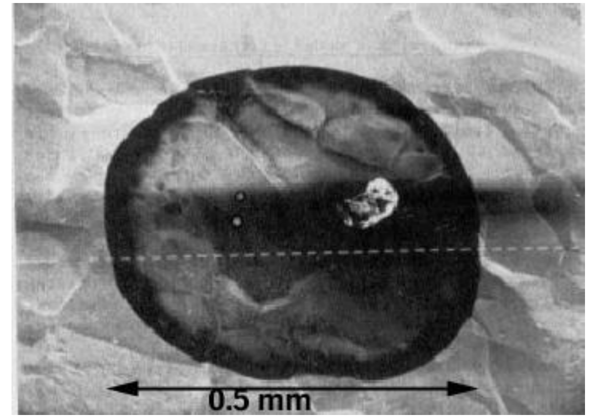

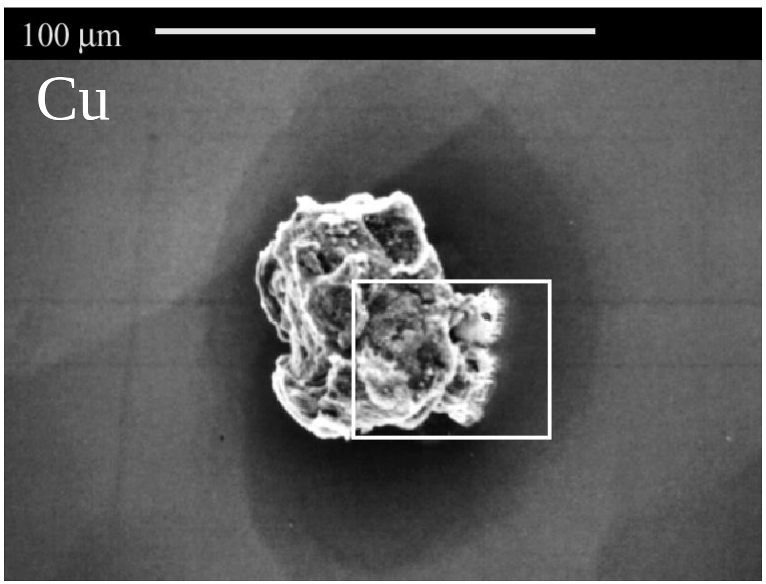

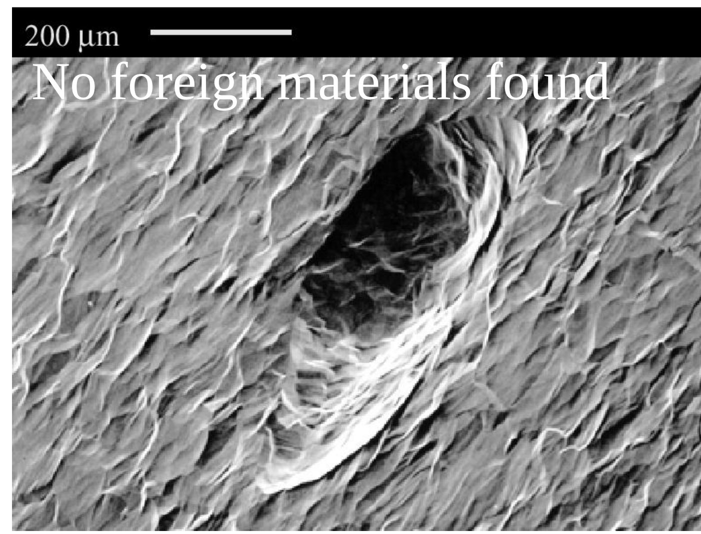

Surface defects, holes can also cause TB

0.1 – 1 mm size defects cause TB

Optical Inspection

- long distance microscope (Cornell)
  - resolution: 12 µm/pixel (limited by camera)
- University Kyoto and KEK camera system
  - resolution: 7 µm/pixel
  - variable light system for height measurement

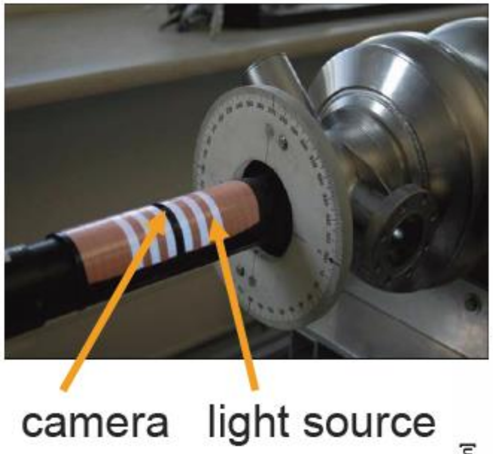

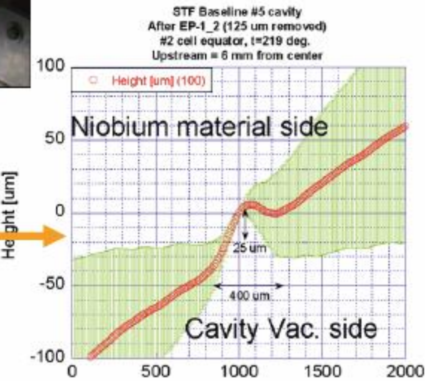

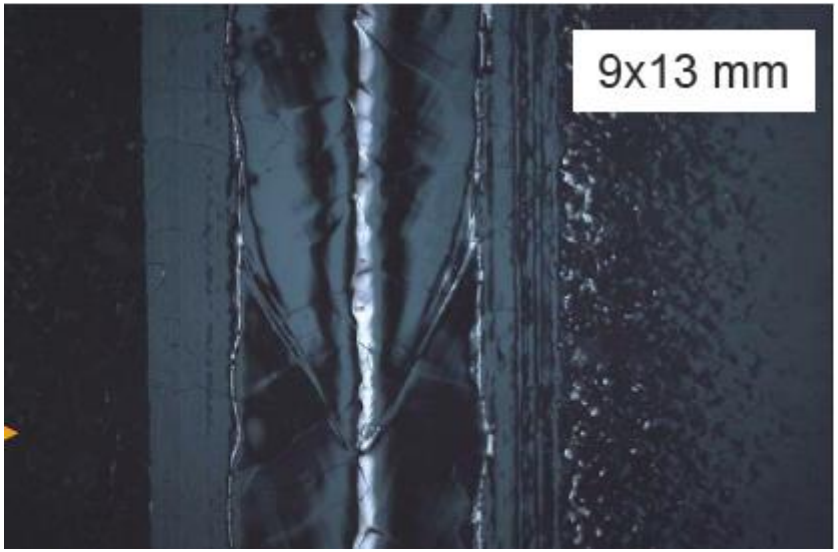

Defects Seen by Optical Inspection

Cell 6, Quench at 16 MV/m on equator

DESY

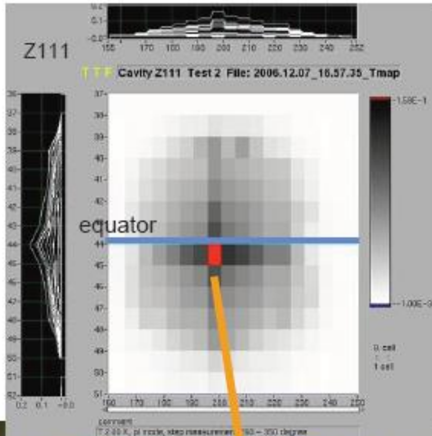

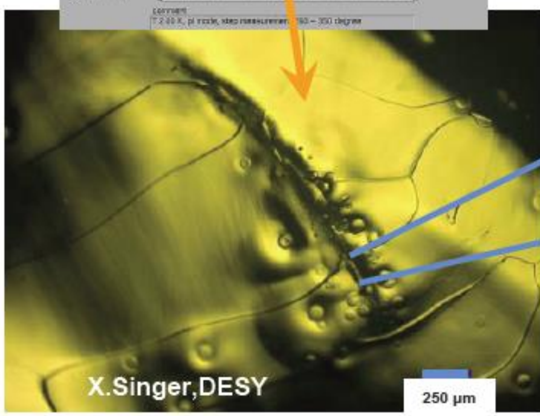

- Holes with sharp edges along the grain boundaries in the equator weld
- Pits around the holes.

SEM

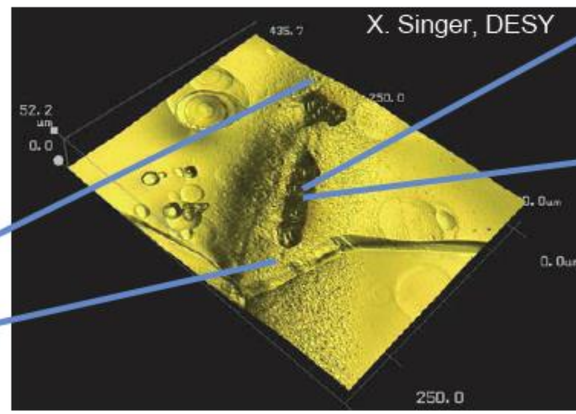

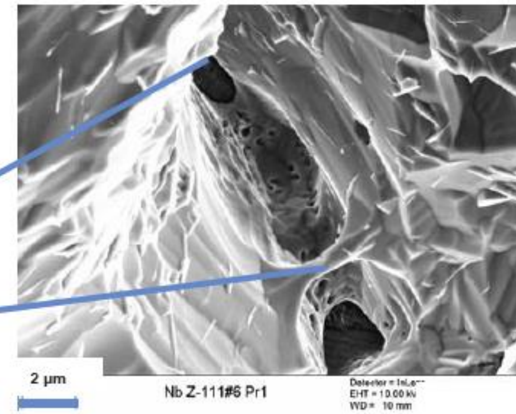

- Auger analysis: no foreign material
- EDX analysis: increased content of carbon in black spots

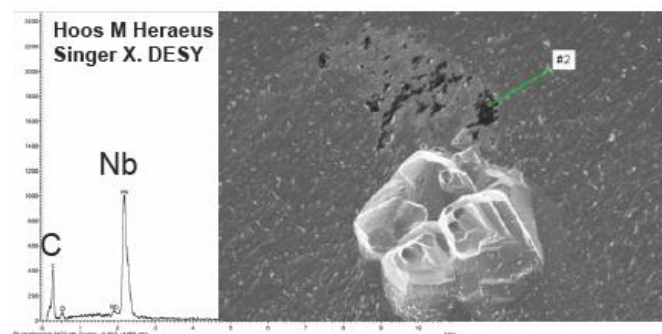

Defects Seen by Optical Inspection

Cell 5, Quench at 23 MV/m on equator

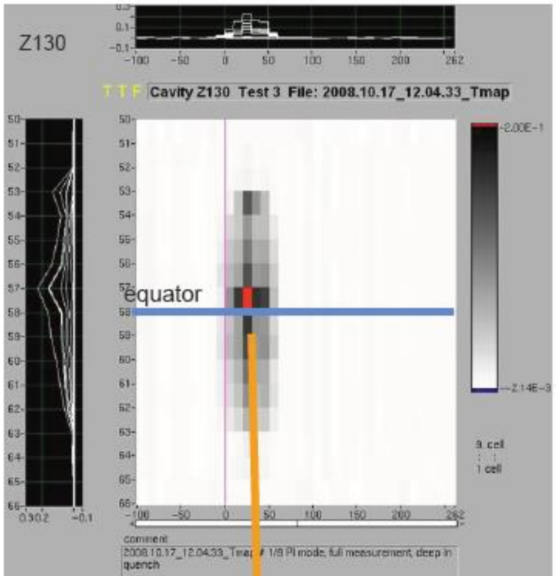

hole in the equator weld

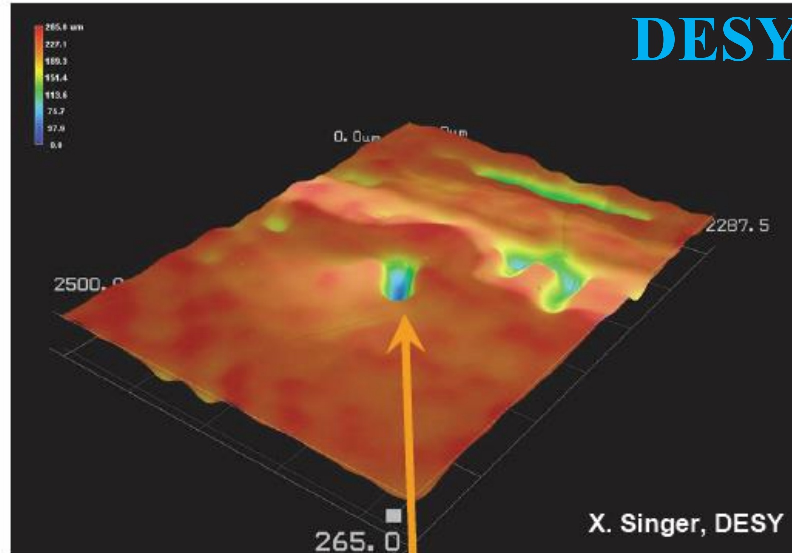

3D image, bump and hole up to 200 µm deep

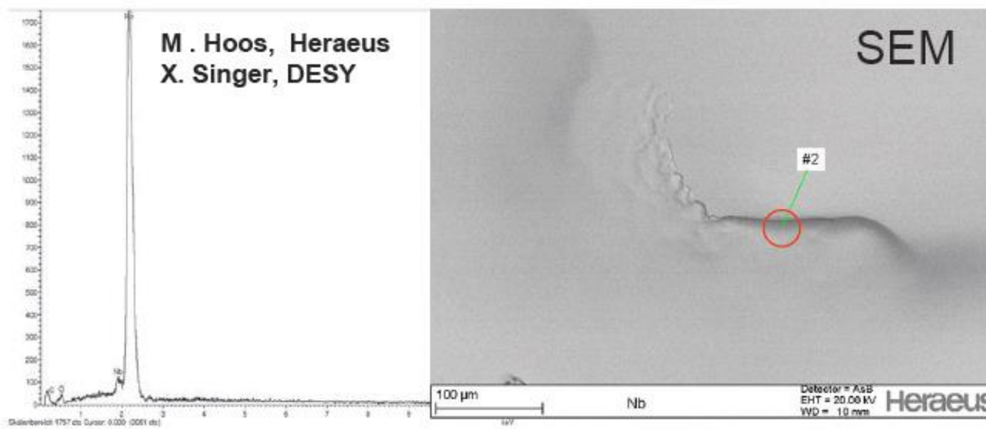

No foreign material inclusions detected by EDX

Cures for Quench

- **Prevention: avoid the defects**
  - High-quality Nb sheets
  - Eddy-current scanning of Nb sheets
  - Great care during cavity fabrication steps

- **Post-treatment:**
  - Thermally stabilize defects by increasing the RRR
  - Remove defects: local grinding

Post-purification for Higher RRR

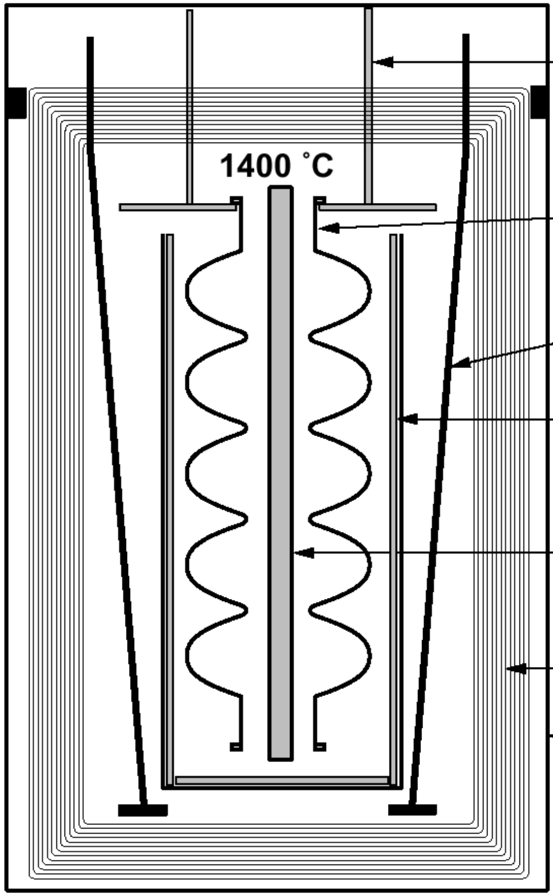

- Post-purification by solid-state gettering
- use Ti (or Y) as getter material => higher affinity for O, (N, C) than Nb
  - coating of cups or cavity with getter material at 1350 C (Ti) under UHV
  - diffusion of O from Nb to Ti until equilibrium

- 1) Increase of RRR = 250-300 to RRR = 500 – 700
  2) Homogenizing impurities

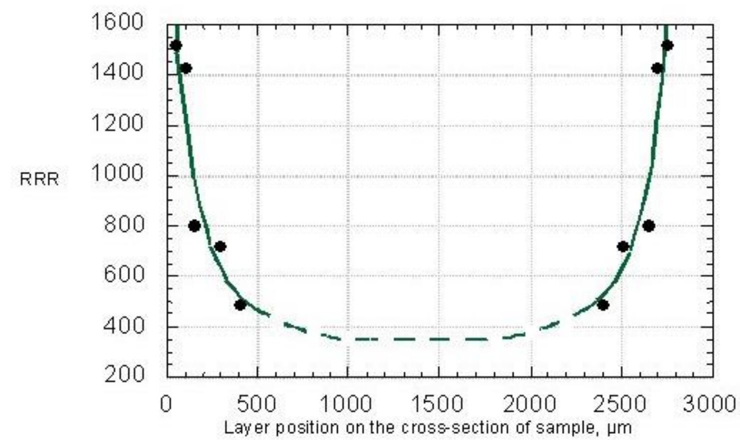

Disadvantages:

- > 50 µm material removal necessary after heat treatment
- Significant reduction of yield strength of the Nb

Post-purification

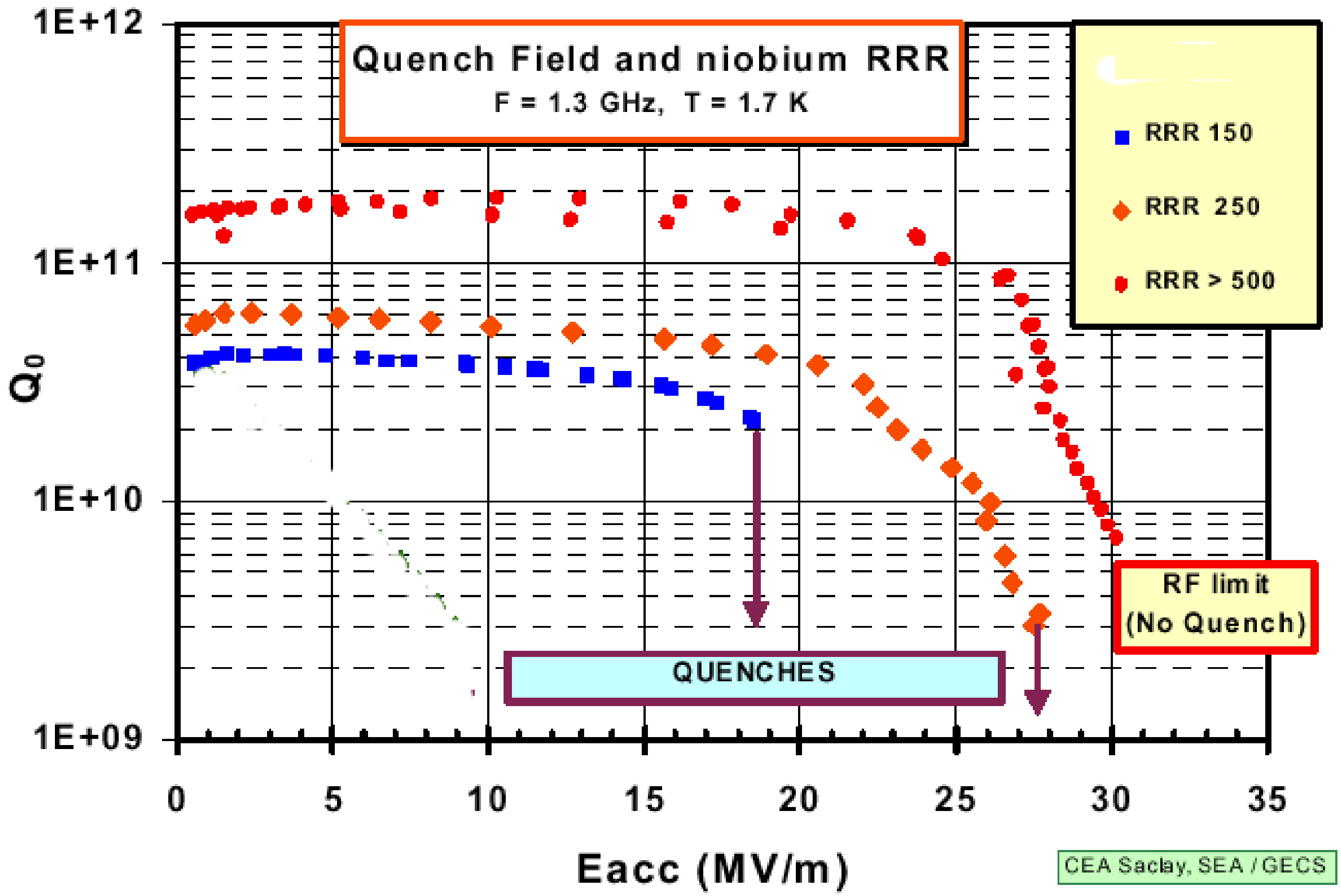

Post-purification

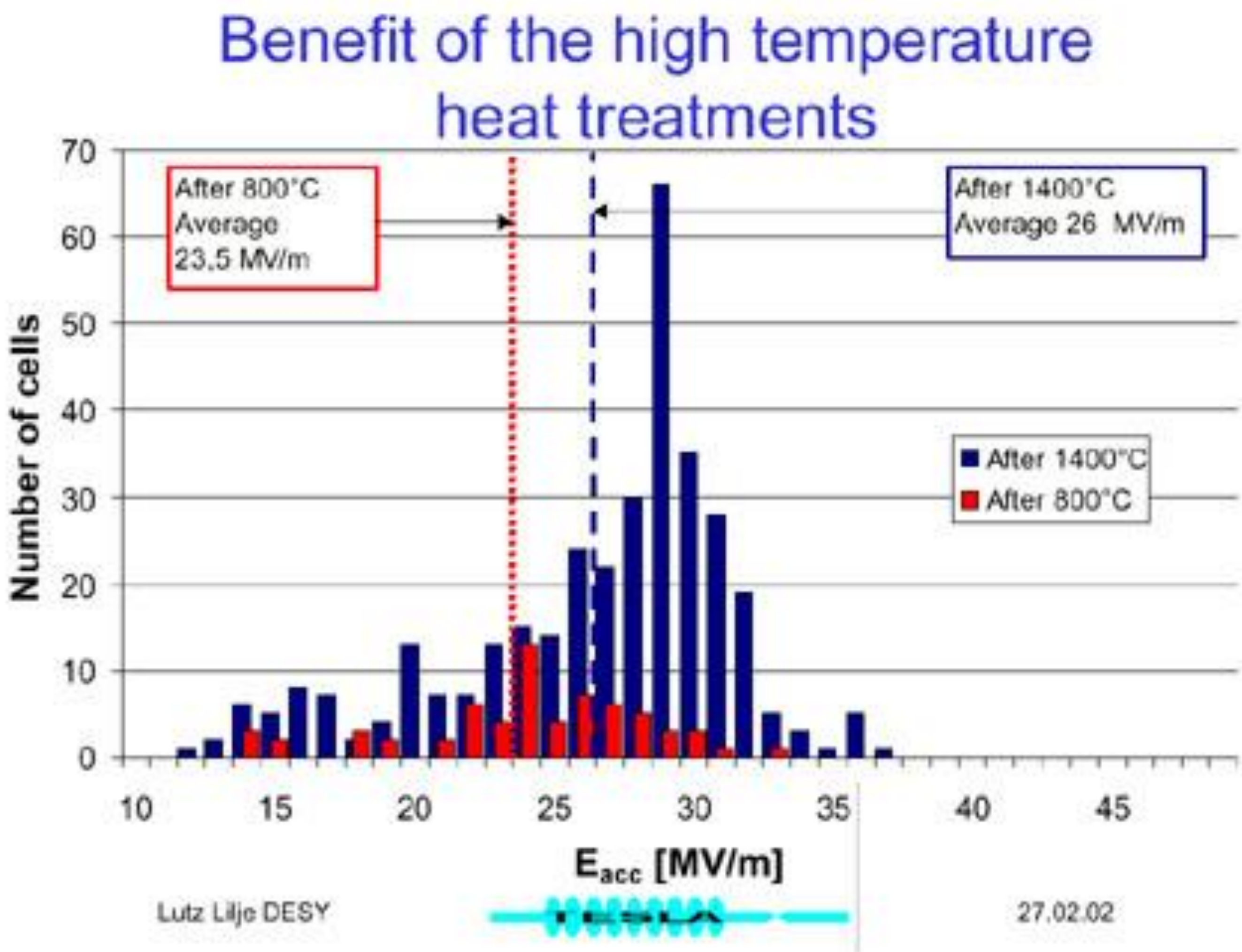

How High of RRR Value is Necessary?

9-cell ILC cavities

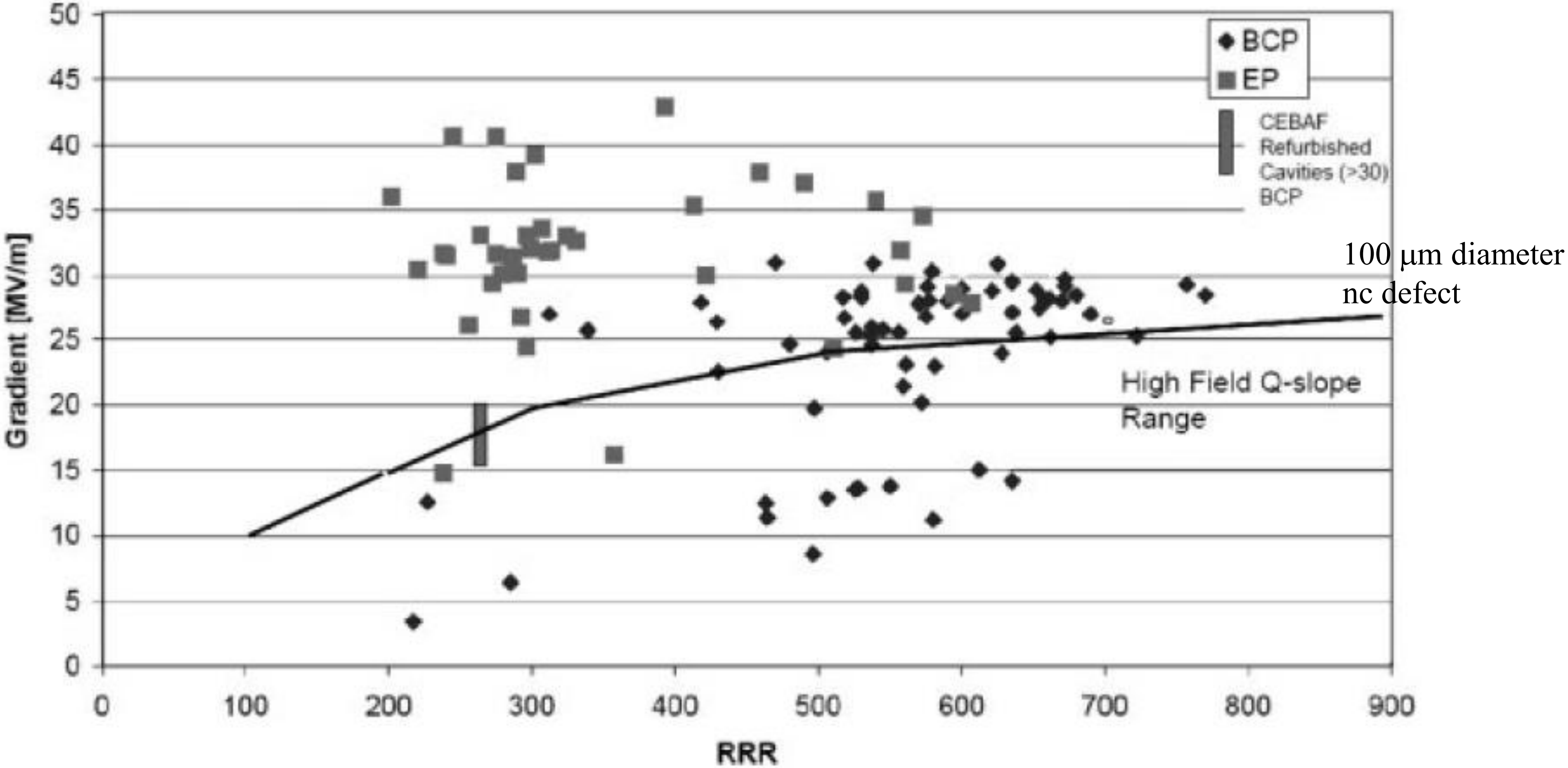

Defect Repair: Local Grinding

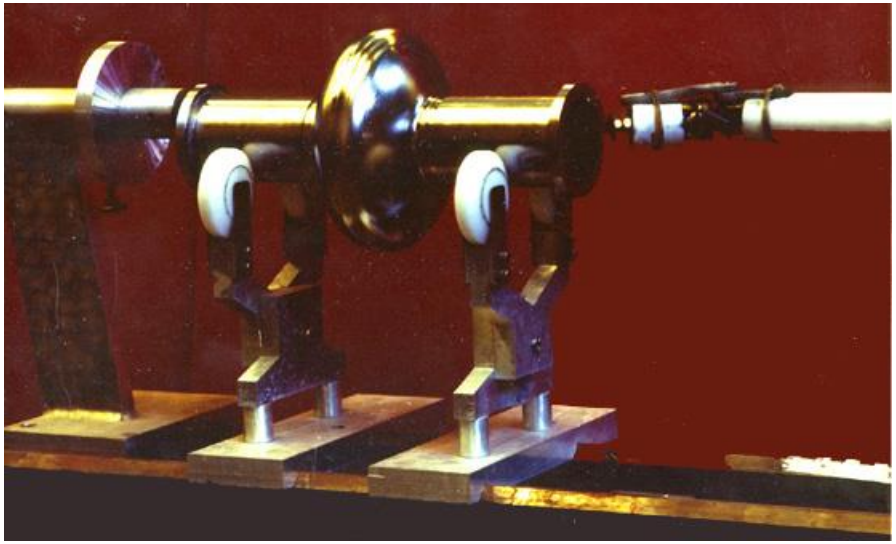

Polymond + water for grinding

Polymond: diamond particles in a resin (particle size = 40 ~ 3 um)

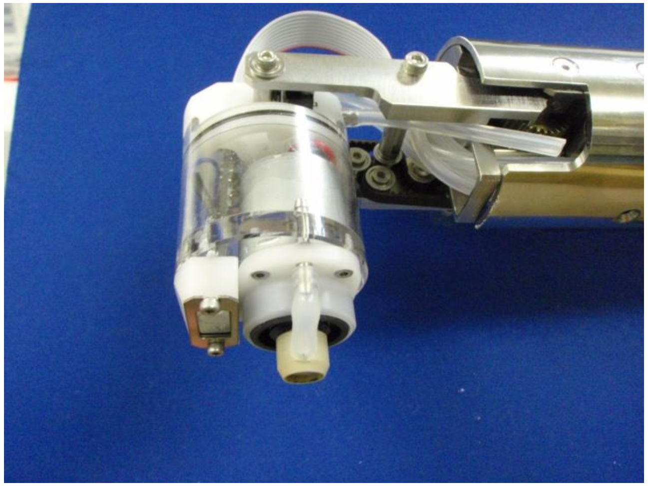

Defect Repair: Local Grinding

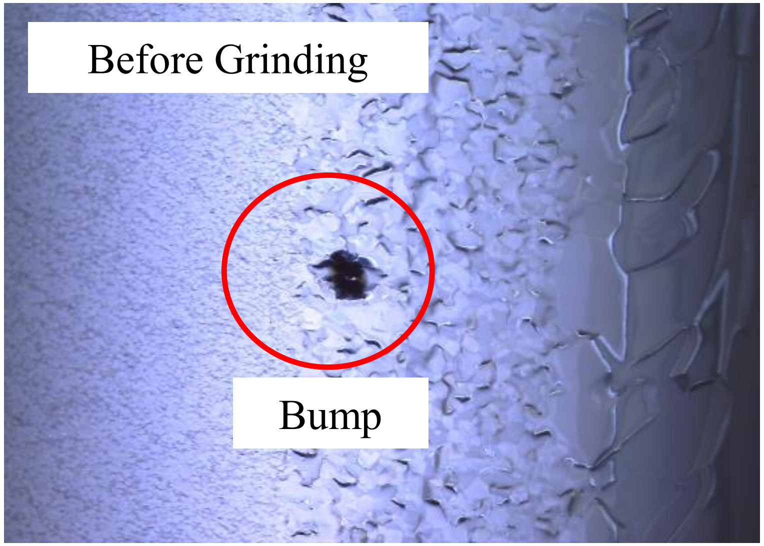

Quench at E_{acc}=20 MV/m

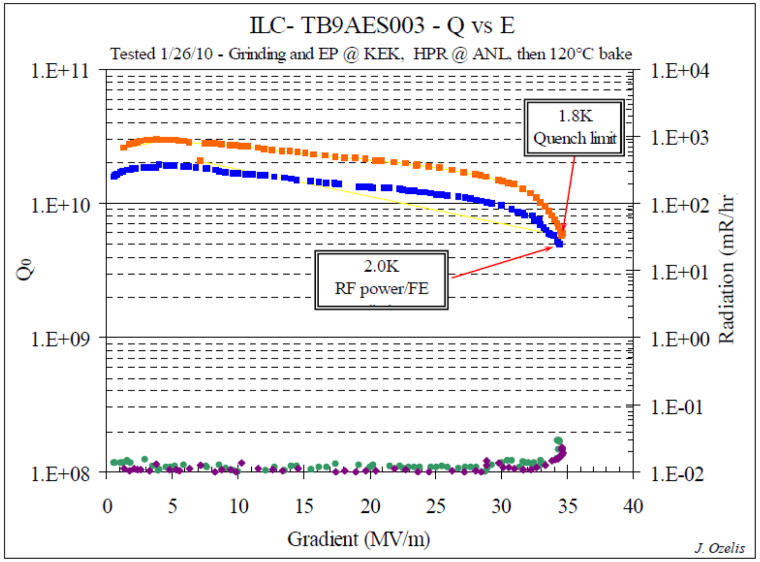

Figure 1.) Q_0 vs E runs at 2.00K and 1.80K.

Summary on Quench

- Big improvement in Cavity fabrication and treatment
  less foreign materials found (at limitations <20MV/m only)

- Visual inspection systems are available
- Many irregularities in the cavity surface are found with this systems during and after fabrication and treatment
  pits and bumps
  weld irregularities
- Often one defect limits the whole cavity
- Some correlations are found between defects and quench locations at higher fields
  But often no correlation between suspicious pits and bumps and quench location
- At gradient limitations in the range >30 MV/m defects are often not identified

High-Field Q-Slope (“Q-drop”)

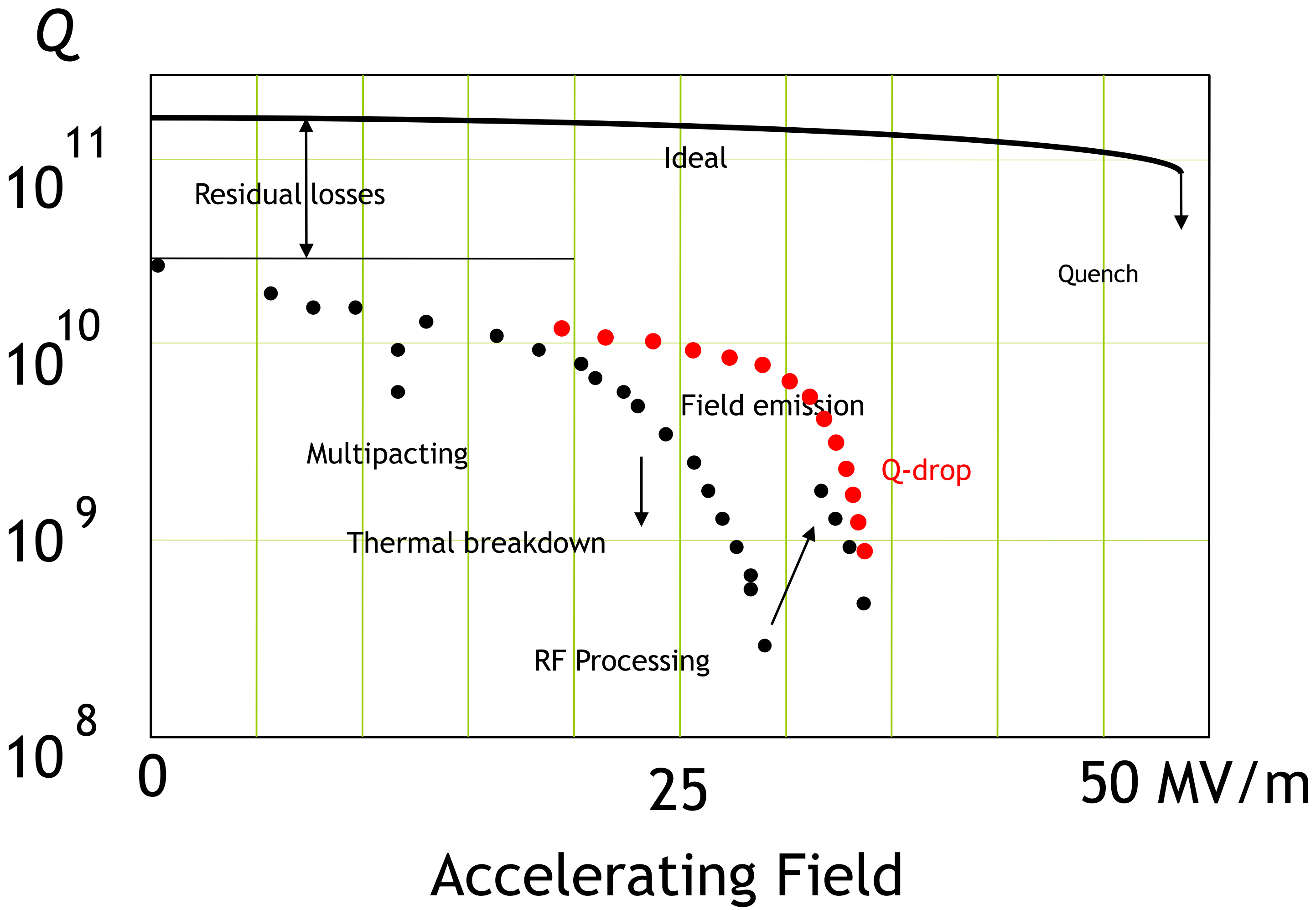

Q-drop and Baking

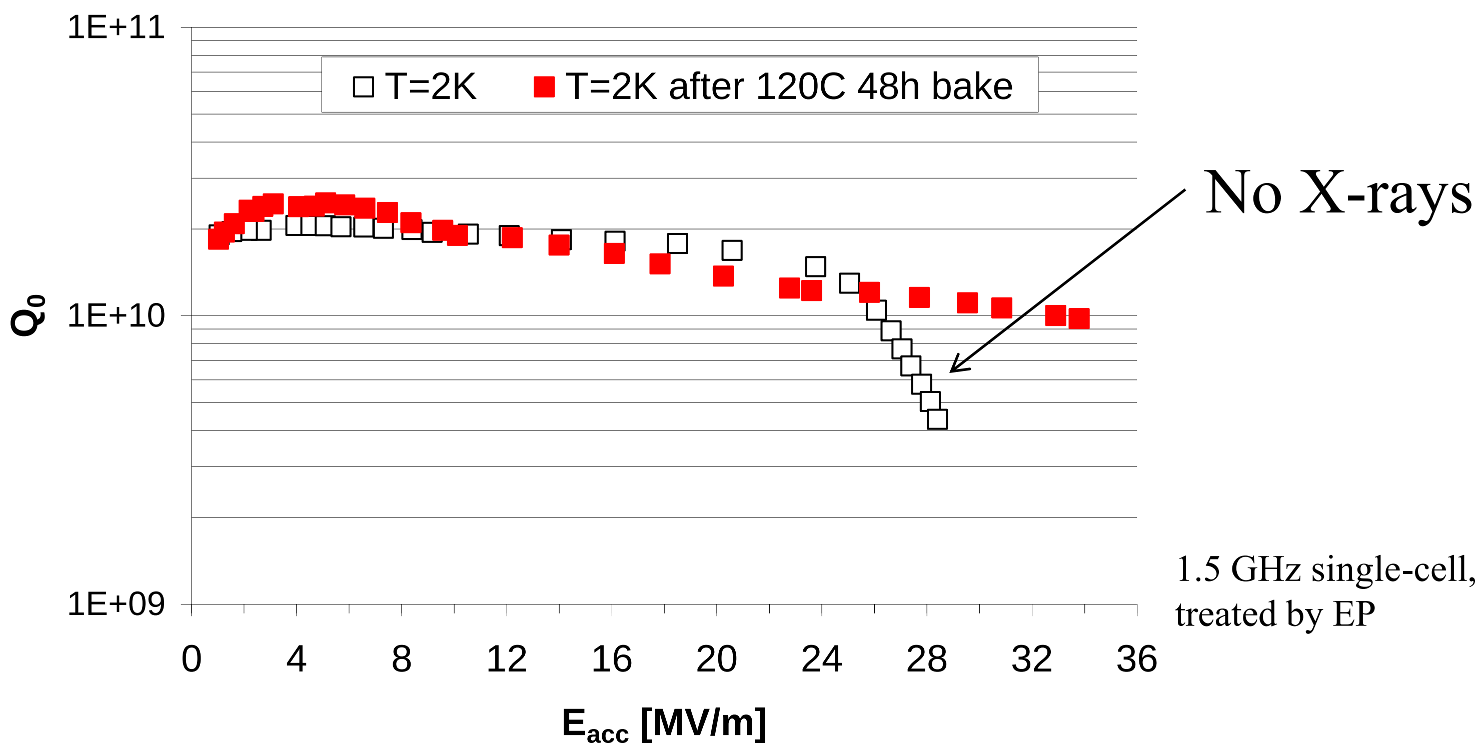

- The origin of the Q-drop is still unclear. Occurs for all Nb material/treatment combinations
- The Q-drop recovers after UHV bake at 120 °C/48h for certain material/treatment combinations

Experimental Results on Q-drop

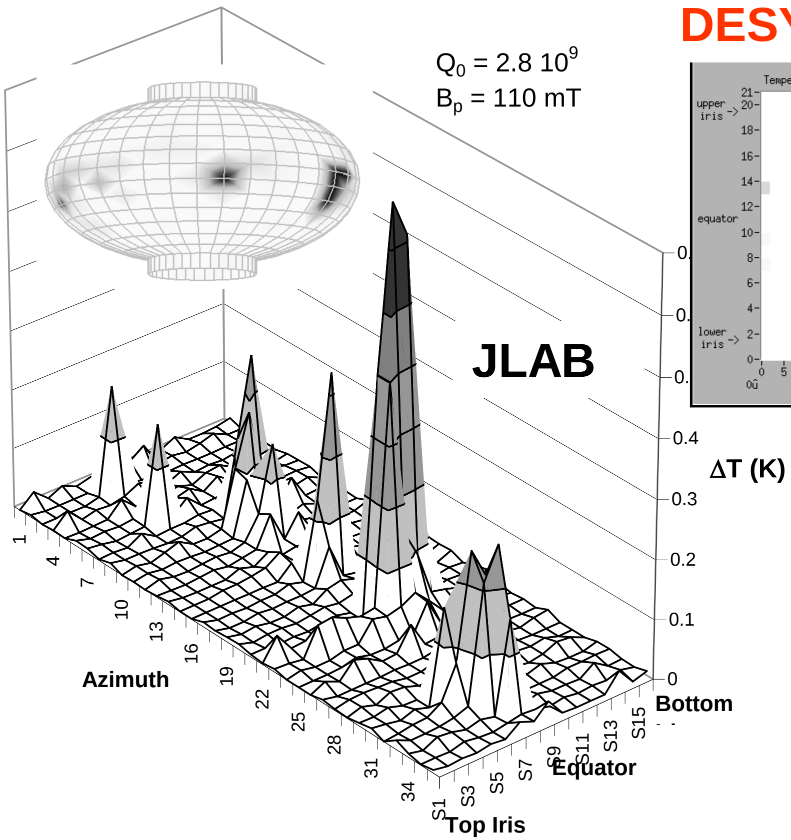

DESY

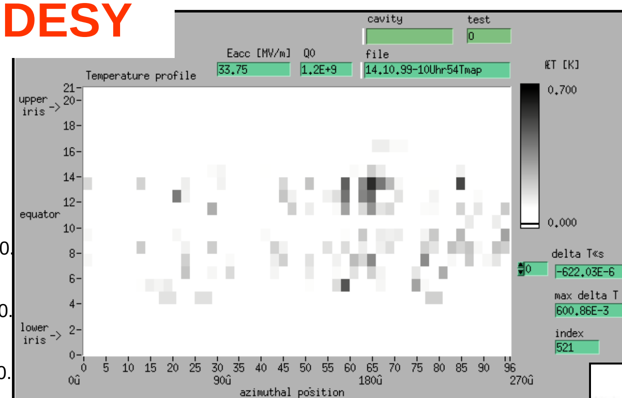

T-Maps

CORNELL

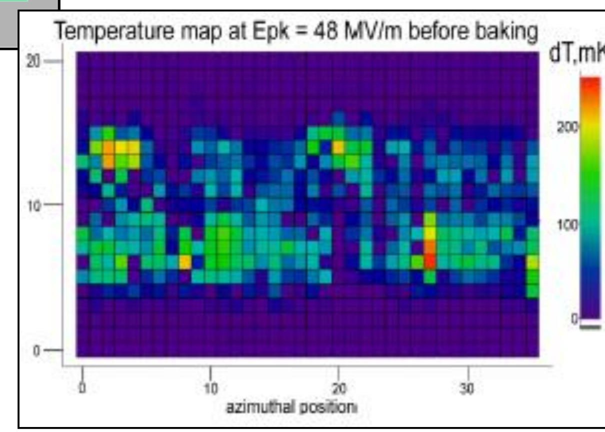

- “Hot-spots” in the equator area (high-magnetic field)

Experimental Results on Q-drop

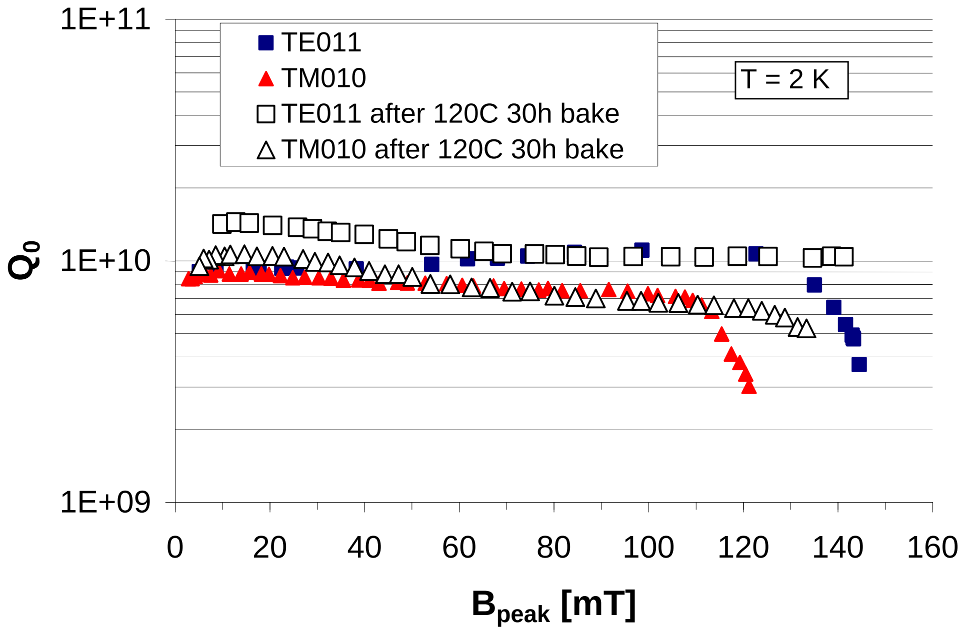

• Q-drop and baking effect observed in both TM_{010} and TE_{011} modes. TE mode has no surface electric field

Q-drop: high magnetic field phenomenon

Onset of Q-drop is higher for
- smooth surfaces
- reduced number of grain boundaries

Baking: Material and Preparation Dependence

Baking **works** on cavities made of:

- Large-grain Nb (buffered chemical polished or electropolished)

50 µm

Smooth surface, few grain boundaries

- Fine-grain Nb, electropolished

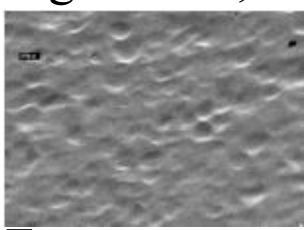

100 µm

Smooth surface, many grain boundaries

- Fine-grain Nb, post-purified, BCP

Smooth surface, fewer grain boundaries

Baking **does not work** on cavities made of:

- Fine-grain Nb, buffered chemical polished

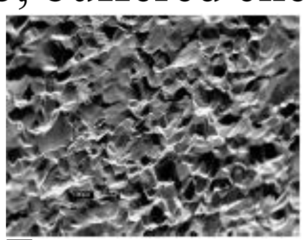

100 µm

Rough surface, many grain boundaries

Recipe against Q-drop

- Recipes necessary to overcome the Q-drop, depending on the starting material, based on current data:

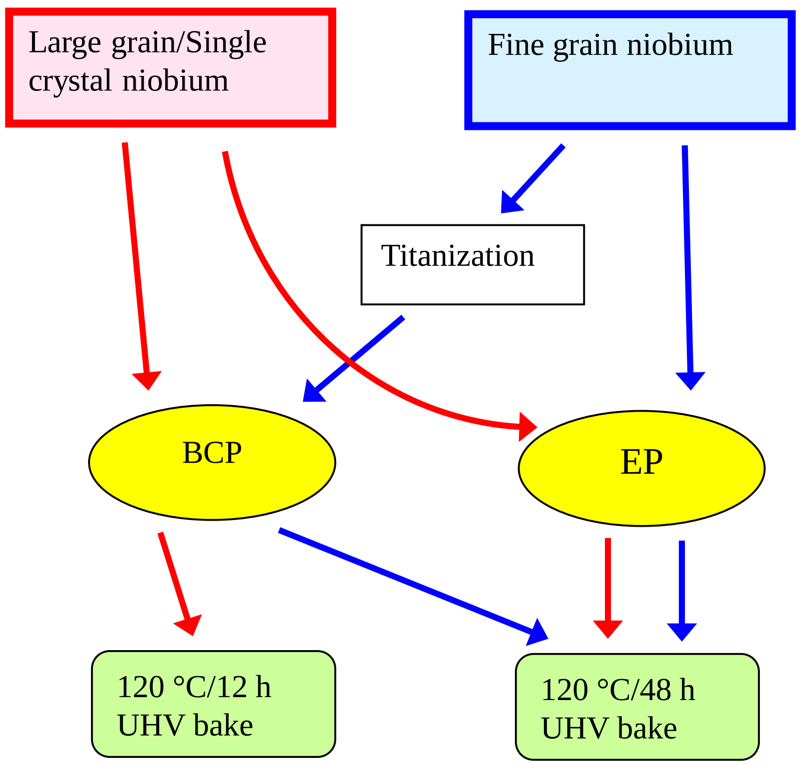

Baking Effects on Low-field R_s and H_{c3}

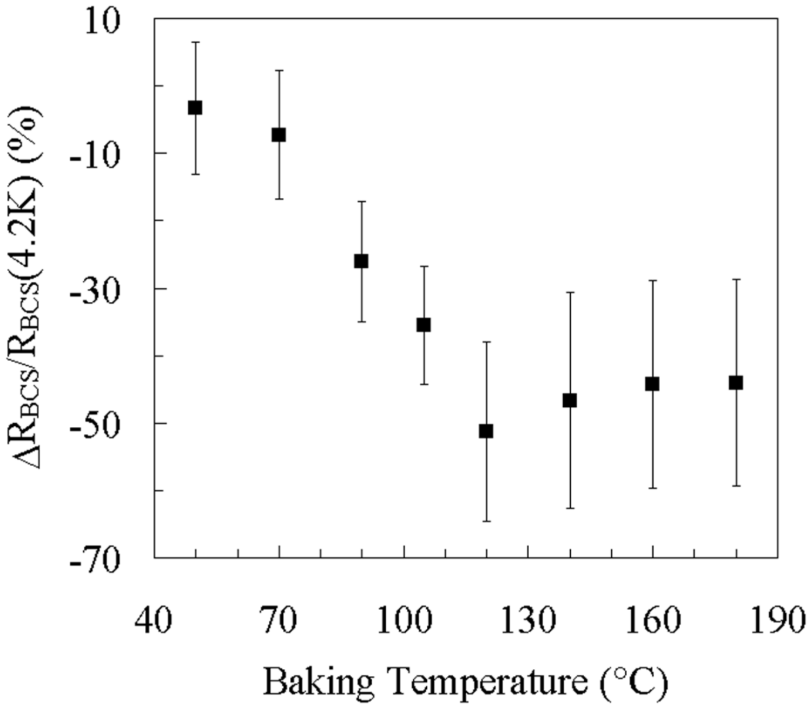

$r_{32}=B_{c3}/B_{c2}$: depends on bake temperature and duration

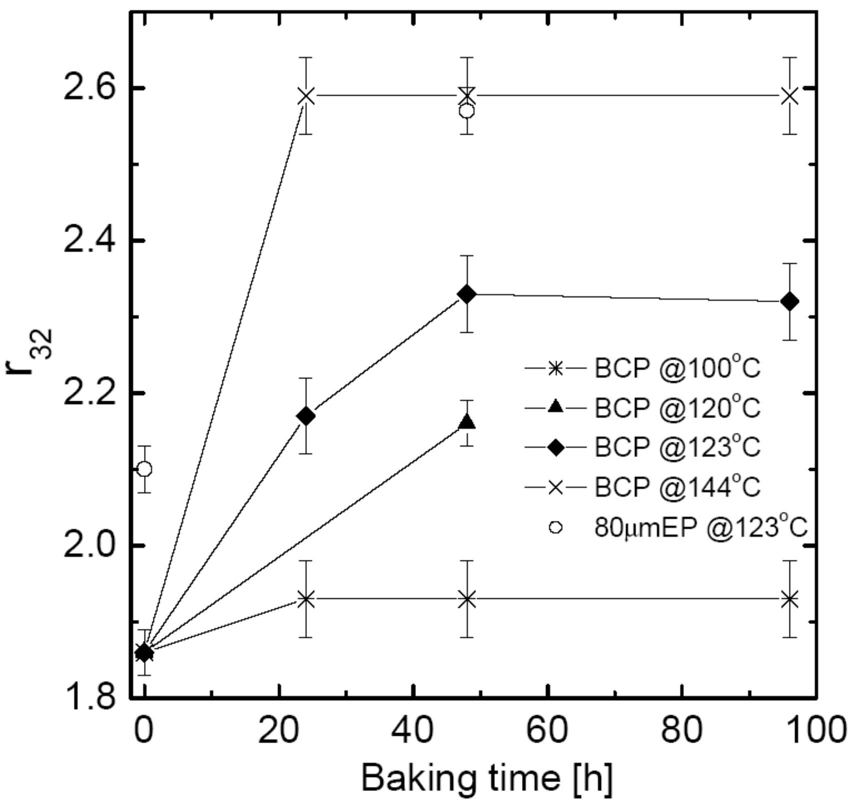

- Decrease of R_{BCS} due to ↓ of l and ↑ of energy gap
- The physics of the niobium surface changes from CLEAN (l > 200 nm) to DIRTY LIMIT ($l \approx 25$ nm $\cong \xi_0$)

Models of Q-drop & Baking

- Magnetic field enhancement
- Oxide losses
- Oxygen pollution
- Magnetic vortices

Magnetic Field Enhancement Model

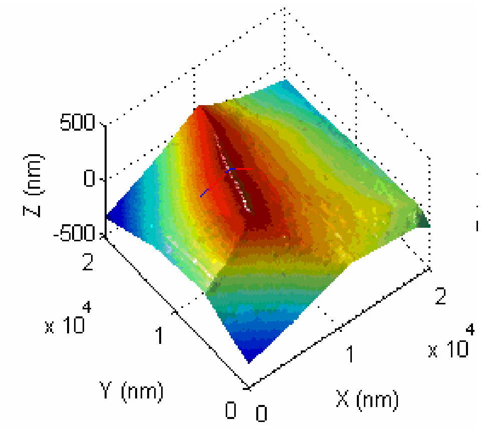

AFM image of a grain boundary edge

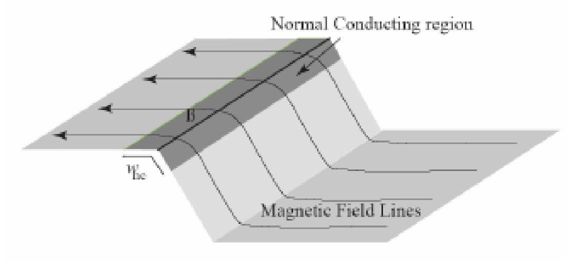

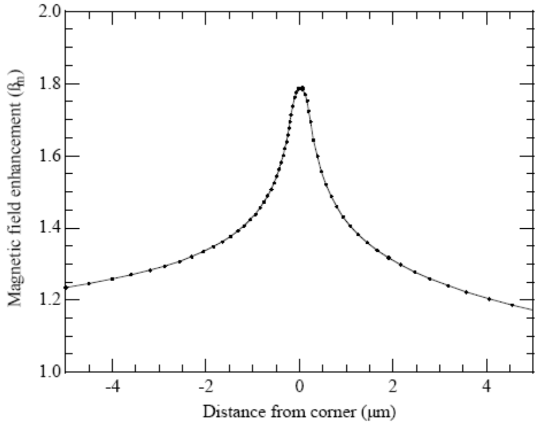

Local quenches at sharp steps (grain boundaries) when $\beta_m H > H_c$

β_m: Field enhancement factor

- $Q_0(B_p)$ calculated assuming
  - ✓ Distribution function for β_m values
  - ✓ The additional power dissipated by a quenched grain boundary is estimated to be ~ 17 W/m

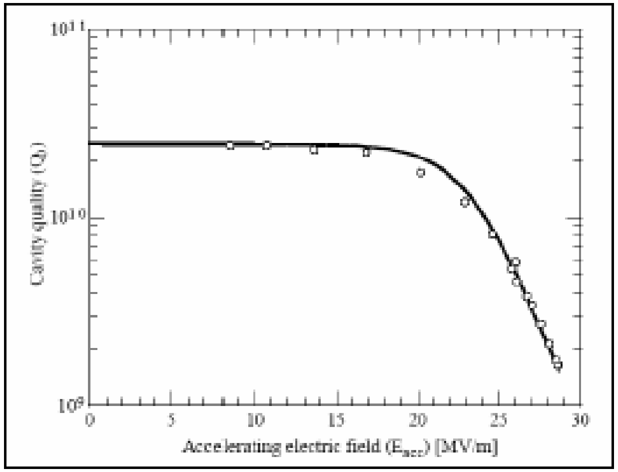

J. Knobloch et al., *Proc. of the 9th SRF Workshop*, (1999), p. 77

MFE Model: Shortcomings

The model cannot explain the following experimental results:

- Single-crystal cavities have Q-drop
- Seamless cavities have Q-drop
- Low-temperature baking does not change the surface roughness
- Electropolished cavities have Q-drop, in spite of smoother surface

Interface Tunnel Exchange Model

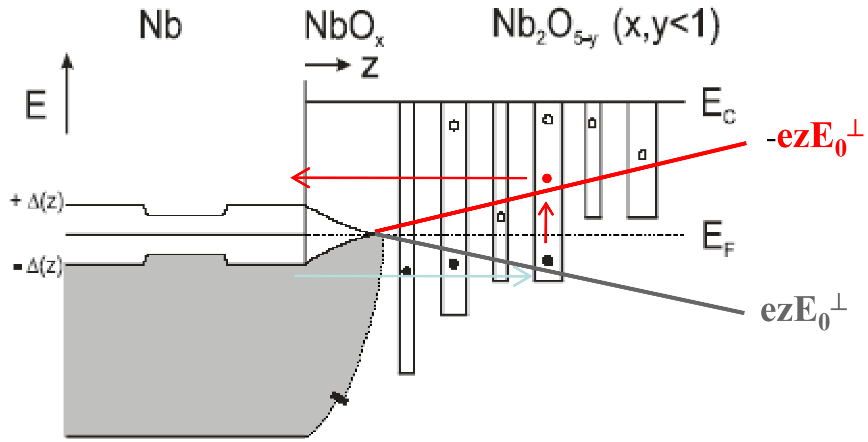

Band structure at Nb-NbO$_x$-Nb$_2$O$_{5-y}$ interfaces

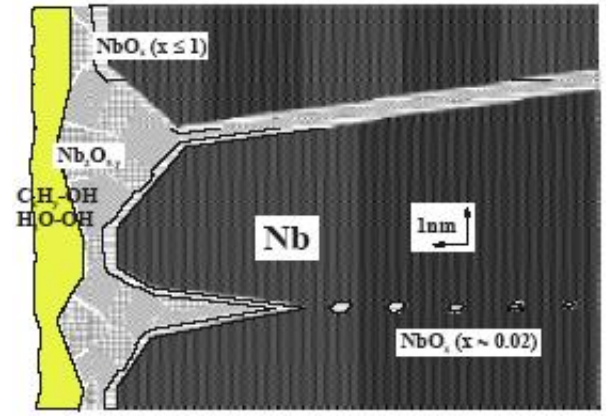

Schematic representation of the Nb surface

- Interface Tunnel Exchange (ITE) model
  - Resonant energy absorption by quasiparticles in localized states in the oxide layer
  - Driven by electric field $E_0 > \frac{\varepsilon_r \Delta}{e\beta^* z^*}$

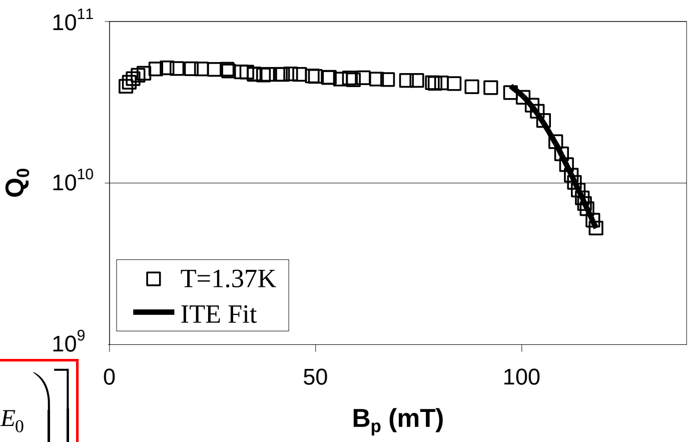

$$R_s^E = b\left[\left(e^{-c/E_p} - e^{-c/E_0}\right) + \left(\frac{c}{E_p}e^{-c/E_p} - \frac{c}{E_0}e^{-c/E_0}\right) + \frac{1}{2}\left(\frac{c^2}{E_p^2}e^{-c/E_p} - \frac{c^2}{E_0^2}e^{-c/E_0}\right)\right]$$

J. Halbritter et al., *IEEE Trans. Appl. Supercond.* **11** (2001) p. 1864

ITE Model: Shortcomings

The model cannot explain the following experimental results:

- The baking effect is stable after re-oxidation
- The Q-drop was observed in the TE_{011} mode (only magnetic field on the surface)
- The Q-drop is re-established in a baked cavity only after growing an oxide ~ 80 nm thick by anodization

Oxygen Pollution Model

- Surface analysis of Nb samples shows high concentrations of interstitial oxygen (up to ~ 10 at.%) at the Nb/oxide interface
- Interstitial oxygen reduces T_c and the H_{c1}

Magnetic vortices enter the surface at the reduced H_{c1}, their viscous motion dissipating energy

- The calculated O diffusion length at 120°C/48h is ~ 40 nm

Interstitial oxygen is diluted during the 120°C baking, restoring the H_{c1} value for pure Nb

Before baking

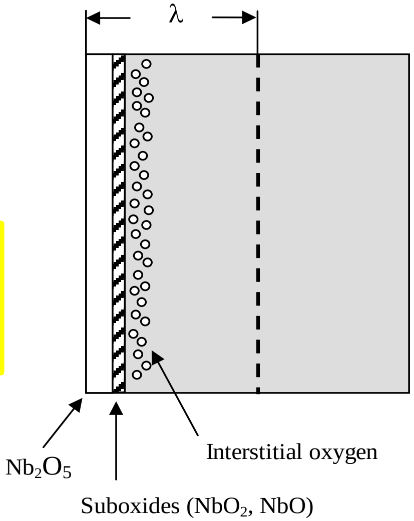

After baking

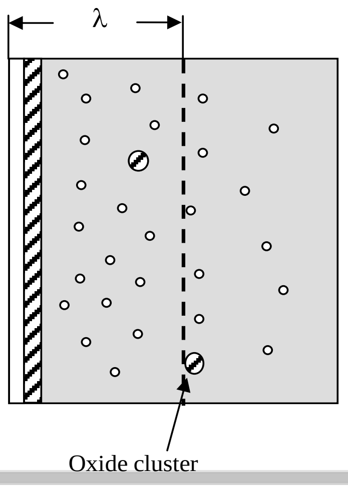

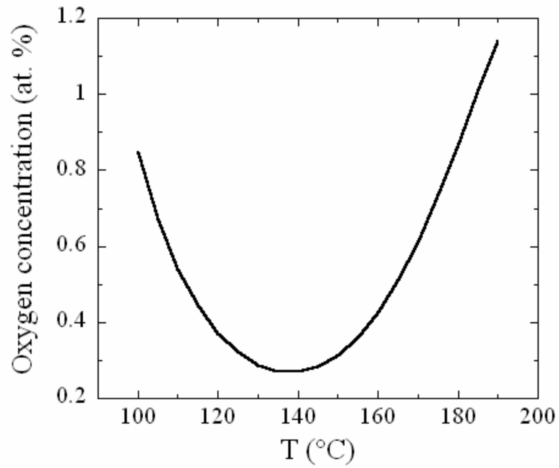

Calculated oxygen concentration at the metal/oxide interface as a function of temperature after 48h baking

G. Ciovati, *Appl. Phys. Lett.* **89** (2006) 022507

Oxygen Pollution Model: Shortcomings

The model cannot explain the following experimental results:

- The Q-drop did not improve after 400°C/2h "in-situ" baking, while O diffuses beyond λ
- The Q-drop was not restored in a baked cavity after additional baking in 1 atm of pure oxygen, while higher O concentration was established at the metal/oxide interface
- Surface analysis of single-crystal Nb samples by X-ray scattering revealed very limited O diffusion after baking at 145°C/5h

Fluxons as Source of Hot-Spots

- Motion of magnetic vortices, pinned in Nb during cool-down across $T_{c,}$ cause localized heating

- Periodic motion of vortices pushed in & out of the Nb surface by strong RF field also cause localized heating

The small, local heating due to vortex motion is amplified by R_{BCS}, causing cm-size hot-spots

Thermal Feedback with Hot-Spots Model

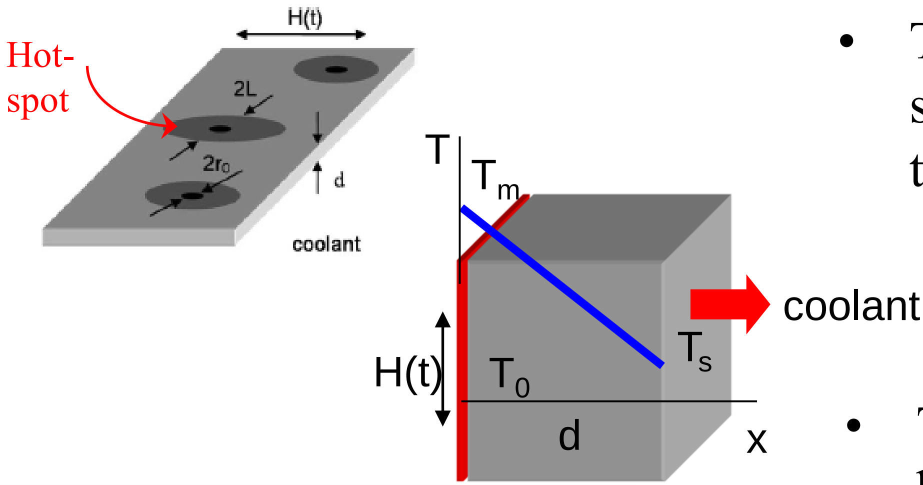

- The effect of "defects" with reduced superconducting parameters is included in the calculation of the cavity R_s

Hot-spots

- This non-linear R_s is used in the heat balance equation

$$u(\theta) = \theta e^{1-\theta}$$

$$\frac{2B_p^2}{B_{b0}^2} = 1 + g + u(\theta) - \sqrt{\left[1 + g + u(\theta)\right]^2 - 4u(\theta)}$$

$$Q_0(B_p) = \frac{Q_0(0)e^{-\theta}}{1 + g \Big/ \left[1 - \left(B_p / B_{b0}\right)^2\right]}$$

Fit parameters:

g related to the No. and intensity of hot-spots

$Q_0(0)$ low-field Q_0

B_{b0} quench field

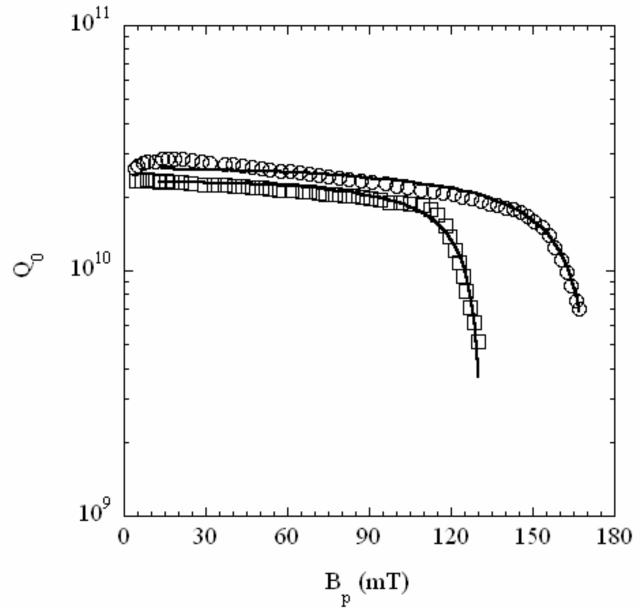

A. Gurevich, *Physica C* **441** (2006) 38

Q-drop: Recent Samples Results

Samples from regions of high and low RF losses were cut from single cell cavities and examined with a variety of surface analytical methods.

No differences were found in terms of:

- roughness
- oxide structure
- crystalline orientation

EBSD

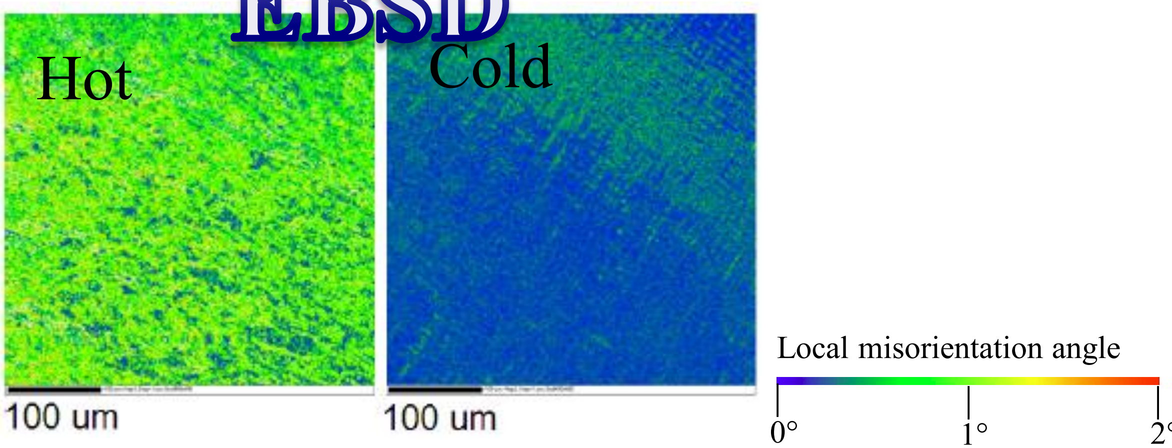

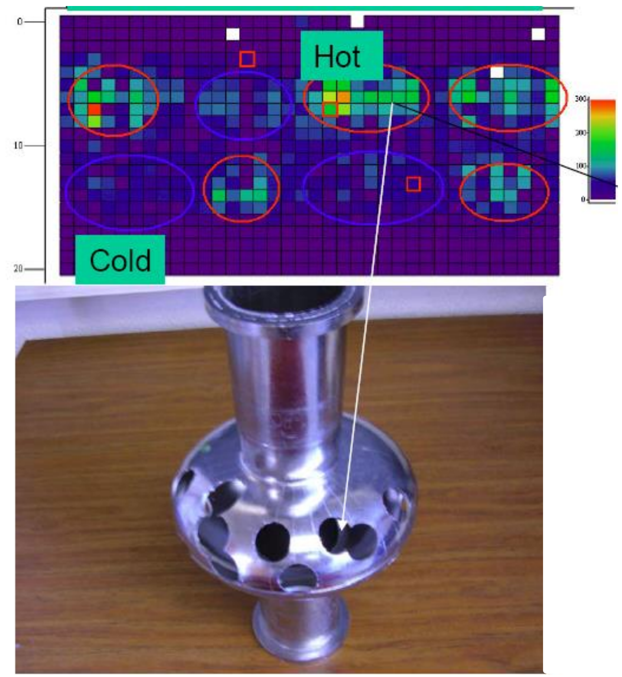

It was found that "hot-spot" samples have a higher density of crystal defects (i.e. vacancies, dislocations) than "cold" samples